Producing Energy and Fertilizer from Organic Municipal Solid Waste: Enhancing hydrolysis and bacterial populations and mixing and thermodynamic modeling of new solid waste treatment technology

Ecology Publication Number 09-07-064

To ask about the availability of this document in a format for the visually impaired, call the Solid Waste and Financial Assistance Program at 360-407-6900. Persons with hearing loss can call 711 for Washington Relay Service. Persons with a speech disability can call 877-833-6341.

FINAL REPORT

Producing Energy and Fertilizer from Organic Municipal Solid Waste: Enhancing hydrolysis and bacterial populations and mixing and thermodynamic modeling of new solid waste treatment technology

Submitted by
Bioprocessing & Bioproducts Engineering Laboratory
Department of Biological Systems Engineering
Washington State University
June 2009

Usama E Zaher, PhD, PE
Shulin Chen, PhD, PE
Project Leaders and Principal Investigators
Bioprocessing & Bioproducts Engineering Laboratory
Washington State University, Pullman, WA 99164-6120

Chenlin Li, PhD, Research Associate
Bioprocessing & Bioproducts Engineering Laboratory
Washington State University, Pullman, WA 99164-6120

Liang Yu, Research Assistant
Timothy Ewing, Research Assistant
Bioprocessing & Bioproducts Engineering Laboratory
Washington State University, Pullman, WA 99164-6120

This project was completed under Interagency Agreement C0700136 with the Bioprocessing & Bioproducts Engineering Laboratory, Washington State University

Legal Notice

The Washington State Department of Ecology provided funding for this project through the Beyond Waste Organics Waste to Resources (OWR) project. These funds were provided in the 2007-2009 Washington State budgets from the Waste Reduction Recycling and Litter Control Account. OWR project goals and objectives were developed by the Beyond Waste Organics team, and were approved by the Solid Waste and Financial Assistance Program. This report is available on the Department of Ecology's website at www.ecy.wa.gov/beyondwaste/organics.

The reader may be interested in the other project reports supported by Organic Waste to Resources and Waste to Fuel Technology funding sponsored by Ecology. These are also available on the "organics" link. The Washington State University Extension Energy Program will make this report accessible in its broader library of bioenergy information at www.pacificbiomass.org.

Table of Contents

Executive Summary

Introduction

As Washington continues its efforts to more sustainably utilize organic wastes, new and better technologies to accomplish this will need to be developed. Washington State currently produces over 16 million dry tons of underutilized biomass, according to the Biomass Inventory and Bioenergy Assessment (Frear et al., 2005) conducted by Washington State University (WSU) and the Washington State Department of Ecology (Ecology). Of that amount, approximately 750,000 tons of post-consumer wastes (food waste, yard waste, yellow and brown grease, other miscellaneous organics) and 360,000 tons of food processing and packing wastes are potentially suitable for digestion, many of which can be co-digested with manures on farm AD facilities. In many cases, though, location, regulations, and economics dictate that treatment of these wastes occurs outside of the farm environment and without co-digestion with manures and their buffering stability. Presently, industry predominantly chooses to not digest the waste materials instead opting for other options such as landfill, compost or incineration, technologies that do not provide as much renewable energy and sustainability benefits as AD. One reason for this choice against AD is the difficulty in digesting highly volatile organic waste solids in an economical and stable manner. Clearly, new technological options must be made available to industry in order to increase the adoption rate of AD for these particular high-strength solids.

High Solids Anaerobic Digestion (HSAD)

Several different types of AD technologies exist to accommodate high-strength solid wastes. These technologies can be broadly classified as those appropriate for low solid concentrations (less than 15% of TS) or high solid concentrations (greater than 15%). High solids anaerobic digestion (HSAD) is a relatively new application of conventional AD technology and can be accomplished through three basic forms of technology:

- Wet systems—approach that dilutes the high solids to low TS capable of being pumped and mixed in typical plug-flow and/or complete mix designs;
- Dry systems—approach the maintains the high solids content in a stackable form that is not actively mixed, but simply uses liquid leachate return as a mechanism for mass transfer;
- Phased systems—approach that breaks the AD process into acidification and methanogenesis steps, each with their own dedicated reactors and units processes—notably, one reactor is making primarily methane while the other reactor produces mostly CO_2 and H_2.

A review of these existing commercial HSAD designs shows that scientific and engineering concerns still exist within each of these approaches. In the wet system, dilution with potentially valuable, costly and scarce water resources makes little engineering sense as larger and more expensive reactors are required to handle the diluted waste stream. In addition the mechanical mixing and solids recycling that occurs to maintain effective bacterial mass transfer and inoculation to protect the system from inhibition are costly from both a capital and operating energy sense. In the dry system, purposeful non-mixing reduces capital and operating energy costs but biological kinetics are severely hampered by the loss in mass transfer efficiency,

resulting in less than impressive biogas production and performance. In the phased system, the separation of biological processes results in added complexity in regard to flow patterns and number of reactors, with consequent capital and operating cost increases. Goals of this study were to develop a new engineering approach towards high solids digestion that combines the best concepts of existing approaches and formulates a new design capable of reducing capital and operating costs while maintaining effective biogas production performance and stability.

New HSAD Design

This research project developed, tested, and modeled an innovative design for a mesophilic (35^{o}C) HSAD system for the biological treatment of biomass consisting primarily of the organic fraction of municipal solid waste (MSW) (Figure 11.30). This system utilizes an innovative dual-chamber digester design to efficiently inoculate high solids waste with a recycled leachate containing a dense concentration of anaerobic organisms. The leachate is separated from the solids chamber, treated in a modified high rate upflow anaerobic sludge blanket (UASB) digester (seed chamber), and recycled back to the high solids chamber to provide mixing, pH control, and seeding of anaerobic microorganisms. At the same time recycling the leachate provides a convenient pathway for nutrient removal and recovery from the digester.

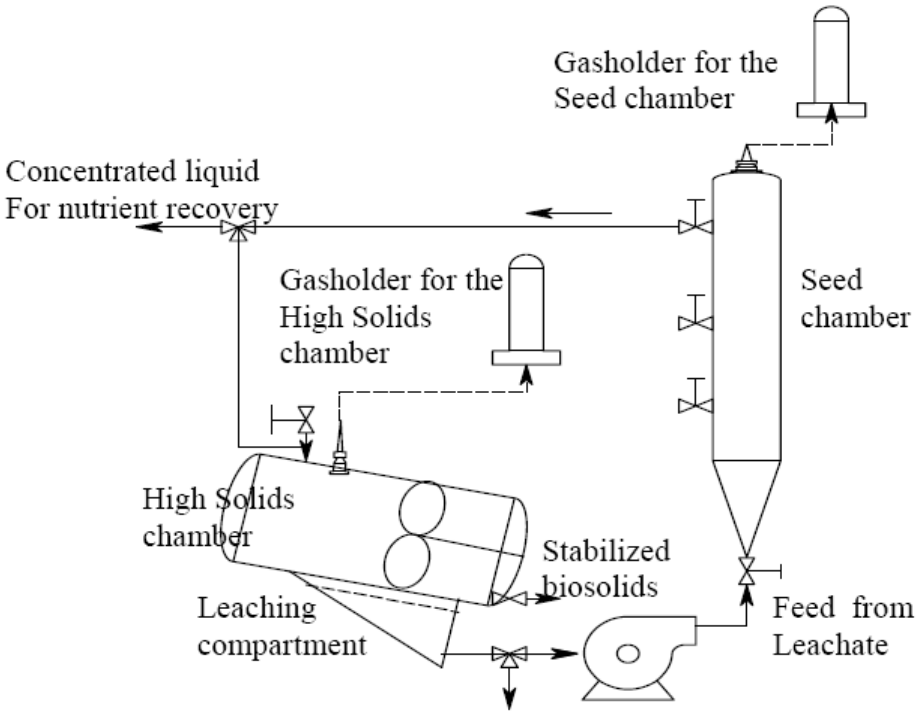

Figure 1 New HSAD design

This hybrid system utilizes dual reactors but is not phased in that both reactors are operating under near neutral pH conditions and producing an effective methane concentration within both reactor headspaces. In addition, this system is in many ways a mix between a dry and wet system in that the high solids are digested with minimal active mechanical mixing, relying mainly on liquid leachate return, but the biological kinetics and stability are enhanced over typical dry systems in that the attached high-rate reactor digests the high VFA liquid leachate--returning a

pH neutral liquid to the pile. Advantages of this high-rate liquid reactor and neutral pH leachate return are:

- Improved biogas production kinetics through the use of a high-rate liquid reactor;
- Enhanced and more cost-effective bacterial inoculation resulting from the release of bacteria from the high-rate reactor to the solids reactor as opposed to using sludge or solids recycle;
- Greater system stability in that high VFA liquids are quickly reacted prior to entry back to the pile, removing a notable product inhibition threat plaguing many digesters;
- Use of VFA removed leachate as a means for mass transfer throughout the system allows for more sustainable use of limited water resources, reduction in reactor sizes and importantly, a means for inducing nutrient recovery as the majority of the mineralized nutrients reside within the liquid leachate.

Proof of System Capabilities and Viability

Preliminary modeling from bench-scale experimental results has indicated that this system compares favorably to the reported performance of current dry digester technologies. Digester loading rate and biogas production rate are improved by about 50%, while achieving comparable chemical oxygen demand and total solids reduction. This compares a bench-scale experimental design to actual facility performance. At full-scale, the system will require optimization to achieve similar or enhanced performance. In addition to the waste treatment benefits of this system, the potential to integrate a nutrient removal and recovery system increases the overall economic value of the system. It is estimated that integrating the leachate recycle loop into a nutrient removal and recovery system would produce 2.1 kg/ton of nitrogen and 3.72 kg/ton of phosphorus from food waste. Based on the bench-scale results, the cost of treating organic waste with this system is estimated to be $1.08/kW-h compared to $1.55/kW-h calculated for an existing technology. These values account for capital and operational costs amortized over the predicted operating life of the facility. This system has potential to lower both capital and operational costs compared to existing technologies.

Public Benefits to Washington State

There are three main ways in which the state can benefit from further development and ultimate deployment of this system. First, capital and operational costs for the treatment of organic waste are reduced compared to existing digester technologies; Second, this new system significantly reduces the emissions of odors and waste gases emitted by utilizing a closed leachate recycle loopFurthermore, the leachate recycle loop provides a pathway for recovering nitrogen and phosphorus nutrients. Third, the methane can be utilized as a renewable source of combined heat and power (CHP) or compressed and utilized as an alternative vehicle fuel.

1. Introduction

As Washington continues its efforts to more sustainably utilize organic wastes, new and better technologies to accomplish this will need to be developed. Washington State currently produces over 16 million dry tons of underutilized biomass, according to the Biomass Inventory and Bioenergy Assessment (Frear et al., 2005) conducted by Washington State University (WSU) and the Washington State Department of Ecology (Ecology). Of that amount, approximately 750,000 tons of post-consumer wastes (food waste, yard waste, yellow and brown grease, other miscellaneous organics) and 360,000 tons of food processing and packing wastes are potentially suitable for digestion, many of which can be co-digested with manures on farm AD facilities. In many cases, though, location, regulations, and economics dictate that treatment of these wastes occurs outside of the farm environment and without co-digestion with manures and their buffering stability. Presently, industry predominantly chooses to not digest the waste materials instead opting for other options such as landfill, compost or incineration, technologies that do not provide as much renewable energy and sustainability benefits as AD. One reason for this choice against AD is the difficulty in digesting highly volatile organic waste solids in an economical and stable manner. Clearly, new technological options must be made available to industry in order to increase the adoption rate of AD for these particular high-strength solids.

This research project developed, tested, and modeled a mesophilic (95^{o}F) high-solids anaerobic digestion (HSAD) system for the biological treatment of organic waste consisting primarily of the organic fraction of municipal solid waste (OFMSW) (Figure 2).

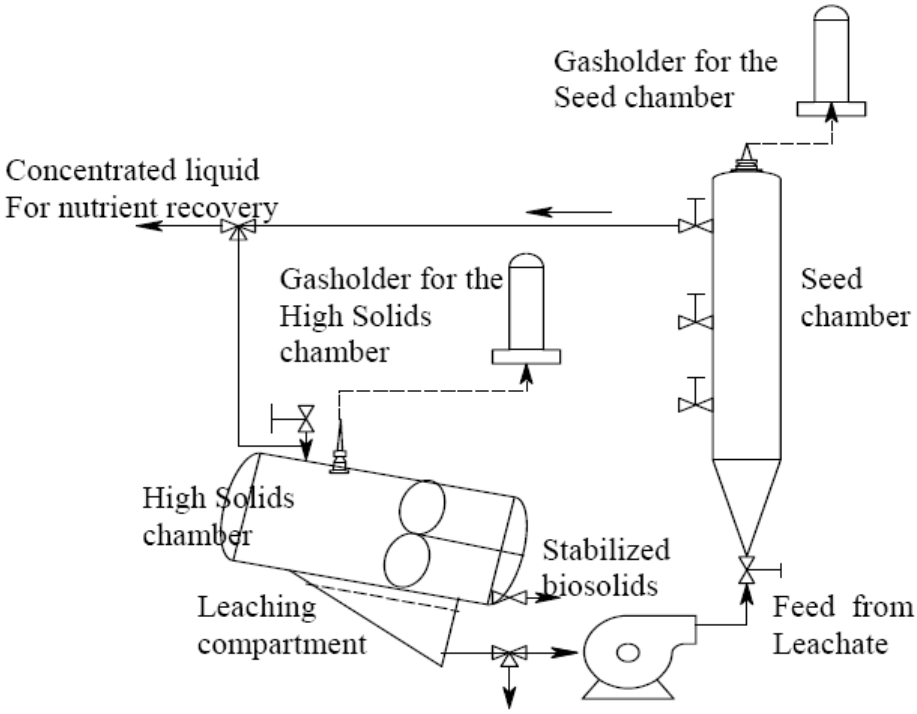

Figure 2 Process Flow Diagram

This system utilizes an innovative dual-chamber digester design to efficiently contact high solids waste with an economically separated and recycled leachate. The leachate is separated from the solids chamber, treated in a modified high-rate upflow anaerobic sludge blanket (UASB) digester (seed chamber), and recycled back to the high solids chamber to provide mixing, pH control, and seeding of anaerobic microorganisms (hydrolytic, acetogenic, and methanogenic). The leachate also serves as a point of contact for an integrated nutrient removal and recovery system. The decoupling of the solids retention time (SRT) from the leachate or hydraulic detention time (HRT) allows for system optimization over a wide range of received feedstocks. It is anticipated that design features, which rely on reduced reactor volumes, less intensive mixing, enhanced bacterial concentrations, and reductions in product inhibition, will allow for increased biogas production at lower capital and operating costs as compared to existing high-solids waste treatment technologies, thereby improving upon the existing adoption rate for application of high-solids digestion.

Specific attributes of the system are many. First, methane is produced in both the high-solids chamber and the seed chamber, as opposed to most systems that utilize a dual-chamber which rely on only hydrolysis and acidogenesis in the first reactor and methane-formation in the second chamber. Second, hydrolysis occurring in the high-solids chamber is enhanced by leachate recycled enzymes as well as anaerobic microorganisms due to the similar chemical and biological environments. The reduced solids recycle allows for reduction in energy and in size of the reactor. Third, the high-solids chamber relies on continuous seeding to improve the overall process of solids degradation and stabilization. Fourth, this system utilizes natural diffusion of leachate through the high-solids chamber. Fifth, the seed chamber is operated as a high rate expanded sludge bed (modified UASB) digester that increases methane production and anaerobic microorganism yield and allows continuous seeding to the high-solids chamber.

This HSAD system has a significant advantage over existing AD systems in that it can be applied to high-solids waste streams containing concentrations of more than 15% total solids (TS) while most of the AD systems that are applied to domestic wastewater treatment, dairy manure, and food processing wastes in Washington State can only handle up to 8-12% TS. Application of these existing systems to targeted high solids biomass would require significant dilution with potentially inhibitory nutrient-rich reclaimed water and larger digester volumes resulting in higher capital costs. Existing European technologies developed for HSAD, be they WET (10-15% TS) or DRY (25-40% TS) depend on pumping or mixing large volumes of treated solids in order to maintain viable anaerobic microorganism populations. This moving or recycling of solids requires additional reactor volume and expensive solids pumping and/or mixing equipment. This HSAD system, though, acts as a hybrid between WET and DRY since it incorporates a high-solids chamber with leaching integrated with a seed chamber containing high activity anaerobic microorganisms, requiring no pumping or recycling of solids which can be expensive or problematic. An additional advantage to this system being hybrid is that along with treating organic waste at concentrations greater than 15% TS, it can accept dilute waste streams directly in the seed chamber for treatment. Another added benefit of the system is that the leachate is home to the majority of the dissolved or suspended mineralized nutrients and therefore can be readily treated for nutrient removal and recovery just prior to re-entry to the

main reactor. By removing and recovering the nutrients, the digestion process is improved as potential inhibitors are alleviated and more importantly, producers can more easily satisfy their nutrient management plans while also producing valuable bio-based co-products.

2. Project Objectives

The goal of this project was to investigate a new design for HSAD with increased biogas production at significantly lowered capital and operating costs compared to existing technologies. This goal was achieved by targeting suitable underutilized biomass, testing the new system experimentally at the bench-scale, and developing mathematical models for process and economic analysis. The following objectives were set to optimize the new process, establish criteria for the system design, and maximize the benefits and energy output.

Objective 1: Select feedstock and test this system at the bench-scale
Selection of the feedstock was made mainly to maximize the benefit to Washington State. A list of the top wastes suitable as feedstocks in biogas plants was developed of which the top two were selected based on their annual production quantities (Q > 1000 tons/year), organic content (OC > 80%) and potential biogas production (PBP > 1 ft^3/lb). Beyond feedstock waste another feedstock within the integrated system is the bacterial biomass produced in the seed chamber. Demonstration of the development of anaerobic microorganisms and biogas production from the seed chamber was necessary to test the effectiveness of the integrated system and in particular the seeding system. The seed production target was set to 10,000 mg volatile solids (VS)/L to improve the anaerobic microorganism activity in the high-solids chamber. Growing anaerobic microorganisms separately on the leachate from the solid waste provides the microorganism population an adaption time to overcome potential inhibitors. Various operation modes of the seed chamber had to be tested in order to check its robustness for continuous seed production. Also, steady-state and intermittent feed conditions were tested.

Objective 2: Develop process models for describing operational and economic benefits
Development of process models includes model implementations in simulation software, model calibration, and model validation. Software implementations of the process models are necessary for the development and the future scale-up of the process. Model calibration is necessary to estimate the most sensitive process kinetics. Model validation is necessary to simulate the new process, predict the behavior of this system, save experimental time, and keep the process development within the time frame of the project. Two targets were set for this objective. The first was the development of an AD process model calibrated for the selected feedstocks. The second target was a complete and validated economic simulation tool of the system. Evaluation of this system via economic modeling was necessary to establish the connection to Washington State and to evaluate the benefit of continued system development to the citizens of the state. The target set for this objective was the improvement of this system's economic value compared to existing systems as follows:

- 20% savings due to improved biogas production per unit volume of digester. The savings were calculated per kWh from solid wastes assuming 30% efficiency of electrical power generation from biogas.

- 30% cost reduction due to savings in solids recycling and improved environmental impact calculated per kWh from solid waste digestion and biogas production.

Testing the experimental setup by integrating the high-solids chamber with the seed chamber was necessary to demonstrate the process improvement due to augmentation and continuous seeding. Two targets were set to evaluate this objective. The first target was to achieve an improvement of the reactor effective volume to 90% of the geometric volume. The second target was to improve the biogas production to 90% of the theoretical biogas production of the organic fraction of the treated waste.

Objective 3: Enhance hydrolysis of cellulosic feedstocks
A case study and experimental methodology for the pretreatment of cellulosic feedstocks in support of AD was detailed by four methods: alkaline and peroxide, thermal, enzymatic hydrolysis, and biofilm-facilitated hydrolysis.

Objective 4: Develop mixing strategies and models
Based on a literature review of existing technologies, mixing strategies for this system were developed, computational fluid dynamic (CFD) models are shown under predicted loads, and selection criteria were detailed.

Objective 5: Disseminate scientific publications developed as a result of this project
A list of scientific publications and conference presentations generated from this project are given. In addition, several relevant publications are attached as appendices.

Additional notes
Objectives 1, 3, and 4 are of technical focus to validate this system, evaluate its efficiency, and design its integrated system of chambers. The seed chamber--microorganism augmentation process, was tested experimentally and the mathematical models extrapolated the augmentation process to the maximum load and production rate. The integrated system of high solids chamber and seed chamber was tested experimentally. Mathematical models were used to determine the system efficiency and its larger scale design. Objectives 2 and 5 are of managerial focus to establish the connection to the market for this new system in Washington and to determine the economic benefit to the electricity rate and tax payers. The potential feedstock and the geographical locations of the system were determined. The potential savings in the biogas production using the new system were calculated per kWh to estimate the economic benefits to the electricity grid and tax payers.

3. Project approach

3.1. Feedstock assessment

A detailed biomass assessment was performed as described in Appendix 1. The biomass inventories of the states of California and Washington were filtered to determine digestible, fermentable, and year-round available wastes. The biomass databases, as recorded for each

county in Washington (Frear et al. 2005), were sorted according to yearly biomass (waste) production at the state level. Each biomass type was classified into four categories: wet, dry, tilled, and seasonal. The databases were filtered to exclude:

1. Agricultural residuals that are tilled within soils to maintain their fertility
2. Seasonal wastes that are not available for year-round feed in reactors as the sole feedstock
3. Solid wastes that are mainly inert

Accordingly, wastes consisting of more than 30% dry content of easily degradable organic fractions were selected for methane production. Other wastes that were mainly cellulosic were assumed to be more suitable for conversion to other fuel such as ethanol which mainly includes feedstocks such as forest residues, land-clearing debris and municipal wood waste. The availability, proximate analysis including the degradability of these types of waste is included in Table 1 of Appendix1. It is observed that the cellulose and hemicelluloses content of green lawn clippings is higher than other feedstocks selected for anaerobic digestion, however green clippings are found to be 41% degradable without any pretreatment; therefore it is recommended as a feedstock for anaerobic digestion. Feedstocks to test in this system were chosen based on potential biogas and power production. The procedure to estimate the power that could be generated from each waste is detailed in Appendix 1. Food waste and manure, though, had the highest biogas and power production potential with milk cow manure at 49% degradability and MSW food waste at 89% degradability. MSW food waste both because of its high degradability and its tie to Ecology *Beyond Waste* efforts was selected as the predominant feedstock for testing the HSAD design. However, a focus on MSW food waste should not be interpreted as meaning that other important municipal feedstocks such as green waste could not be effectively incorporated as a useful feed to the system. Lastly, although manure is not a target feedstock of this municipal HSAD system, it was used as a feedstock for some of the experiments in digestion and hydrolysis as its buffering capacity and known digestion parameters were useful as a control and baseline for experimentation and modeling. In particular, the fibrous solids in the dairy manure were excellent feed for hydrolysis studies, being representative of many of the different classes of municipal green or lignocellulosic waste that could be a potential feedstock in this application.

3.2. Design concept and modeling

The design for this system as shown earlier in Figure 1 requires no solids recycling or intensive solids mixing. Substrate/microorganism contact is primarily induced through use of the leachate recycling, a far less costly and problematic mixing approach than those utilizing movement of solids. The leachate is sent through a high-rate reactor which converts inhibitory soluble acidic compounds to methane while also producing important anaerobic microorganisms which seed the high solids reactor every time that the system is loaded with new feedstock. System capabilities were determined using models developed in part through data resulting from bench-testing of the system. Four mathematical model implementations were developed to estimate the process kinetics and the configuration settings for this system. Two model implementations were used to estimate the degradation kinetics of the selected feedstock, as detailed in Section 3.1. The

other two model implementations were used to estimate and simulate the configuration of the seed chamber and the integrated system detailed in Figure 2.

A simple model (ADM2) was developed to test the three primary steps of AD: hydrolysis, acidogenesis/ acetogenesis, and methanogenesis. The model was used for kinetic parameter estimation using different anaerobic microorganism inoculums. (See Appendix 2 for a full description of ADM2.) The model was used to study the degradation of dairy manure which was being used as a control and comparative feedstock with high buffering capacity. To study the anaerobic degradation and methane production from food waste, a general co-digestion model (GISCOD) was developed using the Matlab-Simulink® implementation of the International Water Association (IWA) Anaerobic Digestion Model no.1 (ADM1). The GISCOD model applies the advanced transformer model procedure to estimate the composition and study the hydrolysis of each waste separately. The transformer model is illustrated in Appendix 3. The integrated co-digestion model in Matlab-Simulink® is presented in Figure 3. The food waste characteristics are assigned to input1. The biochemical characteristics are estimated by the transformer model and assigned to the hydrolysis model to study hydrolysis separately. The same is done for the diluted manure that was added to buffer the system. The hydrolysis products were combined and further digestion steps were performed using the IWA ADM1. The detailed model for IWA ADM1 is described in Appendix 4.

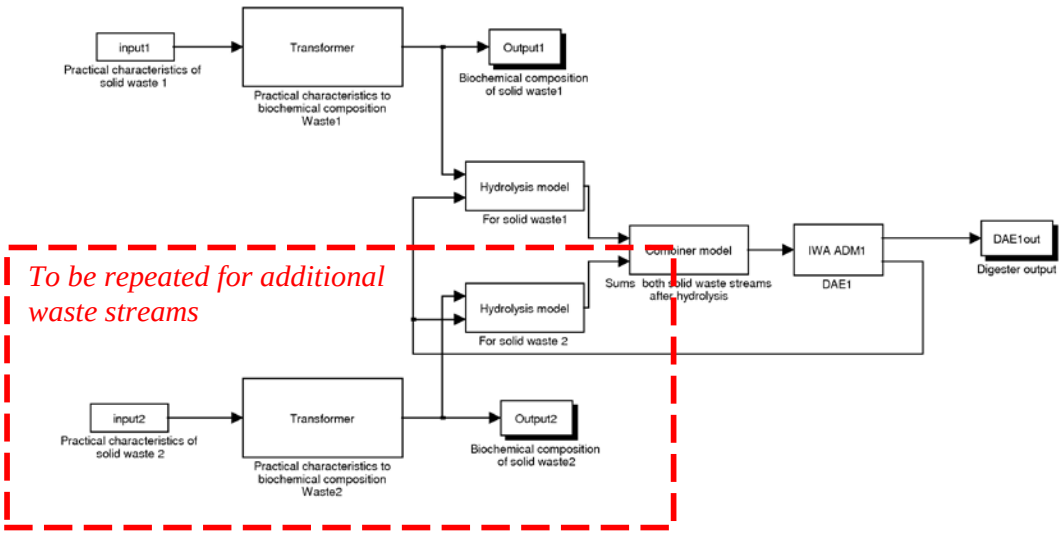

Figure 3 GISCOD Model in Matlab-Simulink®

A third model was built for the seed chamber in Matlab-Simulink® as illustrated in Figure 4. Although the figure shows the scheme horizontally, it should be noted that the flow in the chamber is upward as if the whole scheme was rotated 90º counter clock-wise. ADM1 was updated and used to model the seed chamber as three compartments in series. Each compartment is a masked implementation of the whole model nodes and C-code. A recycle port and a continuous recycle loop were constructed to simulate the continuous leachate recycle loop that was applied to the seed chamber to expand the simulated sludge bed. An inlet compartment was modeled to combine the dilute leachate recycle loop and the intermittent feed. The sludge bed

expansion was modeled by introducing fraction parameters that regulate the solids leaving each compartment. The output from each compartment is sent to the Matlab work space as a simulated time-step matrix. Moreover, two monitor boxes were designed to simulate gas and liquid outputs dynamically.

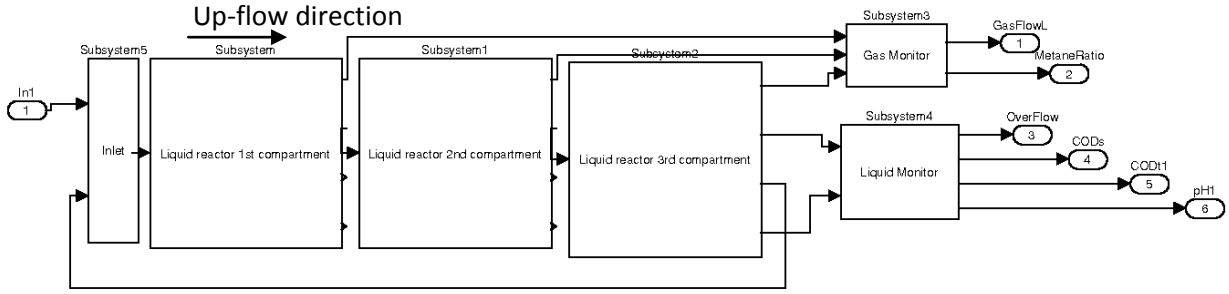

Figure 4 Seed Chamber Process Model

A fourth model was built for this system in Matlab-Simulink® as shown in Figure 5. The solid waste flows and practical characteristics such as chemical oxygen demand (COD), total organic carbon (TOC), total nitrogen (TKN), and total phosphorus (TP) are generated as model inputs from the Matlab workspace. The transformer model estimates the solid waste's biochemical characteristics such as carbohydrates, proteins, lipids, and inert contents. The biochemical characteristics and flows of the solid wastes and the seed are inputs to the high-solids chamber model. The high-solids chamber model was developed by upgrading the IWA ADM1 with the leaching process. The leachate from the high-solids chamber is fed to the seed chamber to grow the anaerobic microorganism seed and recycle it back. The seed chamber is a masked implementation of the model that is shown in Figure 4. All output vectors from the high-solids and the seed chambers are sent to the Matlab work space. Gas, solids, and liquid monitors were implemented for dynamic simulation of the system output and to facilitate optimization and parameter estimation of the integrated model.

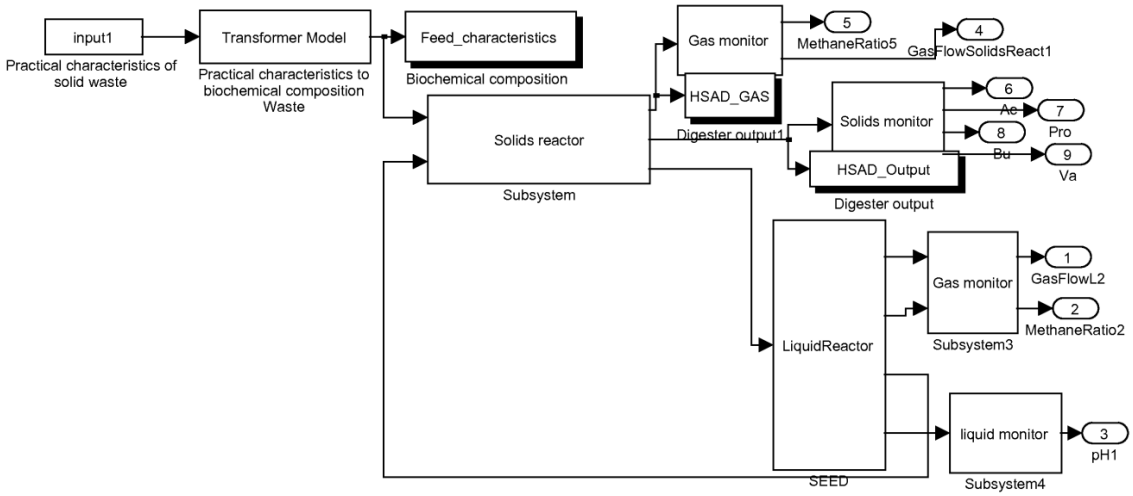

Figure 5 Integrated Process Model

The four models were calibrated using the experiments described in the next two sections: 3.3 and 3.4. The ADM2 parameters were estimated from serum bottle batch experiments. The GISCOD model was calibrated using co-digestion experiments with manure and food waste. Although any set of feedstocks could be used to calibrate the GISCOD model, manure along with the obvious choice of food waste was chosen because of the wealth of available data parameters for these particular feedstocks. The fraction parameters of the seed chamber model were calibrated using two bench-scale experiments digesting leachate from fresh dairy manure and food waste. The fourth model of the integrated system was used to estimate the effective volume of the high-solids chamber. The values of the process model parameters are listed in Appendix 5. The integrated model was validated using a bench-scale experimental apparatus.

3.3. Unit Process and seeding experimentation

Although the original grant proposal plan suggested two sets of experiments to test this system's two unit processes (high-solids and seed chambers) separately with each feedstock, an additional two sets of experiments were performed to understand the failure mechanisms of conventional solids digesters when they are not continuously seeded and leached. Accordingly, four sets of experiments were performed for testing the unit processes as well as studying the solids digestion process kinetics and validation of the seeding process. The four sets of experiments were performed in a temperature controlled hot room set to 95ºF. The four sets of experiments are described below.

The first set of experiments was designed to test the AD of food waste and fresh manure (buffered feedstock control) separately in conventional completely-mixed digesters. The mechanically mixed lab-scale digester shown in Figure 6 was used to test the AD of > 20% TS of each feedstock mixed by volume with 50% inoculum from a domestic sludge AD.

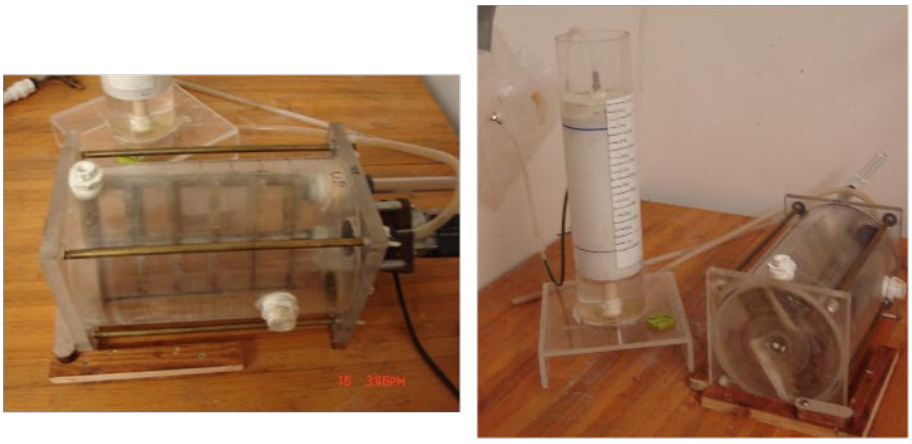

Figure 6 Mechanically Mixed High Solids Chamber (left) with Biogas Collector (right)

The biogas production was measured using the biogas collector that was connected to the digester as shown in Figure 6. Sealed sampling ports were configured to collect waste and gas samples for lab analysis without inhibiting the digester's anaerobic conditions. The solids

digestion experiment with manure was run for 45 days and the experiment with food waste was run for 25 days. The operation was extended once complete inhibition was reached after the first week to test possible recovery after process adaptation resulting from pH control accomplished through addition of various alkaline solutions. Samples from both reactors were tested using laser scanning and SYTO® 9 (Invitrogen Co., Carlsbad, CA) staining and confocal microscopy techniques to evaluate the microorganism viability.

The second set of experiments was designed to investigate the microbial activity and digestion of diluted dairy manure, again used as a representative control feedstock with high alkalinity and buffering capacity. The experiment was designed to study the effects of different inoculum sources and concentrations on the AD. ADM2 was used to analyze these effects. The experiments and analysis are described in detail in Appendix 2.

The third set of experiments was to study the degradation of food waste and the effect of co-digestion with dairy manure, and its ability to supply buffering and alkalinity, in semi-continuous intermittently mixed lab-scale reactors. The GISCOD model was used to analyze the anaerobic degradation mechanisms and estimate the hydrolysis parameters of both the food fraction of MSW and manure. A detailed description of the experiment and the analysis are described in Appendix 4.

The fourth set of experiments was designed to test the seed chamber. Two bench-scale modified UASB digesters were used to grow the anaerobic microorganism seed on the extracted liquid from dairy manure and food waste. Both feedstock's were homogenized and preserved at 5 ºC. Each digester was started with diluted inoculums from an anaerobic sludge digester. The dilution ratio was 1:2 of anaerobic sludge to distilled water. The characteristics of the extracted liquid from manure (control) and food waste and the inoculums are listed in Table 1. The as-built seed chamber is shown in Figure 7.

Each chamber was connected to a peristaltic pump to maintain continuous recycle. The leachate recycle loop is connected to a compartment with a valve system to divert the flow during feeding. The feed was started after a starvation period of the initial inoculum and was kept at a constant rate of 50 mL/day of liquid manure and 100 mL/day of liquid food waste until the process reached steady state in both digesters. The steady state was followed by a dynamic process operation imposed by intermittent feeds of 200 mL and 300 mL for manure and 300 mL and 400 mL for food waste, which was repeated every 3 to 5 days. The steady state results were used to estimate the initial state of the seed chamber model and fraction parameters of the bacteria (f_b) and solid substrate (f_s) leaving the model compartments. The dynamic results from each chamber were used to validate the seed chamber model. The anaerobic seed production was quantified by analyzing the effluent solids volatile VS, laser scanning using confocal microscopy and SYTO 9 staining, and the model estimate of the viable microorganism populations.

Table 1 Characteristics of Dilute Liquid Feed and Initial Inoculums

Characteristic	Unit	Liquid food waste	Liquid Manure	Anaerobic sludge
Total solids (TS)	g/l	5.2	38.1	2.5
Volatile solids (VS)	g/l	4	24.8	0.9
Particulate COD (CODp)	gCOD/l	6.5	30.2	1.19
Soluble COD (CODs)	gCOD/l	5.6	5.6	0.36
Total organic carbon (TOC)	gC/l	4.6	11.3	
Inorganic carbon (IC)	mole/l	10.7	60.4	
Total Kjeldahl nitrogen (TKN)	gN/l	0.45	3.4	
Total ammonium (TAN)	gN/l	0.17	1.9	
Total phosphorus (TP)	gP/l	0.03	0.2	
Total ortho-phosphorus (OP)	gP/l	0.015	0.03	
Volatile fatty acids (VFA)	gCOD/l	0.53	1.5	
pH	-	3.8	7.3	7.4

Figure 7 As-built Seed Chamber

3.4. Experimental validation

The integrated seed chamber and the high solids chamber system was tested at bench-scale. The as-built setup is shown in Figure 8. The high solids chamber was laterally mixed with continuous percolation along the digester, and it was extended by a leaching compartment at the bottom. The leachate was recycled to the seed chamber and its overflow was recycled. Both the high solids and seed chambers were operated under mesophilic conditions at 98.6^{o}F and were connected to gas holders for collection and sampling of biogas. Food waste digestion was maintained in the integrated system with biogas production collected from both the high solids and seed chambers.

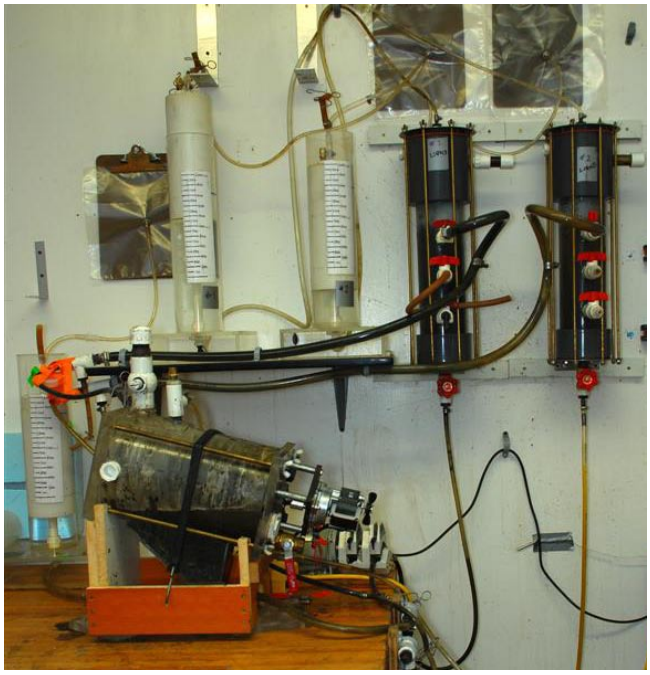

Figure 8 Integrated HSAD System with continuous leachate recycle loop

The high solids chambers were initialized with anaerobic sludge inoculum from the previous seed chamber experiment. After startup, continuous feed of solid wastes was made to the high solids chambers, and the high solids chambers were integrated into the leachate recycle loop of the seed chambers. The integrated system experiment with manure was not possible since the leaching compartment and tubes were frequently clogged with fibers. For bench-scale experimentation, small tube and fitting sizes would not allow for the continuous flow of small fibers that escaped from the screen between the high solids chamber and the leaching compartment. The integrated system experiment with food waste was completed since it contained less fiber. The food waste characteristics are listed in Table 2. The feed rate to the high solids chamber was maintained at a constant rate of 10 g/day until a steady state of biogas production was reached. After the steady state process dynamics were reached the feeding was continued by alternating 100 g, 150 g and 200 g every 3 to 7 days according to the observed process performance. An overload condition was imposed by feeding 200 g for 3 subsequent days followed by reduced feed and a dilution period for process recovery. The solids volume was maintained at 3 L, and the liquid volume in the seed chamber was maintained at 2 L. The intermittent recycle rate of leachate through the seed chamber was maintained at 250 mL/h for 2 hrs each day (500 ml/day feed rate to the seed chamber). For the rest of the daily operation, the high solids chamber was disconnected from the leachate recycle loop and the recycle flow was maintained for the seed chamber to keep the up-flow velocity and suspension of the sludge bed. Although found optimal by process simulation, continuous leaching and seeding was impractical at the bench-scale since it required a very low pumping rate and small easily clogged tubing.

Table 2 Characteristics of Solid Waste Feed

Characteristic	Unit	Solid food waste
Total solids (TS)	g/l	154
Volatile solids (VS)	g/l	118
Particulate COD (CODp)	gCOD/l	182
Soluble COD (CODs)	gCOD/l	18.8
Total organic carbon (TOC)	gC/l	53.3
Inorganic carbon (IC)	mole/l	10.7
Total Kjeldahl nitrogen (TKN)	gN/l	5.3
Total ammonium (TAN)	gN/l	1.3
Total phosphorus (TP)	gP/l	4.6
Total ortho-phosphorus (OP)	gP/l	0.9
Volatile fatty acids (VFA)	gCOD/l	2.3
pH	-	

The steady state methane production results were used to estimate the effective volume of the high solids chamber. The experimental results during steady state operation and the imposed process dynamics were used to validate the model predictions.

3.5. Model based scale-up of the design

The design parameters of this system were determined by optimization using the validated integrated system model. The maximum methane production was evaluated from Equation (1) and used as the optimization target.

$$P_{CH4} = f_O \cdot f_b \cdot \frac{COD_t}{64 \cdot SG} \cdot 24.789 \quad \textbf{(1)}$$

Where:

P_{CH4} : Maximum methane production in L/kg

f_O : Organic fraction of the waste as VS/TS

f_b : Biodegradable fraction of the waste, assumed 0.8

COD_t : Total COD of the feedstock in g COD/L

SG : Specific gravity of the feedstock, typically 1.2

According to the food waste characteristics in Table 2, the maximum methane production rate is 39.7 L/kg of waste calculated at 95ºF. The design parameters of this system were evaluated by estimating the high solids chamber volume, seed chamber volume, and seed contained in the leachate recycle from a basis of 1 ton/day of waste. The optimization minimized the root mean square between the theoretical and simulated methane production rate to estimate the design parameters and to determine the methane production efficiency of the system.

3.6. Benchmarking the economic value

For comparison with existing HSAD systems, a second optimization was performed using only the high solids chamber model with continuous solids recycle (excluding the seed chamber). The maximum methane production was used to estimate the high solids chamber volume by applying the same recycle rate that was estimated in the first optimization of this system. For the purpose of comparison only, this second optimization assumes that the high solids chamber mixing system will be as efficient mixing recycled solids as mixing recycled liquid seed. The recycled solids are typically mixed with the feedstock in a blending chamber. The cost of the blending chamber was evaluated as an additional unit in existing systems and is not needed in this system. For the purpose of comparison, the seed chamber was assumed to have the same capital cost as the high solids chamber. The seed chamber is, however, less expensive compared to the high solids chamber since it is operating with liquid waste and does not require mechanical mixing. Additional savings from this system for the operation and capital costs were also evaluated.

The operational costs of this system were benchmarked by evaluating the savings of pumping liquid instead of solids and of mixing a smaller high solids chamber. The savings were evaluated by comparing this system with optimized existing systems per kWh. Solids pumping at 20% TS assuming d_{50}=0.6 mm, costs 3.6 cents/ton (Wilson K. C., Addie G. R. et al. 2006), 4.3 cents/m^3 of waste recycle rate. Accordingly, the cost of pumping liquids is calculated by the ratio of pumping power savings in this system with Equation (2), where W_L and W_S are the powers of pumping liquid and solids, respectively. The relative efficiency (η_r) is typically 0.8, and the specific gravity of the solid waste SG is typically 1.2.

$$\frac{W_L}{W_S} = \frac{\eta_S \cdot \rho_L}{\eta_L \cdot \rho_S} = \frac{\eta_r}{SG} \qquad \textbf{(2)}$$

The typical cost of mixing solids using paddle or screw mixers is 0.14 \$/ft^3 (Paul, Atiemo-Obeng et al. 2004), 4.94 \$/m^3. According to Equation **(3)** the mixing power and, therefore, mixing costs are proportional to digester volumes assuming similar viscosity (μ) and mixing intensity (G) in the high solids chambers of this system and the solids reactors of existing systems.

$$W_{mixing} = G^2 \cdot \mu \cdot Vol \qquad \textbf{(3)}$$

The capital cost was evaluated in comparison to a typical installation of the Kompogas system at Braunschweig, Germany. The Kompogas system has a solids reactor with solids recycle similar to what is considered in the optimization case studies. The plant installation cost was \$10,200,000 and was treating kitchen waste at 17,640 tons/year feed rate (Zaher, Cheong et al. 2007). The capital cost per ton was evaluated according to Equation **(**4) assuming lifetime of the existing plant equals twenty years and an annual interest rate of four percent. The capital cost of the novel HSAD system at maximized loading rate was scaled from the cost of this installation on the basis of the high solids chamber volume. The system optimized in this study is presented in detail in section 4.2.2 which illustrates the design and performance of the anaerobic digested system developed.

$$\text{Capital cost } \$/\text{ton} = \frac{\left(A/P, i\%, n\right)P}{Q} \quad (4)$$

All costs were evaluated per kWh of electrical power (E), using Equation (5) and assuming electricity generation efficiency of 30% and heating value of methane W_1 =35.8 MJ/m^3. The savings of the new system to Washington State were evaluated according to the total power production from waste that was estimated in Section 3.1.

$$E = \frac{\eta \cdot Q_{CH_4} \cdot W_1}{3.6} \quad (5)$$

3.7. Enhancing hydrolysis of cellulosic feedstocks

The objective of this portion of the project was to develop technologies for enhancing the hydrolysis of materials containing cellulose, hemicelluloses, and lignin in order to accelerate the AD process. According to the Biomass Inventory and Bioenergy Assessment (Frear, Zhao et al. 2005), approximately 420 thousand dry tons/year of yard non-wood biomass is underutilized in Washington State. With proper pretreatment this biomass can be fully exploited as a co-substrate with food waste, yellow and brown grease, and other organics for the production of renewable biogas and the recovery of nutrients with this system. Due to seasonal availability of this organic waste along with the parallel development of AD technologies for the treatment of animal manures by the Bioprocessing & Bioproducts Engineering Laboratory (BBEL), dairy manure fibers were selected as a representative lignocellulosic test material for this study.

Anaerobic processing has grown into a mature technology for wastewater treatment in the last two decades but still has limited applications in high solids waste treatment (De Baere 2000; Fang and Liu 2001). In this process, organic pollutants are degraded through a series of chain reactions, namely hydrolysis, acidogenesis, acetogenesis and methanogenesis, each being carried out by individual groups of anaerobic microorganisms. Generally, complex organic pollutants are first hydrolyzed and then fermented into fatty acids. Fatty acids are then converted into acetate and hydrogen, both of which are converted into methane. In this four-stage process, hydrolysis is always considered the rate-limiting step due to the complexity and recalcitrant characteristics of organic pollutants (Verstraete, de Beer et al. 1996; Barnes and Keller 2003). This case is especially notable in the dairy manure anaerobic digestion system.

Current hydrolysis technologies

To date, a considerable number of approaches to pretreatment and hydrolysis have been made to improve the degradation of ligncellulosic materials, such as wheat straw, wood, grasses, etc., for further energy recovery (Fan, Gharpuray et al. 1981; McMillan 1994; Curreli, Agelli et al. 2002; Sun and Cheng 2002; Fan, Zhang et al. 2006; Stephanopoulos 2007). Pretreatment breaks down

complex organic structure into simpler molecules, which are then more susceptible to microbial degradation. This type of pretreatment will produce similar results to physicochemical or biological processes (Mata-Alvarez, Mace et al. 2000; van Lier, Tilche et al. 2001).

Physicochemical pretreatment includes mechanical comminution, acid/base treatment, thermochemical treatment, and ultrasonic treatment. These methods open the cell-wall matrix, remove the lignin and hemicellulose, reduce cellulose crystallinity, or increase the porosity of the materials in order to significantly enhance the hydrolysis (Sun and Cheng 2002; Mosier, Wyman et al. 2005; Wyman, Dale et al. 2005). Dar and Tandon (1987) observed an improvement of 31-42% in microbial digestibility and an almost twofold increase in biogas when alkali treated (1% NaOH for 7 days) plant residues were used as a supplement to cattle manure. Patel et al. (1993) found that thermochemical pretreatment of water hyacinth improved biogas production and the best results were obtained when water hyacinth was treated at pH 11.0 and 250°F. Ultrasonic pretreatment of waste activated sludge for 30 minutes resulted in a 64% increase in methane production (Wang, Kuninobu et al. 1999).

Enzymatic hydrolysis using hydrolytic enzymes such as ligninase, cellulose, and hemicellulase, is one promising method. In nature, various microorganisms produce enzymes that function synergistically or act independently (such as fungal and many bacterial cellulases) (Himmel, Ding et al. 2007). The utility cost of enzymatic hydrolysis is low compared to chemical treatment because enzymatic hydrolysis is usually conducted at mild conditions (pH 4.8 and temperature 113-122ºF) and does not cause corrosion problems with equipment (Duff and Murray 1996). However, general lignocelluloses hydrolysis might be advisable unless the economics associated with using purified enzymes improve substantially. The current approach of using enzyme mixtures is still expensive and not economically feasible at the industrial-scale (Angenent 2007; Gusakov, Salanovich et al. 2007).

Bioaugmentation or enhancing biomass concentration is another promising approach to pretreatment; however, technical challenges still need to be overcome. In nature, both bacteria and fungi can produce cellulase for the hydrolysis of lignocellulosic materials (Sun and Cheng 2002). The usual techniques for the biological treatment are to allow growth and enrichment of a cellulolytic and lignolytic microorganism in order to open up the fiber structure and to remove some lignin. The fibers can then be more easily attacked by fermentative and methanogenic microorganisms. The advantages of these biological conversions include low energy requirements and mild environmental conditions (Hobson and Wheatley 1993; Sun and Cheng 2002). An approach to solve this problem could be to harvest robust hydrolytic microorganisms from natural sources and then form a biofilm with concentrated enzymes to biologically hydrolyze lignocellulosic materials. Molecular biology techniques are expected to be part of the future breakthroughs in advancing this promising process.

3.8. Developing mixing strategies and models

This portion of the research project aimed to investigate mixing strategies and to select and design suitable operational parameters to support the HSAD system during the scale-up process.

Mixing operations are encountered widely throughout industry in processes involving physical and chemical change. A combination of physical motion and molecular diffusion causes mixing and heat transfer to occur within any biochemical process (Nagata 1975; NIENOW, Harnby et al. 1997). Failure to provide adequate mixing may result in lower than expected productivity on scale-up. This could result in costly corrections to expensive equipment or even complete failure of a complex process. In 1989, the cost of poor mixing was estimated at $1 billion to $10 billion in the U.S. chemical industry alone.

AD consists of a series of microbiological processes that convert organic compounds to methane and carbon dioxide, and reduce volatile solids by 35% to 60%, depending on operating conditions (Gabriel 1999). Complicated biochemical reactions can take place only based on close contact between anaerobic microorganisms, enzymes, and degradable substrates. When considering HSAD over existing low solids technologies, the digester working volume and effluent contain significantly higher concentrations of solid organic material which equates to increased fluid viscosity. This change in viscosity can decrease mass and heat transfer within the digester. Therefore, the effect of mixing and the mode or method of mixing is a major concern to HSAD design (Karim, Hoffmann et al. 2005). The director of research and development for Philadelphia Mixing Solutions, Dr. Wojciech Wyczalkowski said that "AD mixing has traditionally been a cost factor in industrial processing, and companies want to use it to provide a reliable source of reusable energy to offset rising energy costs."

Hoffmann et al. (2005) concluded that mixing plays several essential roles during AD of sludge, including enhancing substrate contact with the microbial community, improving pH and temperature uniformity, preventing stratification and scum accumulation, facilitating the removal of biogas from the effluent, and aiding in particle size reduction (Hoffmann, Garcia et al. 2008). In Seok et al.'s (2003) opinion, good mixing promotes the efficient transfer of substrates and heat to microorganisms, maintains uniformity in other environmental factors and assures effective use of the entire digester volume by preventing stratification and formation of dead spots, and prevents pockets of VFA from forming (Seok and Komisar 2003). Smith et al. (2005) made a sensitivity analysis of the hydraulic parameters and showed that increasing dead zone volume and bypass flow significantly reduced digester performance and pathogen removal, whereas increased mixing improved pathogen destruction (Smith, Lang et al. 2005).

Types of mixing for AD

There are three general categories of mixing used for slurry-type AD. These types include mechanical (impeller) agitation, gas-recirculation, and slurry-recirculation. Among these types, mechanical agitation has been proved to be the most efficient in terms of energy input and mixing performance (Karim, Klasson et al. 2005). However, due to the mechanical nature of the impeller and design location, maintenance costs often make it more of a disadvantage compared to the other two.

Karim et al (2005; Karim, Hoffmann et al. 2005; Karim, Klasson et al. 2005) studied the effect of these three mixing types on biogas production at bench-scale. Three sets of experiments were

performed using cow manure slurry feed with either 50, 100, or 150 g/L total solids (TS) concentrations (referred in the text as 5%, 10%, and 15% manure slurry). The experiments were conducted at a controlled temperature of 95^{o}F and a hydraulic retention time of 16.2 days, resulting in TS loadings of 3.1, 6.2, and 9.3 g/L d for 5%, 10%, and 15% manure slurry feeds, respectively. Results showed that the unmixed and mixed digesters performed quite similarly when fed with 5% slurry and produced biogas at a rate of 0.84-0.94 L/L d. The methane yield was found to be 0.26-0.28 LCH_4/g volatile solids loaded. However, the effect of mixing and the mode of mixing became important when the digesters were fed thick manure slurry feeds (10% and 15%). Digesters fed with 10% and 15% manure slurry and equipped with external mixing produced about 10-30% more biogas than the unmixed digester. While the mixed digesters produced more biogas than unmixed digesters, digester mixing during start-up was not beneficial, as it resulted in lower pH, performance instability and prolonged start-up time. Mixing using biogas recirculation system was found not to be effective in the case of 15% slurry feed under the experimental conditions studied. Digesters fed with 10% slurry and mixed by slurry recirculation, impeller, and biogas recirculation produced approximately 29%, 22% and 15% more biogas than the unmixed digester, respectively. Deposition of solids inside the digesters was not observed in the case of 5% manure slurry, but it became significant in the case of 10% slurry.

Zábranská et al (2002) compared mechanical mixers with sludge recirculation combined with biogas mixing in a two-stage digester. Mixing in the first stage was by sludge recirculation combined with biogas mixing. Hydraulic dead zones in the digester and short-circuiting reduced the effective hydraulic retention time and thus had a detrimental effect on the digestion efficiency. Results of the experiment with a tracer showed that the installation of biogas recirculation mixing in addition to sludge recirculation increased hydraulic efficiency, but only 75% of the digester volume was utilized. The mean retention time of sludge particles in the first stage was determined to be 5.1 days. The quality of the output sludge from the second stage non-mixed digester indicated an insufficient homogeneity in the tank and a short-circuiting of sludge. The working volume of the second tank was only 40%. The installation of new mechanical mixers (with propellers) in the first stage was planned and a preliminary determination of hydraulic efficiency of those mixers indicated the improvement of the working volume in the first stage to be 82%.

UC-Davis developed the Anaerobic Phased Solids Digester System (APS-Digester) to process high solids organic waste streams (Figure 9). The process of AD is divided into two units. The first unit is a hydrolysis reactor where feedstock is contacted with the recycled effluent of the second unit to produce hydrogen and acetate. The recycled flows have abundant enzymes that can enhance hydrolysis. This reactor contains high solids loading up to 30% TS. Although the recycled flow could enter into the first step hydrolysis reactor, it is difficult to completely mix with feedstock because there is no fluidity in high solids flow when TS is greater than 20%. Since the feedstock was not completely contacted with enzymes, the enhancement of hydrolysis reaction rate is diminished. In their second unit where methanogenic microorganisms dominate, methane was produced. Due to dilute liquid in the second reactor, they use jet mixing to improve the contact of substrate with microorganism. Jet mixing depends on a high pressure pump and a

nozzle to inject high velocity fluid into the digester. Jet mixing is a very effective way to distribute mixing energy while minimizing power input in large diameter reactors. The in-tank components are Fiberglass-Reinforced Plastics (FRP) and/or stainless steel with no moving parts. Conventional pumps are used for the jet motive flow and are located just outside the tanks for ease in maintenance. Compared to alternative mixing technologies, a K_La jet mixing system offers the following advantages. (1) long design life; (2) low installed cost; (3) low maintenance cost; (4) superior process performance; (5) superior corrosion and abrasion resistance.

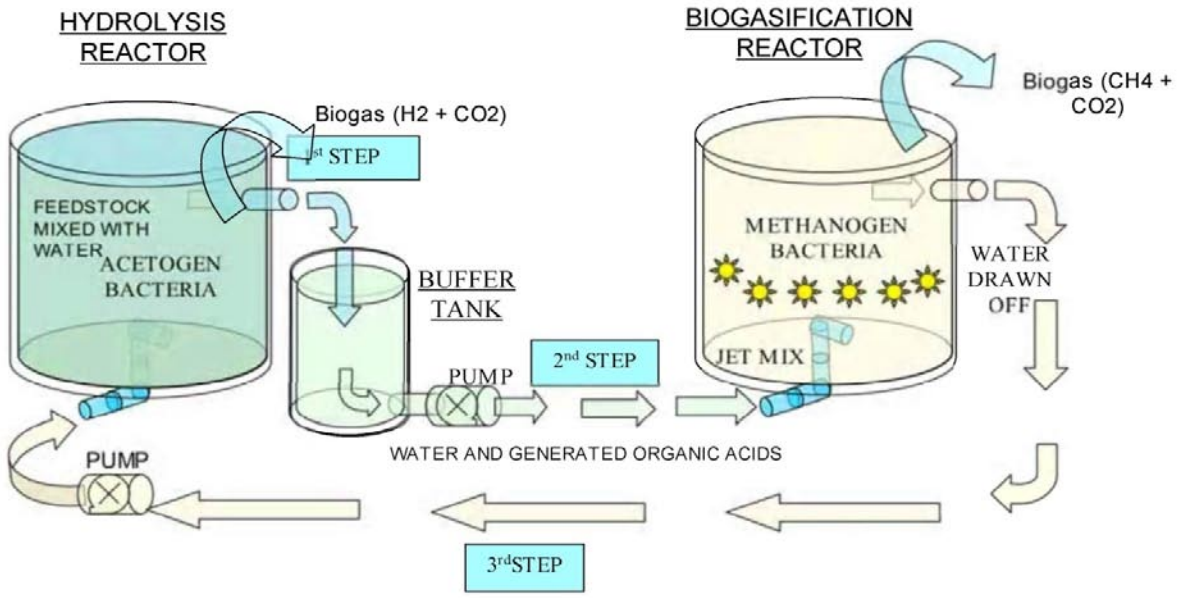

Figure 9 UC-Davis Anaerobic Phased Solids Digester System (APS-Digester)

A Bio-funnel reactor (Figure 10) is an expending, radial-overflow digester for continuous high solids loading (Nijaguna 2002). It is designed to handle both dilute liquids (solid content below 10%) as well as farm wastes (solid content 25 to 30%). The digester is continuously fed through a hydraulic cylinder which presses the fresh material into the digester and up through a funnel. The geometry of the design induces a natural and gentle mixing as the material passes through the funnel and outer chamber. The material splits apart as a result of expanding movement through the digester. This geometry also eliminates the problem of floating scum formation. The system is self-seeding. An integrated gate valve serves as an opening for seeding. The residence time is about 10 days and yields of over $1m^3/m^3$ of biogas/day can be expected.

Research on HSAD has been conducted at the National Renewable Energy Laboratory and found that high solids slurries (TS>20%) are very viscous and resemble solid materials more closely than typical fluid (NREL) (Rivard, Duff et al. 1998). NREL postulates that conventional mixers such as those employed in continuous stirred-tank reactor (CSTR) systems do not ensure homogeneity within the reactor, and problems develop in providing adequate dispersion of substrate, intermediates and microorganisms while minimizing power requirements. Therefore, they designed a slow-speed, tine-blade agitation in order to enhance microbial film formation in the digester. No significant difference in fermentation performance was observed between

agitator speeds of 1 and 25 RPM (Rivard 1993). Figure 11 shows their efforts to scale-up to a pilot-scale system.

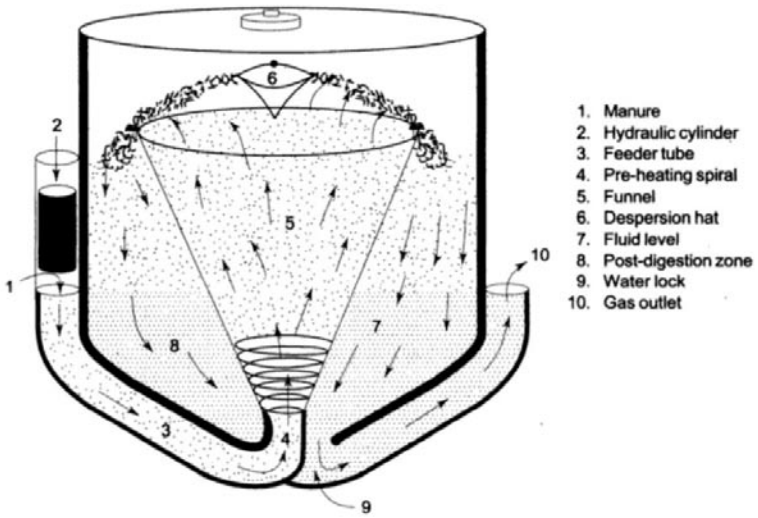

Figure 10 Biofunnel Reactor

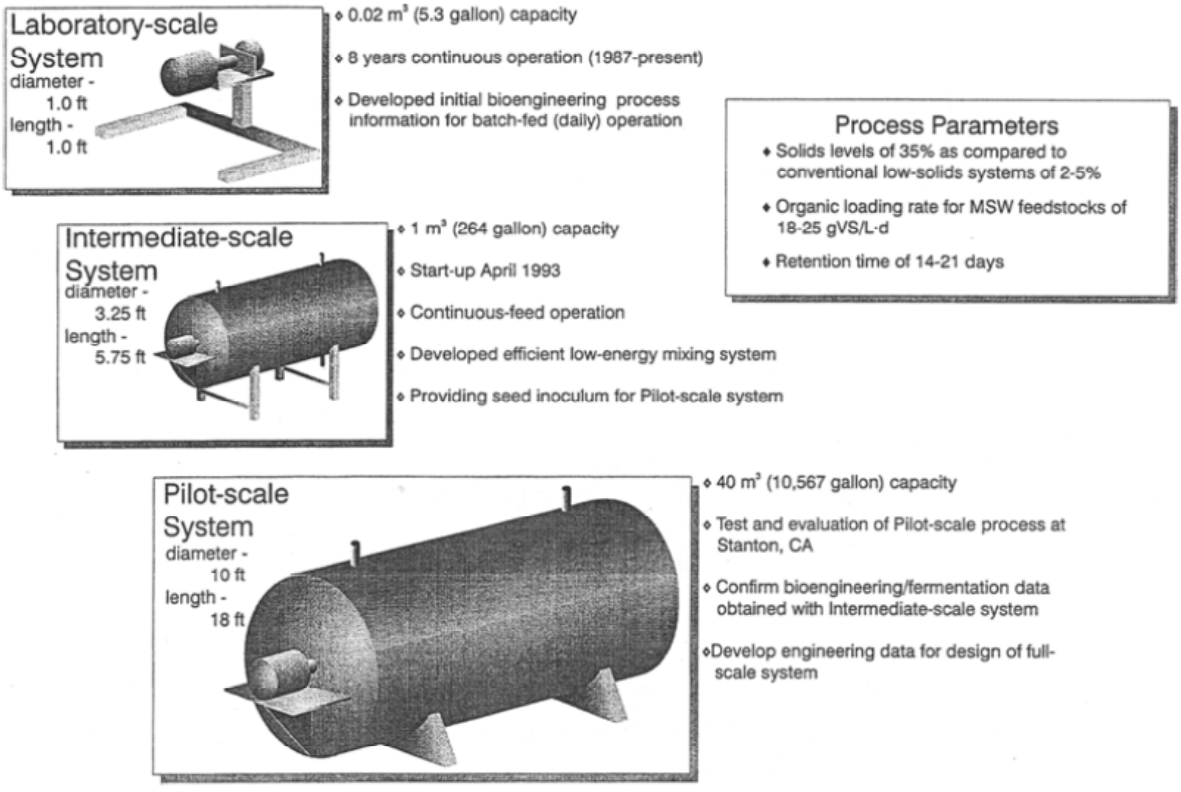

Figure 11 Scale-up efforts detailing laboratory-, intermediate-, and pilot-scale system dimensions and operational parameters

Rivard et al. (1995) researched actual horsepower requirements of a mechanically-mixed HSAD system. A 20 L bench-scale, HSAD at NREL was used to evaluate the minimum required horsepower for mixing high solids sludge. The data shown in Figure 12 indicate that a minimum of 100 psi was required to maintain motor rotation and overcome the frictional losses of the digester shaft seal.

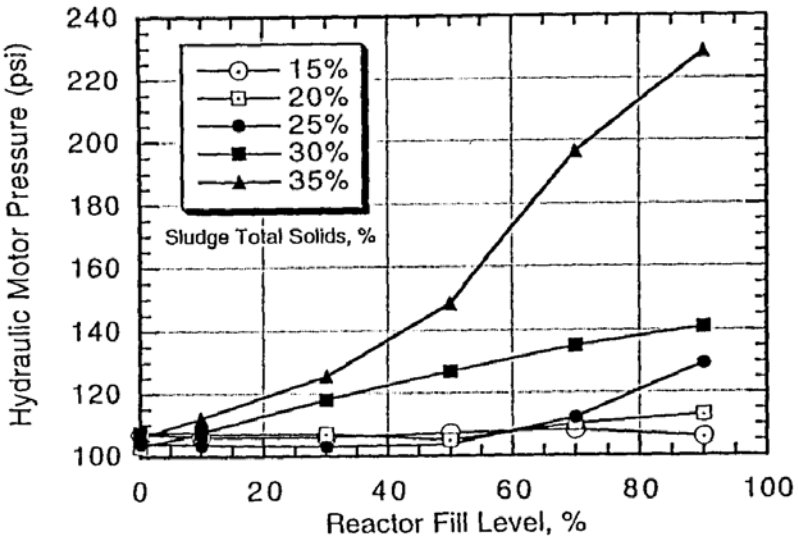

Figure 12 Effect of increasing sludge total solids and digester fill level on mixing horsepower (expressed as hydraulic motor pressure). The study was conducted with the HB12 roller stator motor at 1 rpm

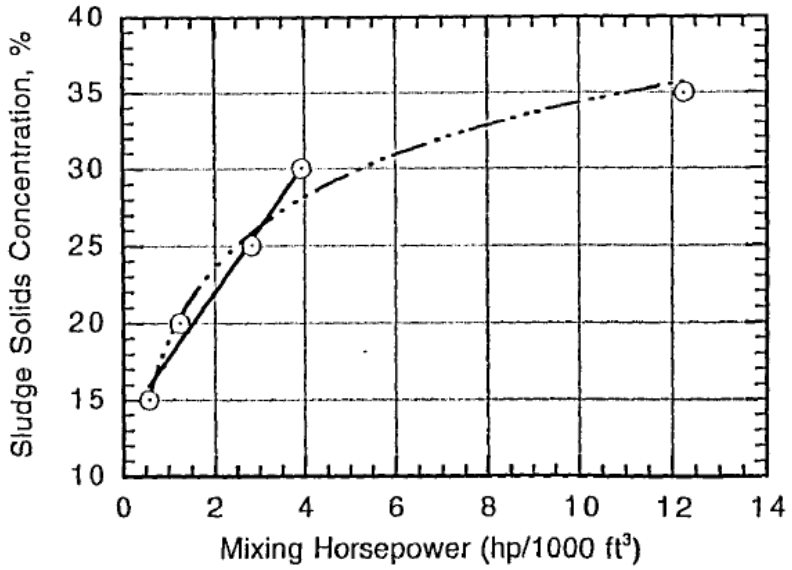

Figure 13 Effects of increasing sludge total solids on required mixing horsepower for the 90% digester fill level

Increasing the solids concentration of the sludge within the 15-25% sludge solids range did not significantly alter the required hydraulic pressure for mixing. However, at sludge solids levels of 30 and 35%, dramatic increases in hydraulic pressure were required to maintain mixing in the digester. Digester fill level also demonstrated an effect on required horsepower for the 30 and 35% sludge solids levels. The data for 90% fill volume were used to predict the effects of sludge solids on mixing horsepower as given in units of HP/1000 ft^3. These data are shown in Figure 13 and indicate that two relationships may be inferred. Data for the first four solids levels (i.e., 15-30%) conform to a linear regression (R=0.989). However, all five data points were best described using an exponential curve (Figure 13 dashed line).

Data in Table 3 compares actual mixing horsepower requirements for the intermediate-scale, high solids digester system with those predicted, by extrapolating the low solids data for Mixco and RefCoM. Additionally, the linear relationship of higher sludge total solids on minimum mixing horsepower as determined using the bench-scale NREL high-solids digester (Figure 13 solid line) was also used to predict mixing horsepower for the intermediate-scale digester system. In general, the mixing horsepower requirements for the intermediate-scale, high solids digesters are best approximated by the data developed from the bench-scale system. The actual horsepower required for intermediate-scale, high solids mixing was substantially less than that predicted by extrapolating low solids data from either Mixco or RefCoM.

Table 3 Analysis of Mixing Horsepower Requirements for the NREL High-Solid Intermediate-Scale Digester System

Sludge solids, %	Sludge volume, L	Motor pressure, psi	Motor rpm	Mixing horsepower, HP/1000ft^3				
				Mixco	RefCoM	NREL	Actual	Actual, W/m^3
19.0	400	175	1	9.5	5.43	1.32	1.42	37.4
19.0	500	225	1	9.5	5.43	1.32	1.48	38.98
21.0	625	300	1	10.5	5.84	1.78	1.57	41.35
26.5	300	275	1	13.3	6.95	3.07	3.02	79.53
30.0	312	355	1	15.0	7.65	3.88	3.74	98.49

Williams et al. (2004) of the Animal and Poultry Waste Management center, North Carolina State University cooperated with ORBIT Company to evaluate a HSAD system. There were two operating digesters. The first digester processed human waste from Fort Bragg and began operating in April, 2003. This HSAD was constructed on ORBIT's Timber Ridge Farms. On this site, two digesters are being fed using the same system. The design was implemented by connecting two digesters to one ribbon blender. Several unit processes can be eliminated, including the entire feed screw system and surge bins. The second reactor had a feeding capacity of up to 3 tons/day and was fed with a mixture of swine manure solids and cardboard. In this system, manure solids would be fed directly from the ribbon blender to the digester. A single ribbon blender discharge screw would be needed for this process—not the series of screws and

bins constructed at Timber Ridge Farms. Additional unit processes that would be eliminated for the stand-alone system include the grinder and the solids separator.

Figure 14 and Figure 15 show the ORBIT pilot digester and diagram. The ORBIT HSAD system utilizes a closed vessel for the conversion of swine waste organics to methane. For economy, this project has been paired with the Super Soil Systems project. The Super Soil Systems project will provide solids separation and feedstock generation for the HSAD project. Treated liquids will be used to generate a liquid fertilizer product, and final digester sludge will be used by Super Soil Systems to generate a value-added soil amendment.

Figure 14 ORBIT pilot digester

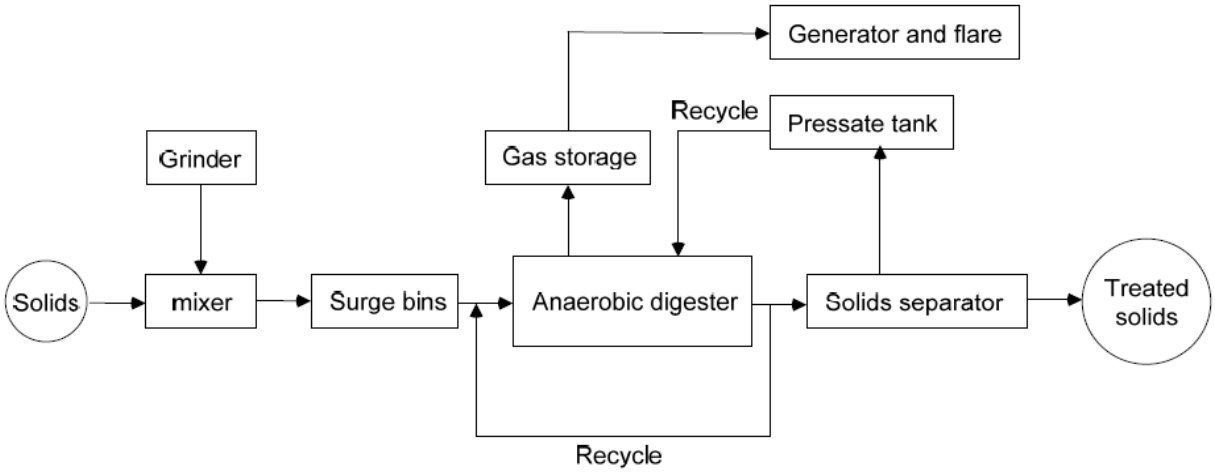

Figure 15 ORBIT flow diagram

The DRANCO, Kompogas, Linde-BRV and Valorga AD systems are examples of Single Stage High Solids (SSHS) processes. All four systems consist of a single-stage thermophilic reactor (mesophilic in some Valorga plants) with an HRT of 14-20 days (Verma 2002). There are typical mixing modes applied in these four commercial-scale systems. In the DRANCO digester (Figure 16), the feed is introduced from the top and digested matter is extracted from the bottom. There is no mixing apart from that occurring due to downward plug-flow of the waste. Part of the extracted matter is reintroduced with the new feed while the rest is de-watered to produce the compost product.

Figure 16 Dranco solids digester installation at Aarburg, Switzerland

The Kompogas digester (Figure 17) works similarly, except the movement takes place in plug flow in a horizontally disposed cylindrical digester. Mixing is accomplished by the use of an agitator. The process maintains the solids concentration at about 23% TS. At solids content lower than 23%, the heavy fraction such as sand and glass can sink and accumulate at the bottom; higher TS concentrations impede the flow of materials (Vandeviviere, Baere et al. 2002; Zaher, Cheong et al. 2007) .

Figure 17 Installation at Niederuzwil, Switzerland, Kompogas system

The Linde-BRV dry digestion system of Lemgo, Germany is similar to the Kompogas system. After solids separation only the liquid fraction is recycled which leads to a lower inoculation rate and, hence, a longer HRT. As shown in Figure 18, the process is not a plug-flow system because feedstock mixing is more pronounced with the transverse paddles and the walking floor.

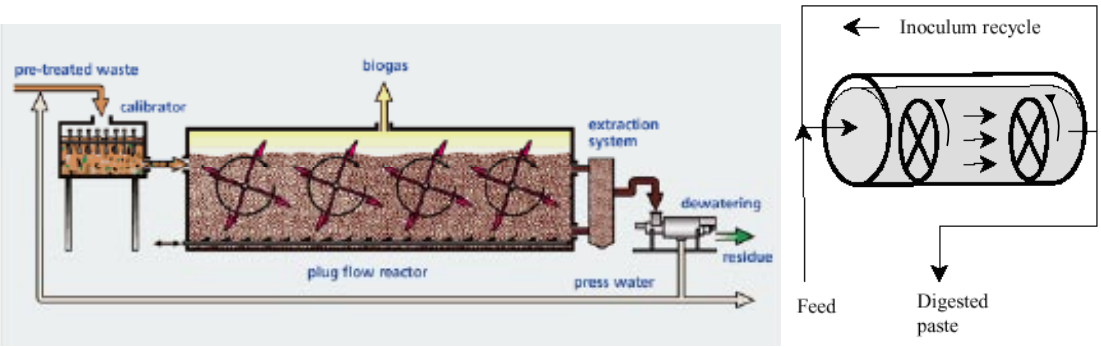

Figure 18 Linde-BRV solids digestion system

The design of the Valorga system is unique. The digester is a vertical cylindrical reactor divided by a partial vertical wall in the center (Figure 19). Feed enters through an inlet near the bottom of the reactor and slowly moves around the vertical plate until it is discharged through an outlet that is located opposite to the inlet. Re-circulated biogas is injected through a network of injectors at the bottom of the reactor and the rising bubbles result in pneumatic mixing of the slurry. The injectors require regular maintenance, as they are prone to clogging.

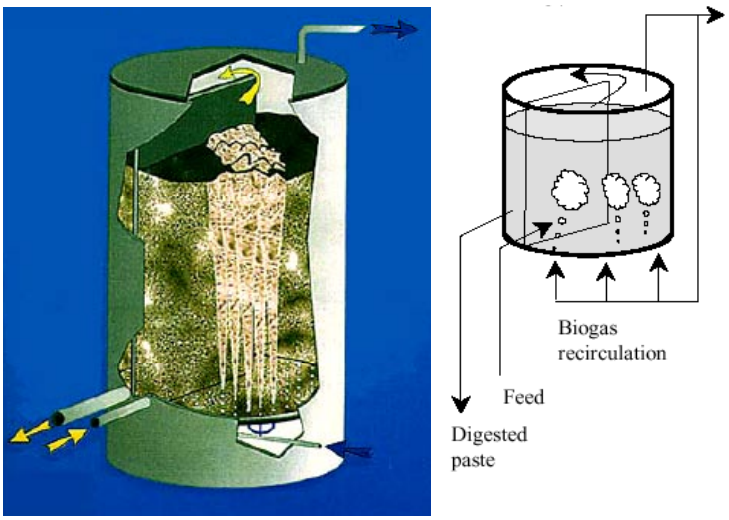

Figure 19 Compressed biogas mixing of the Valorga System

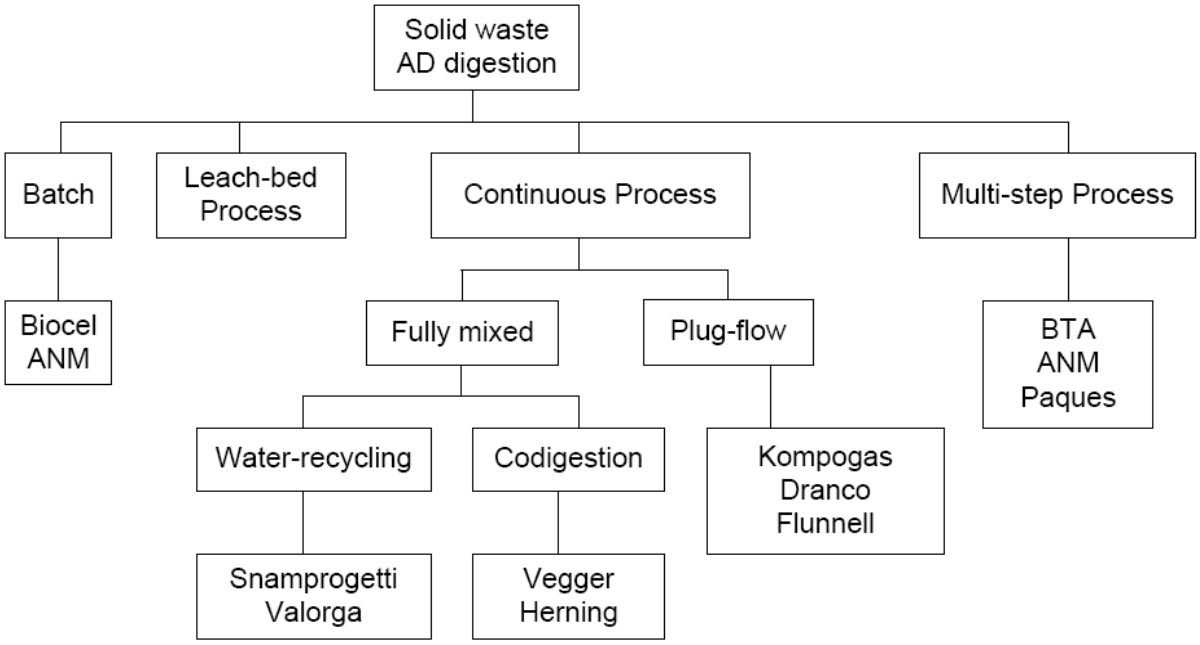

Figure 20 Classification of an anaerobic solid waste digestion system

As shown here, there is a wide variety of configurations for anaerobic treatment of solid wastes at the industrial-scale. One way to classify these reactor systems is depicted in Figure 20 (Angelidaki, Ellegaard et al. 2003). The batch systems can be considered as accelerated landfill systems. These systems are simple and comparatively cheap. An alternative to batch digestion is the leaching bed process, where the leachate from the base of the digester is exchanged between established and new batches to facilitate start up, inoculation, and removal of VFA. This concept has also been described as Sequential Batch Anaerobic Composting (SEBAC).

The continuously operating systems can be divided into completely mixed and plug-flow systems. The completely mixed systems can again be classified as systems based on recirculation of process water for dilution of the incoming MSW and in systems based on the co-digestion concept. Co-digestion is especially well established in Denmark. Several systems are operating on the multi-stage digestion concept. However, one-stage systems are much simpler and cheaper and therefore, considerably more widespread.

4. Project Outcomes

4.1. Objective 1: Select feedstock and test this system at the bench-scale

4.1.1. Feedstock assessment

The biogas and power potential from the bioconversion of different biomass feedstocks were evaluated and used as references to benchmark the economic value of this system. The results for the different feedstocks are detailed in Appendix 1. The underutilized organic waste is shown in Figure 21.

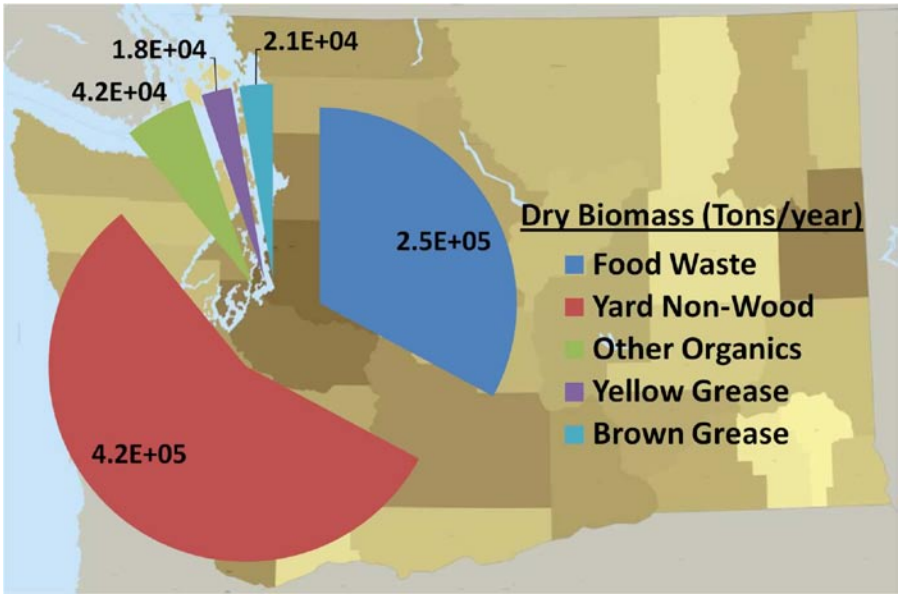

Figure 21 Underutilized organic waste

Food waste and dairy manure feedstocks are the largest quantities that are produced year round. The estimated potential electrical power generation from methane produced by this system from food waste in Washington State is 730 million kWh. The methane and power that can be produced from food waste and dairy manure constitute around 50% of the total energy production utilizing all digestible wastes.

4.1.2. Process kinetics

Digesting high solids concentrations without continuous seeding of the reactors by either recycling of solid wastes (existing systems) or augmentation (this system) was not possible for dairy manure (even with its alkalinity and buffer capacity) or food waste. As shown in Figure 22, complete inhibition of the HSAD system was reached in 10 days for both wastes. At high solids feed concentrations above 15%, the accumulation of volatile fatty acids (VFA) and the release of ammonia reach high inhibitory levels to methanogens. Most of the biogas produced was carbon dioxide. Accumulation of VFA also leads to a drop in pH. The pH drop could be recovered in the case of food waste by adding alkaline solutions (such as NaOH); however, the batch system still soured due to insufficient increase in pH as required. This can be referred to as inhibition

due to the acids accumulation and ammonia. Manure alkalinity was too high to resist pH drop but the process inhibited due to accumulation of ammonia.

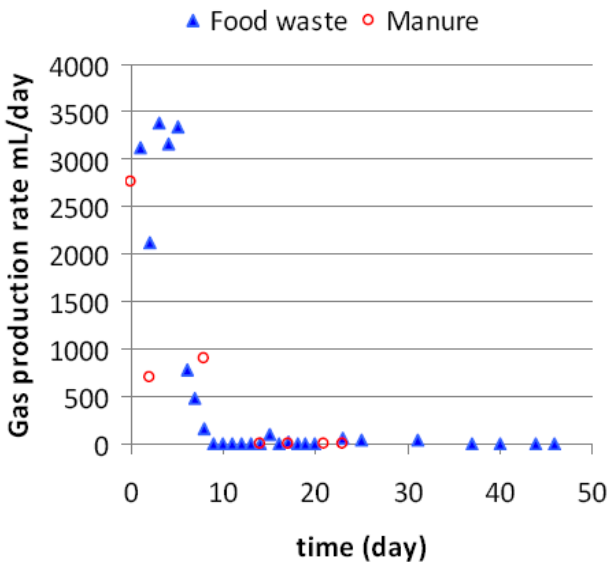

Figure 22 Inhibition to HSAD without continuous seeding

The treatment mechanism was investigated by studying the effect of seeding and co-digestion in reducing such inhibition. As illustrated in Appendix 2, different anaerobic inoculums were suitable for the degradation of manure after dilution, but the most important behavior of manure anaerobic degradation is presented in Figure 23.

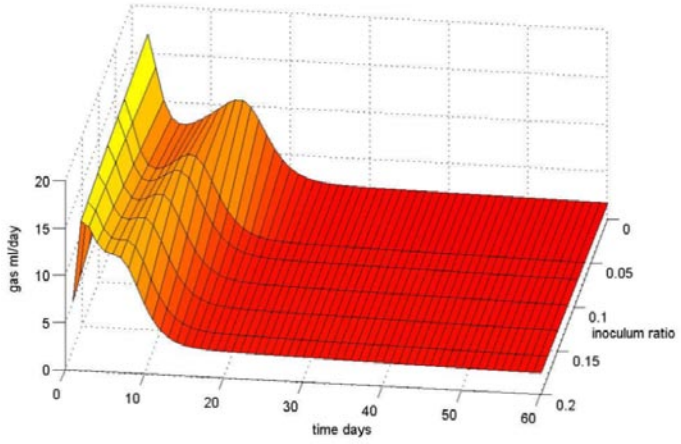

Figure 23 Effect of the seed to substrate ratio on manure degradation

Notably, increasing the inoculum concentration improved the degradation within the time frame of the short hydraulic retention times (HRT) and had no significant effect on longer HRT. The manure has a high fiber content that is not easily digestible and would not be improved in HSAD even with continuous seeding. ***Thus, the most effective system would leach the easily degradable portion as suggested in this system and use a high rate digester with increased seed concentration, as suggested for the seed reactor, for improved methane production.***

When considering HSAD application to the degradable fraction of MSW (food waste) the main barrier is rapid acidification. Such inhibition factors are avoidable using co-digestion. In Appendix 4, co-digestion in an experiment of food waste with diluted manure was performed to calibrate the GISCOD model parameters. Since the GISCOD uses the transformer procedure in Appendix 3, it was possible to model the hydrolysis of each waste separately. Hydrolysis kinetics of diluted manure and food waste were estimated by fitting the biogas production data. The model predictions were in agreement with experimental measurement as shown for biogas production and pH in Figure 24. The GISCOD model applied the ADM1 parameters that are listed in Appendix 5. The pH was in the normal operating range of the anaerobic digestion process due the alkalinity of the manure. The first order rates for hydrolysis of carbohydrates, proteins and lipids were 5.22, 1.86 and 1.24 d^{-1} for food waste and 0.019, 0.025, 0.022 d^{-1} for manure. The low hydrolysis rates confirm the conclusion from the previous experiments that it is not economical to design the high solids chamber for manure digestion since the reactor would need to be excessively large to complete a large conversion. Again leaching the easily degradable portion and treating it in a high rate digester would be the most practical solution.

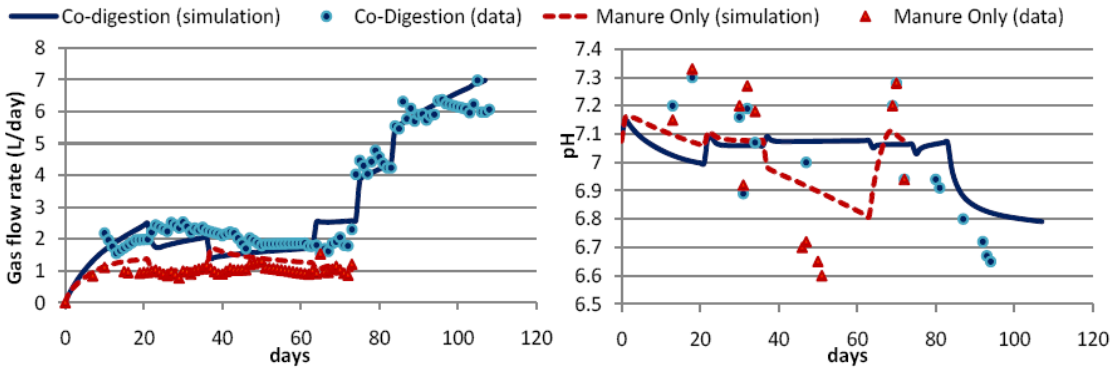

Figure 24 Comparison of simulated and measured biogas production (left) and pH (right) after calibration of the hydrolysis parameters

The seed chambers were validated experimentally by digesting the leachate from manure and the extracted liquids from food waste. The steady state biogas production results were used to estimate the fraction parameters added to ADM1 to describe the distribution of solids along the reactor. The fraction parameters f_b and f_s were estimated to be 0.68 and 0.48, respectively, which represent fractions of anaerobic microorganisms and solid substrate leaving each compartment of the seed chamber model. The fraction parameters were the same within two digits in both manure and liquid food waste digesters. Both digesters were physically identical,

and the same leachate recycle rate was applied in both experiments. Therefore, the up-flow velocity was the main factor that influenced the solids distribution (i.e. solids retention) in both digesters. Using the estimated fraction parameters, the model simulations were in agreement with experimental measurements when applying the ADM1 process parameters listed in Appendix 5.

In the seed chamber experiment with food waste, simulated seed chamber model outputs were compared with experimental results in Figure 25. After a starvation period of the initial inoculum, the biogas production started the second day (day 41) after feeding the digester. The biogas production was kept steady at 0.6 L/day by applying 100 mL/day feed for 4 weeks.

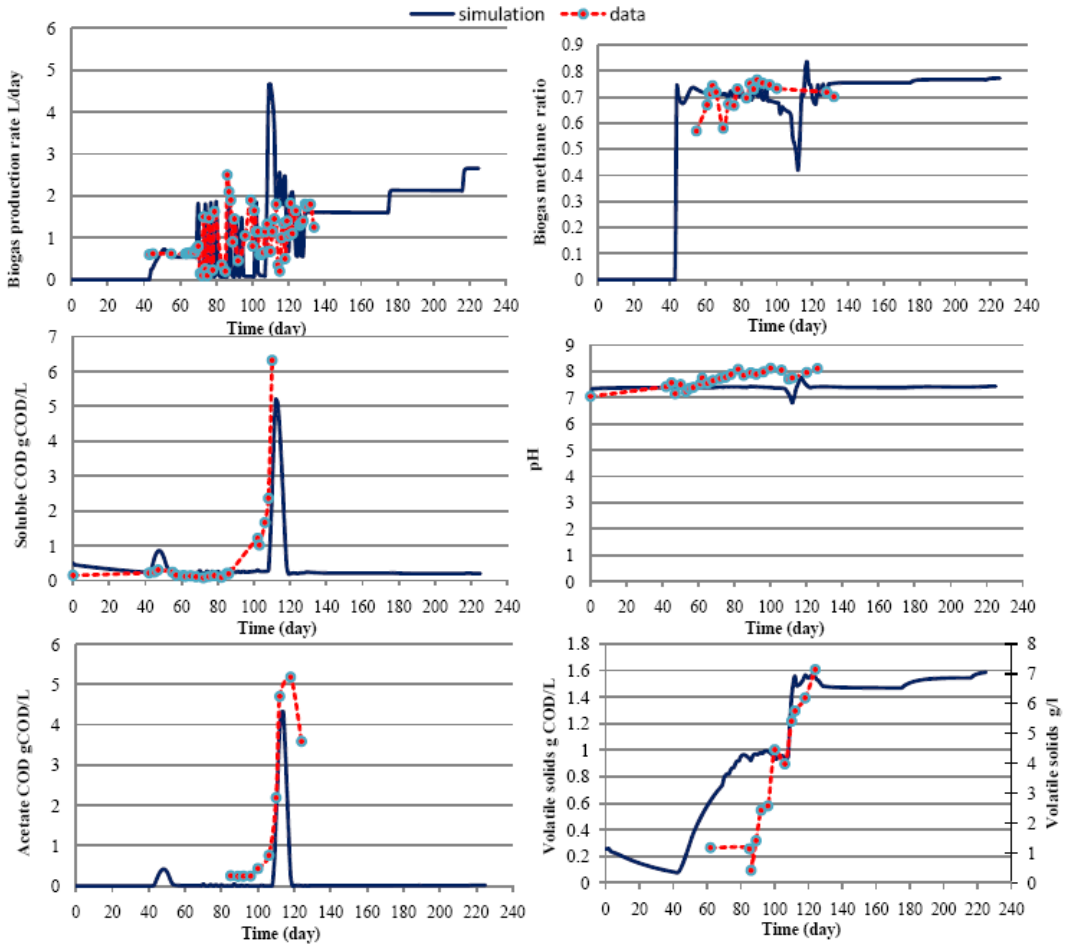

Figure 25 Model validation and extrapolation of the seed chamber with food waste

More dynamics were produced afterwards by intermittent feed twice a week for 9 weeks. Intermittent feeding produced spikes of biogas production as dynamics for model validation. The seed chamber was robust and recovered after each spike load. One intermediate leak event started on day 107 and was accompanied with an increased feed rate of 1000 mL/day for 4 subsequent days to maintain the digester liquid volume. Such overload led to a rapid VFA accumulation as shown in the COD and acetate results. The new system rapidly recovered from

the overload event after the leak was stopped and an intermittent feeding of 300 mL every 3 days was made. Extrapolating the seed chamber performance at higher steady state flow rates of 300, 400, and 500 mL/day (corresponding to 7, 5 and 4 HRT, respectively) showed that the methane ratio was steady around 70% with correspondingly higher biogas production rates. The pH was stable slightly above 7 and quickly recovered after the overload event. The seed chamber design was therefore robust enough to handle intermittent feeding and shock loads. Anaerobic microorganism seed production can be assessed by comparing VS simulation results in g COD/L units with measurements in g/L units. Both the simulation and measurements of VS have the same trend. The VS concentration increased to 7 g/l with the increased volumetric feed rate. ***The seed production from food waste could reach only 0.7% compared to the set target in the project proposal of 1% VS.*** The VS measurements in mass units was around 5 times the simulation in COD units which indicates that the washed out solids were mainly stabilized and the low COD/mass ratio was mainly related to the simulated active biomass. The activity in the anaerobic microorganisms was also confirmed by the microscopic analysis described later.

In the seed chamber experiment with screened manure, the simulated seed chamber model outputs were compared with the experimental results in Figure 26. The experiment followed the same protocol applied to the food waste experiment and the model simulation was in positive agreement with the measurement.

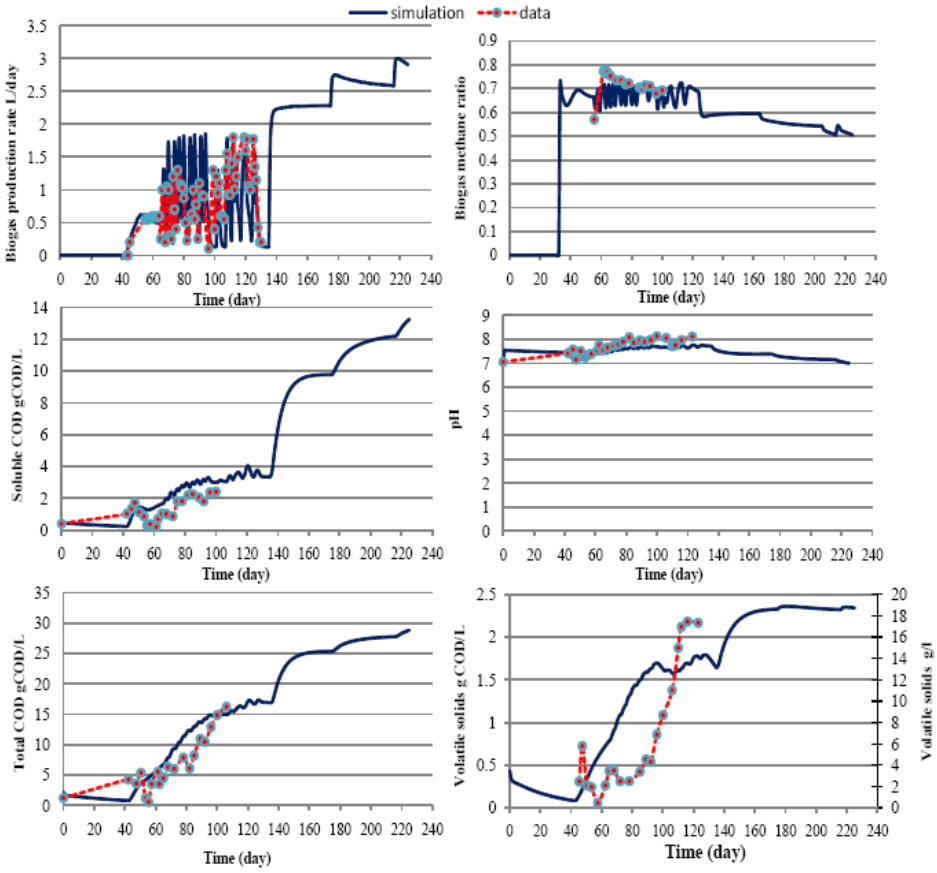

Figure 26 Model validation and extrapolation of the seed chamber experiment with manure

However, there were some differences in comparing both experiments. The applied volumetric loading was slightly less than the food waste experiment but the COD load was much higher. The pH was stable due to the high alkalinity in manure. Particulate and soluble COD accumulated after day 100, corresponding to feed rates higher than 200 ml/day (10 day HRT). ***From the VS results, the seed reactor application to the screened manure would ultimately produce 2% VS***. However, the VS measurement in g/L was 8 times the simulated VS in g COD/L. The latter corresponds mainly to the active anaerobic microorganism populations, which indicates that the active anaerobic seed was not as high as in the case of the food waste. Essentially, there would not be enough anaerobic seed concentration to continuously seed the high solids chamber. The high solids chamber would optimally be used as a leaching compartment and liquid manure would be treated in a high rate digester such as the seed chamber. From the total COD and VS results, 60% COD and 50% VS removal is achieved at day 100 (10 day HRT). The continuous leaching of manure produces washed fibers that can be recycled as bedding material on the farm.

The pictures in Figure 27 were taken using the confocal microscope and SYTO 9 staining to illustrate the difference between the seed produced in the liquid food waste and manure seed chambers. With SYTO 9 staining, living anaerobic microorganisms (with intact cell membranes) appear fluorescent green, whereas dead cells (with damaged membranes) appear fluorescent red. The seed from the chamber digesting liquid food waste is shown in picture (a) as dispersed flocks of active anaerobic microorganisms.

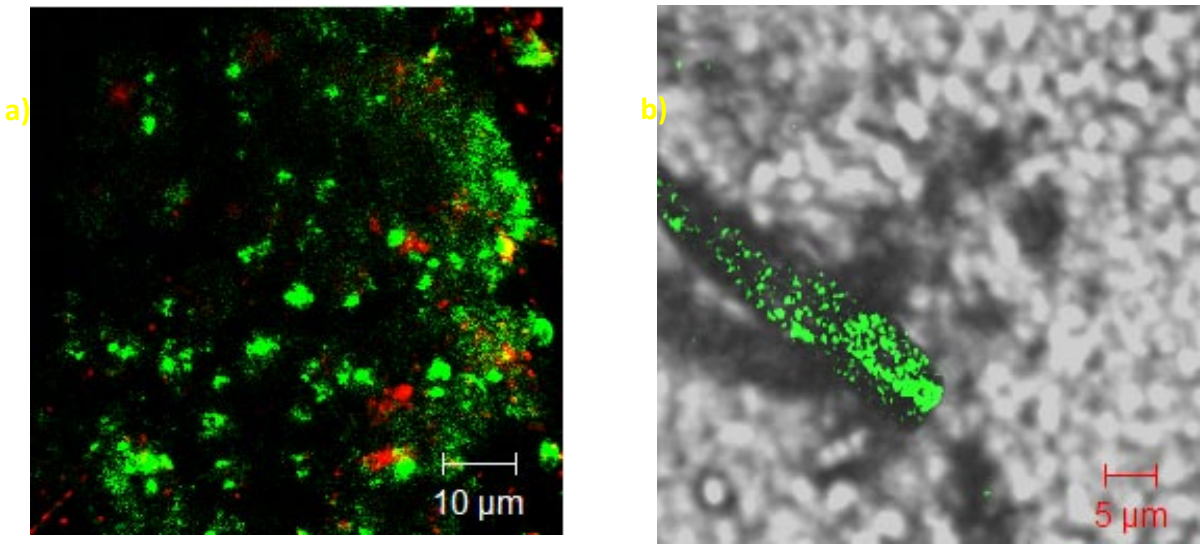

Figure 27 Confocal microscope laser scanning of the anaerobic seed samples: a) from the seed chamber digesting food waste and b) from the seed chamber digesting screened manure

The seed from the chamber digesting liquid manure is shown in picture (b) as attached growth to small fiber pieces that escape the leaching screen. The ratio of active anaerobic seed to the VS (fibers) in the case of manure is much less compared to the case of dispersed growth in the liquid

food waste. The detected morphology and the comparison of simulation and experimental results confirm that the active portion of the seed produced from manure was low compared to that of the seed produced from food waste. Considering the low hydrolysis rate of the manure fiber, the optimal manure treatment system would consider manure digestion only in the seed chamber (high rate digester). The high solids chamber is not needed and could be designed as a leaching compartment only. Therefore, manure was not considered further for testing this system. Recycling the seed in the attached form to small fibers as shown in Figure 27 would not be as efficient as dispersed seed from food waste due to less contact with the solid substrate in the high solids chamber.

4.2. Objective 2: Develop process models

4.2.1. Prototyping of the system

The simulation and experimental data results for gas production from the integrated system lab-experiment are shown in Figure 28 for the high solids chamber and Figure 29 for the seed chamber. The integrated model simulation results were generally in agreement with the observed experiment dynamics without any extensive model calibration. ***Thus, the integrated system model was validated and can be used to scale-up the process.*** Only the steady state results of biogas production rate from the high solids chamber from day 25 to day 45 were used to estimate its effective volume. The estimated high solids chamber effective volume was 2.9 L. ***Compared to the applied 3 L experimental volume, the high solids chamber effective volume was 97%, which was greater than the target of 90%.*** Beginning at day 57 of the integrated system bench-scale experiment, dynamics were imposed on the digester by intermittent feeding and gradual overload. The high solids chamber pH was dropped below 6 by feeding 200 g of the solids waste for 3 subsequent days from day 82 to 85. During this overload, VFAs were accumulating as shown from the acetate and propionate results in Figure 28.

VFA accumulation caused a drop in the pH, biogas production, and methane content. This system recovered from the overload conditions in two weeks and the seed chamber was minimally affected and continued to produce biogas during the entire overload event. The VFA rapidly decreased after stopping the solid waste feed and maintaining the seed recycle for two weeks. ***This system does not suffer from acidification when maintaining the correct feed rate and it is robust enough to recover quickly from overload conditions***. Comparing the TS and VS simulation results in COD units and experimental results in mass units, it can be seen that the COD difference between effluent TS and VS is larger than the mass difference. VS were calculated by summing the simulated concentrations of all particulate substrates and anaerobic microorganisms while TS was calculated by adding the simulated inert particulate fraction. ***Thus, the effluent solids are mainly inert and non-biodegradable and are significantly stabilized in this new system.***

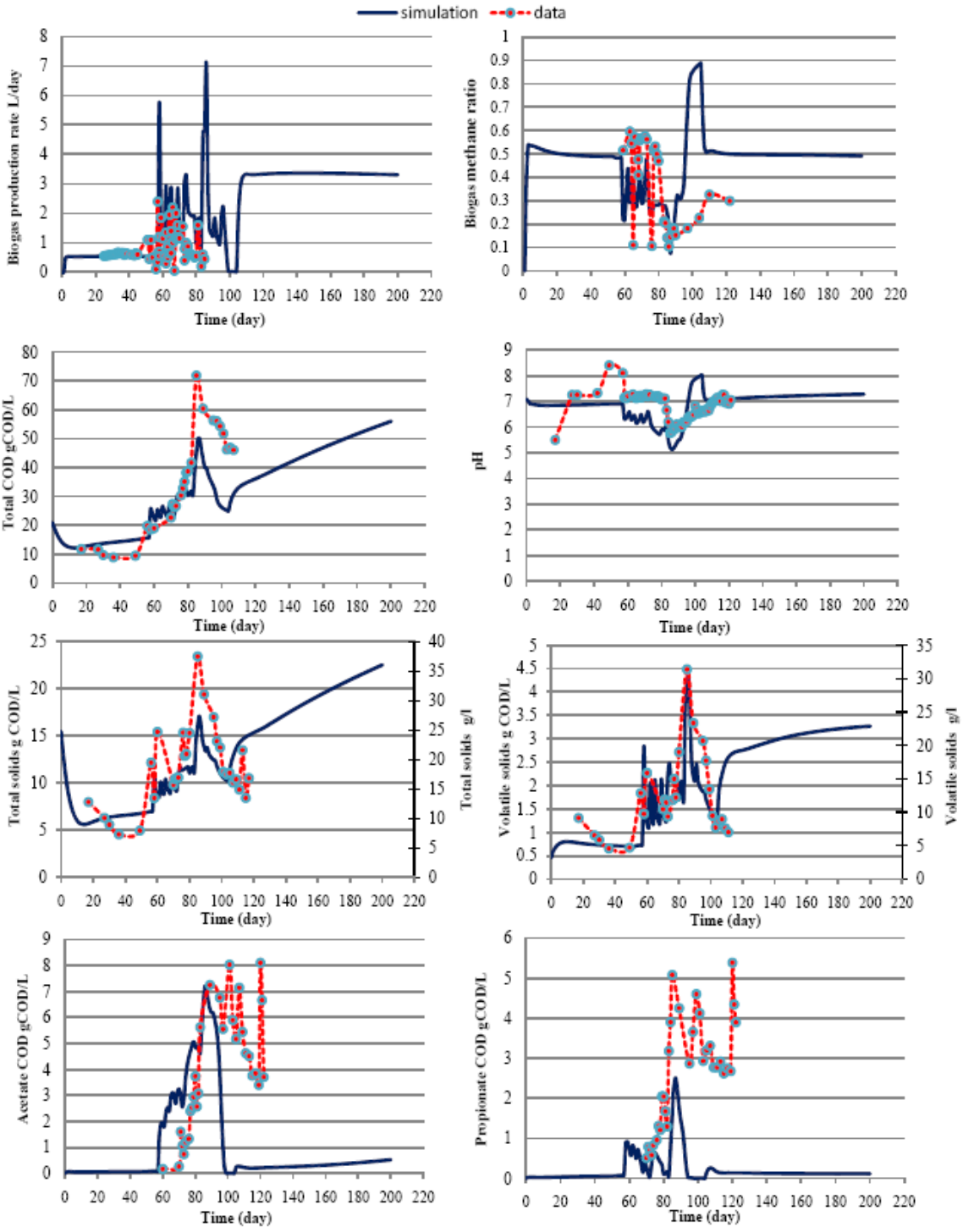

Figure 28 Validation of the virtual and bench-scale prototypes of this system comparing the solids digester simulated output with experimental data of solid food waste digestion

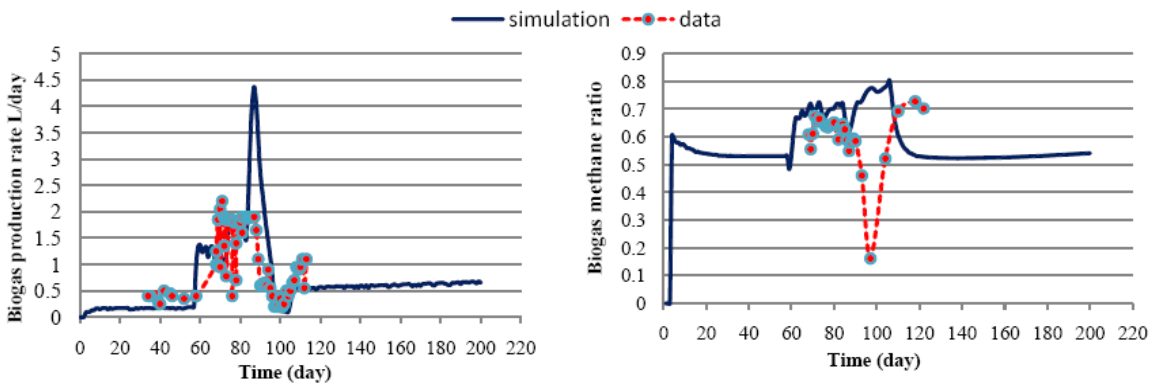

Figure 29 Validation of the seed chamber biogas output during bench-scale experimentation

The confocal laser-scanning microscope image of a solid sample, from the high solids chamber, is shown in Figure 30. The SYTO 9 staining makes the living anaerobic microorganisms (with intact cell membranes) appear florescent green. It can be clearly seen that most of the living microorganisms are attached to the particulate solid substrate.

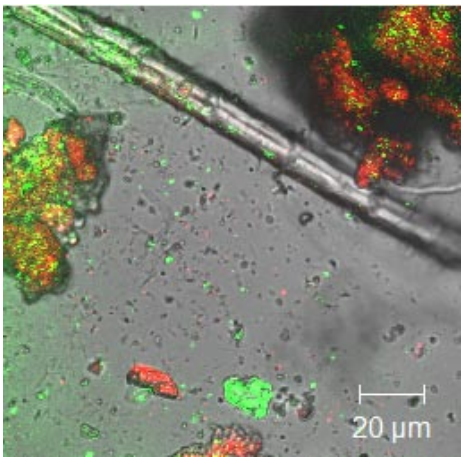

Figure 30 Confocal scanning laser microscope image of solid waste sample from the high solids chamber after SYTO 9 staining procedure

This indicates that in this system, the anaerobic seed will be retained in the high solids chamber and not washed out with the leachate. This observation also explains why the existing conventional HSAD systems should use an efficient blender ahead of the solid digester. The active anaerobic seed would be immobilized on the recycled solids and the blender would efficiently mix the recycle flows with the feed to increase anaerobic seed contact with new substrates. ***Another advantage of this system is that the recycled seed is mainly liquid, which diffuses and blends easily with the high solids chamber content, and no blending chamber is needed ahead of the reactor***.

4.2.2. Optimized performance of the system

The optimization results that were used to scale-up and determine the design parameters of this system are listed in Table 4.

Table 4 Comparison of HSAD systems

Design/performance parameter	Optimization		Typical HSAD w/ solid recycle Kompogas design
	This system with augmentation	Conventional HSAD w/ solid recycle	
MSW Feedstock:	Kitchen waste	Kitchen waste	Kitchen waste
Total solids g/L	154	154	
Total COD g/L	200	200	
Optimization target m^3 CH_4/ton/day	39.7	39.7	
Optimization results for feed rate of 1 ton/day:			
Methane production rate m^3 CH_4/day	38	38	
Methane production efficiency	96%	96%	
Solids digester volume m^3	17	25	38.3*
Solids recycle m^3/day	--	4	9**
Liquid recycle m^3/day	4	--	--
Solids blending chamber m^3	--	5	10
Seed chamber m^3	18	--	--
Performance parameters			
Solids digester loading rate ton/m^3/day	0.06	0.04	0.026*
Biogas production rate m^3/ m^3/day	4.62	3	2.8*
Methane production rate m^3/ m^3/day	2.28	1.52	
COD removal %	47.33	45.38	
Solids removal %	70.31	69.46	50-70*
Potential fertilizer:			
kgN/ton waste	2.10	--	--
kgP/ton waste	3.72	--	--
Capital cost $/ton including post composting	18.9***	27.8***	48.6*

** according to reported performance of typical installation of Kompogas system (Braunschweig, Germany)*
*** according to reported performance of typical installation of Dranco system (Aarburg, Switzerland)*
**** predicted on the scale of the solid reactor volumes compared to the existing system*

This system has a smaller high solids chamber compared to existing systems. To have a common basis for comparison, the volumes of the digesters were optimized by assuming a reasonable biogas production target. The optimized systems achieved the same 96% efficiency compared to the target methane production. Both loading rate and methane production rate per unit volume of solids digesters were higher in this system. Other advantages include the potential for recovering nutrients from the leachate recycle loop. The potential environmental impact is reduced due to

the nutrient recovery and lessened waste biogas emissions from the closed leachate recycle loop. Existing systems seed the digester by blending recycled solids with the feed, which often releases odorous and toxic GHG. This system operates at mesophilic temperatures and can be controlled efficiently in both chambers by heating the leachate recycle loop. The methane production rate was similar to varous thermophilic systems (i.e. UC Davis) even though this system utilizes significantly less high solids chamber volume.

4.2.3. System economics

The economic analysis of this system and the potential savings are listed in Table 5. The costs and savings were normalized to the kWh unit.

Table 5 Economic analysis of this system

Cost and economic benchmarks	(1) This system with augmentation	(2) Conventional HSAD system with solids recycle	Annual Savings of this system	
			US$/KWh	%
Capital cost including post composting $/ton	18.89	27.78		
Electricity production rate kWh/ton	113.37	113.37		
Capital cost of solids digester including post composting $/kWh	0.16662654	0.245039029	0.078412489	32%
Cost of the seed chamber assuming similar capital cost as solid reactors $/kWh	0.16662654		-0.16662654	
Cost of solids recycle $/m^3		0.043		
Cost $/m^3 of liquid recycle	0.029			
Recycling Recirculation cost $/kWh	0.0010165	0.0015172	0.0005007	33%
Mixing cost solids digester $/m^3	4.94	4.94		
Mixing cost solids digester $/kWh	0.7407821	1.0893855	0.3486034	32%
Mixing cost for recycled solids blending $/kWh		0.2178771	0.2178771	100%
Total cost production $/kWh	**1.0750517**	**1.5538188**	**0.4787671**	**31%**
kWh from food waste	157,000,000	157,000,000		
Total cost utilizing all food waste (annual savings)	**$168,783,121**	**$243,949,552**	**$75,166,430**	**31%**

4.3. Objective 3: Enhance hydrolysis of cellulosic feedstocks

4.3.1. Alkaline/peroxide and thermal pretreatment

Some organic materials discharged from the acidic environment of the animal rumen might be resistant to the commonly used acid hydrolysis method. The alkaline condition is hypothesized to be effective in breaking down the structure of these materials. The mechanism of alkaline hydrolysis is believed to be saponification of intermolecular ester bonds crosslinking xylan hemicellulose and other components (Ile. lignin and hemicellulose). The porosity of the lignocellulosic materials increases with the removal of the crosslinks. Dilute sodium hydroxide (NaOH) treatment of lignocellulosic materials causes swelling, leading to an increase in internal surface area, a decrease in the degree of polymerization, a decrease in crystalinity, separation of structural linkages between lignin and carbohydrates, and disruption of the lignin structure (Sun and Cheng 2002). Furthermore, in the presence of hydrogen peroxide, the oxidative delignification process can further be performed to enhance the conversion efficiency. Additionally, alkali is also helpful for buffering the co-digestion system for food waste and dairy manure. A thermal pretreatment process causes the fiber materials to undergo hemicellulose degradation and lignin transformation due to high temperature, thus improving the efficiency of cellulose hydrolysis and digestion by fermentative and methanogenic bacteria.

Fibers separated from manure were used in this study. Hydrolysis experiments were conducted in flasks with 5.0 g fiber in 50 mL water or alkaline solution (2.4% dry weight) for 24 hours. Three methods were investigated to evaluate their enhancement of fiber digestibility, including thermal (248 ºF, 20 min), alkaline, and alkaline peroxide pretreatment. The effect of pretreatment can be reflected by three parameters, including the increase of COD solubilization (SCOD, soluble COD measured after pretreatment), weight loss, and composition change of lignocelluloses (i.e., lignin, cellulose and hemicellulose). The SCOD after 24 hrs was measured in this study, whereas the observations of weight loss and composition variations are under consideration. After pretreatment, the hydrolyzed fibers were investigated for their methane production performance in batch serum bottles.

In this experiment, various pretreatment methods (thermal, chemical, and thermochemical pretreatments) of fibers were performed for 24 hrs to improve treatment efficiency. First, the influence of thermal pretreatment on COD solubilization was evaluated. The control experiment was performed using non-pretreated fibers. Figure 31 illustrates that, at ambient temperature, a SCOD value of 560 mg/L was obtained. Fibers were successfully liquidized by thermal pretreatment at 248 ºF for 20 min and a SCOD of 1455 mg/L was achieved. This result indicates that the organic particulates in fibers were liquidized to soluble substances or converted into lower molecular weight compounds by thermal pretreatment. Second, alkaline pretreatment was performed at pH 12 with alkaline agents NaOH at three temperatures (Figure 31), and the SCOD were 4366, 6896, 8687 mg/L, respectively. When NaOH was added, COD solubilization increased through various reactions such as saponification of uronic acids and acetyl esters

reactions occurring with free carboxylic groups and neutralization of various acids formed from the degradation of particular materials.

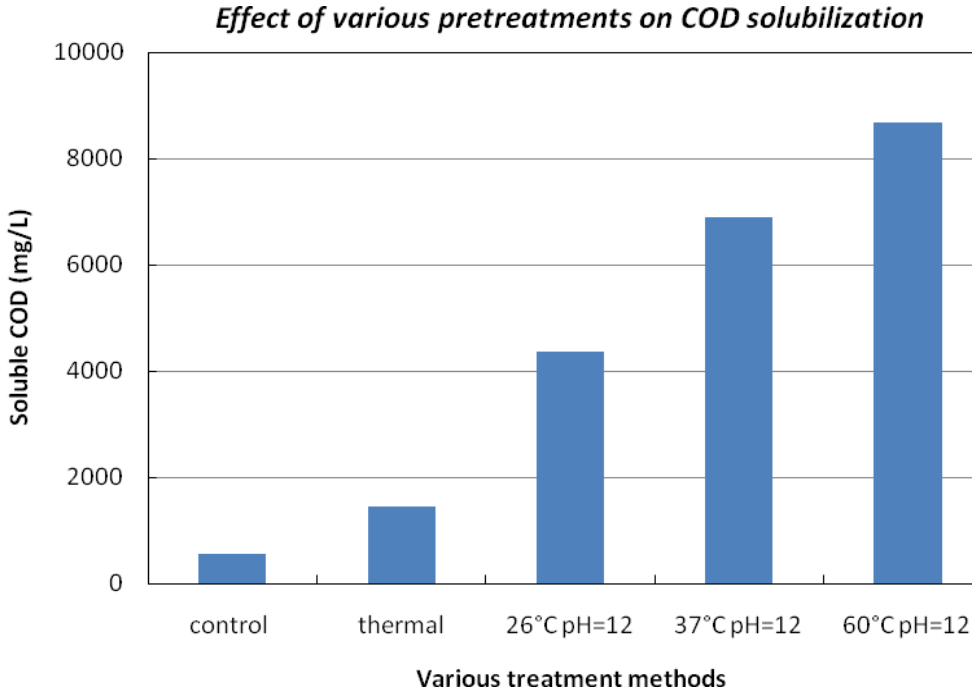

Figure 31 Thermal pretreatment methods for COD solubilization

Hydrogen peroxide under alkaline conditions is widely reported as an environmentally friendly way to bleach fiber and partly break down the fiber structure. In this work, the effect of pH was investigated to obtain the optimal conditions on COD solubilization by fixing the hydrogen peroxide concentration at 1.5%, and the results are presented in Figure 32. The SCOD stays stable in the pH range of 7.0-9.0, but increases when the pH increases from 10 to 12.5. Results indicate that alkaline conditions are beneficial for hydrogen peroxide treatment.

Furthermore, the effects of three peroxide concentrations were investigated with the highest COD solubilization occurring at 3.0% (Figure 33). However, high levels of alkali and peroxide become uneconomical since potentially expensive acids will be needed to neutralize the system prior to anaerobic digestion. Considering both the COD solubilization and the economic aspect, pH 12.5 and 1.5% were chosen as the optimal condition for peroxide treatment.

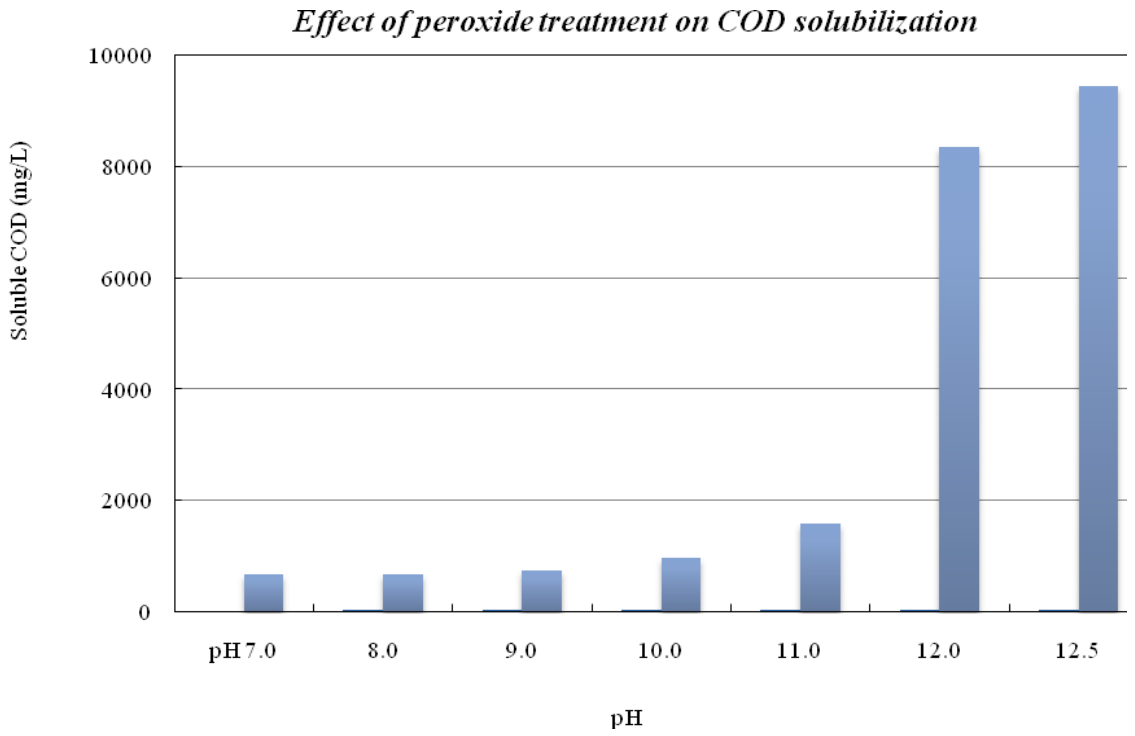

Figure 32 Effect of varying peroxide treatment with increasing pH on COD solubilization

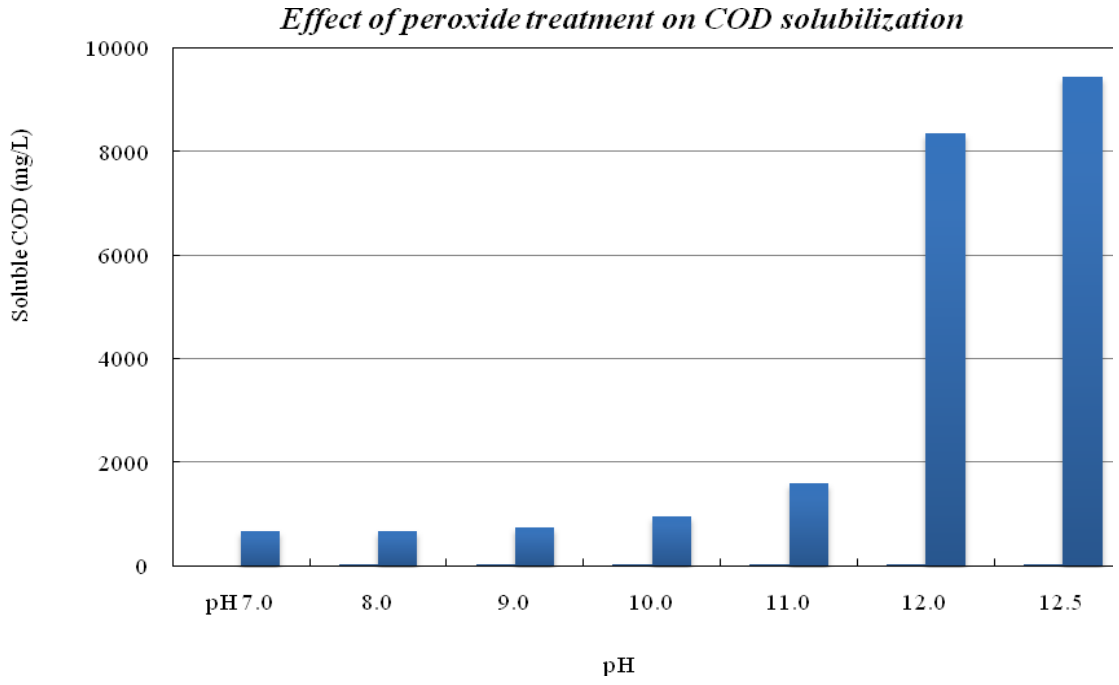

Figure 33 Effect of three peroxide treatments on COD solubilization at 3.0% hydrogen peroxide

The methane production with pretreated manure fibers and control was conducted in this study and the results from the first 21 days are presented here. Figure 34 shows the methane yield was 45 mL for the control (assumed from easily biodegradable small molecules and some cellulose and hemicellulose). Methane production was significantly increased by the three pretreatments at 500 h. The maximum methane production of 132 mL was achieved by thermal pretreatment. Alkaline and peroxide pretreatment slightly increased the methane production by 1.24 and 1.33 times, respectively. Unexpected side reactions might produce inhibitory compounds during the alkaline and peroxide pretreatment, which could possibly decrease the methane production. It is expected that better results may be obtained by optimizing the pretreatment conditions of these two methods.

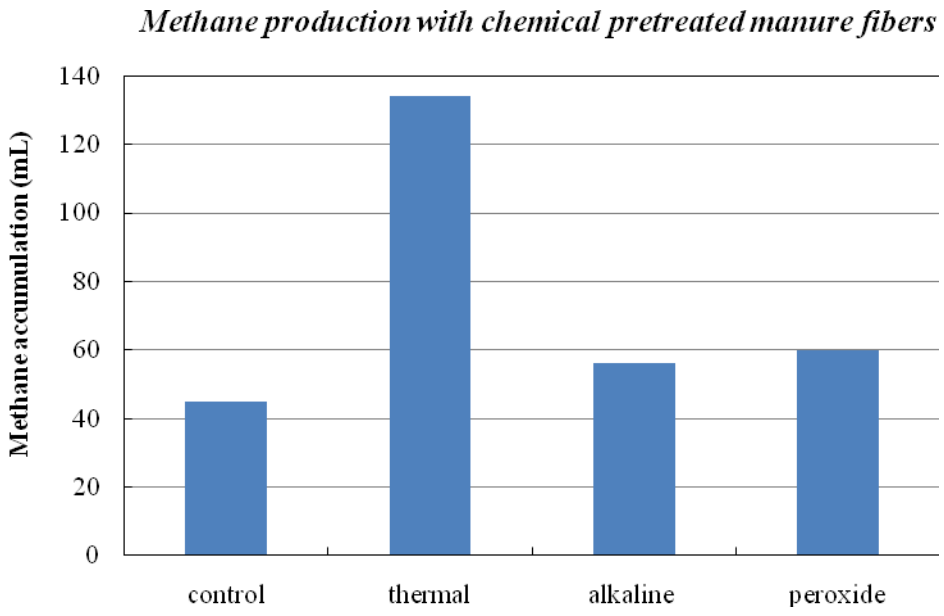

Figure 34 Methane Production from chemically pretreated manure fibers

4.3.2. Enzymatic hydrolysis

The objective of this portion of the study is to produce enzymes directly from dairy manure using white rot fungi and then apply the crude enzyme to AD to further degrade lignocellulosic fibers. In this way, operational costs will be decreased, and this method shows future promise for widespread application compared with utilization of expensive commercial enzymes. Ligninase is a generic name for a group of isozymes that catalyze the oxidative depolymerization of lignin (Glenn, Akileswaran et al. 1986; Asgher M., Asad M. J. et al. 2006). These ligninases are extracellular and can be produced by *Phanerochaete chrysosporium.* The ligninases are capable of catalyzing a wide range of one- and two-electron oxidations. The substrates of ligninase, exhibit much higher reduction potentials. This property, along with its low pH optimum, gives ligninase the unique ability to catalyze the oxidative depolymerization of lignin and the oxidation

of methoxybenzene-containing lignin-like substrates. In this study *P. chrysosporium* was maintained and spore formation was induced in malt extract broth medium in batch flasks. This was used to inoculate autoclaved dairy manure to produce ligninases.

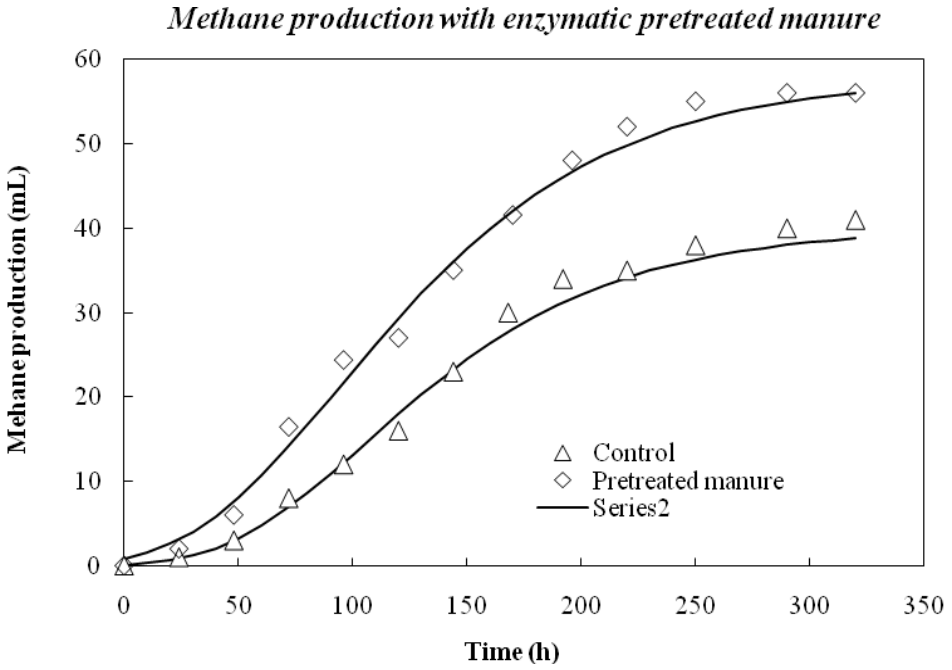

Figure 35 Enhancement of methane production by enzymatic pretreated manure

The enzyme produced directly from the dairy manure using the white rot fungi was then applied to anaerobic digestion for further degradation of lignocellulosic fibers. Methane production with enzymatic pretreated manure and control were conducted and results are presented in Figure 35. The methane yield was 40 mL for the control, which is assumed to be from the easy biodegradable small molecules attached on the fibers plus some fiber materials such as cellulose and hemicellulose. The fiber concentration for this test was about 2% of total suspended solids. Interestingly, the methane yield of pretreated manure increased by 30% and a maximum methane production of 55 mL was achieved.

4.3.3. Biofilm enhanced enzymatic hydrolysis

In this project, a novel idea is proposed. That is, using biofilm to enhance hydrolysis of concentrated biomass and promote interspecies synergy on insoluble manure fibers. This idea is under validation for its effectiveness and deserves further detailed investigation. In AD, manure fibers can serve as natural carriers for anaerobic microorganisms to attach, grow, and possibly form biofilms. In most instances, the effective biodegradation of insoluble substrates, i.e., manure fibers, require that anaerobic microorganisms must remain attached to the substrate surface. This proximity can be facilitated by the formation of microbial biofilms in which

microbes are held on the substrate surface by an extracellular polysaccharide matrix, which can also mediate the formation of colonies of the anaerobic microorganisms and structured consortia with physiologically cooperative species. More importantly, the effect of this biofilm structure is to hold hundreds of cells of a particular microbial species and enrich the excreted enzymes, in a stable polymeric matrix at one particular locus on the substrate surface. Cellulolytic microorganisms have a very strong affinity for cellulose and most of these organisms adhere to the insoluble substrate. They produce deep pits by the activity of their associated enzymes and digest insoluble substrates (Costerton 1992). If end product saturation threatens to dampen this biodeterioration by feedback inhibition, cooperative microorganisms can degrade these products and drive the catabolic reactions towards more complete degradation for methane production. The multispecies biofilm is then considered effective in the focused microbial and enzyme attack on an insoluble substrate (Costerton 1992). Particularly, it should be pointed out that AD is carried out effectively in many natural anaerobic microbial ecosystems including the rumen of animals such as sheep, cows, deer, and kangaroos.

Some research has shown that a multispecies biofilm can be formed in the rumen and provides an example of the intricate relations between the cells in a microbial community (Macfarlane and Macfarlane 2006; Shinkai and Kobayashi 2007). Using immobilized high concentration of enzymes for the development of novel anaerobic digestion technology could significantly improve conventional systems by providing increased depolymerization rates and possibly greater extents of degradation of lignocellulosic material through the function of biofilm. In the biofilm, large numbers of microorganisms may exist in structural juxtaposition, which allows them to cooperate physiologically in the step-by-step oxidation of organic materials to produce methane. It is necessary to employ molecular tools to probe the genetic information for following:

- To verify their synergetic functions,
- To understand the complex communities of microorganisms, such as what microorganism are present,
- To understand the metabolic potential for bio-methanation
- To verify what part of the potential microbes are realizing, and how they interact with each other and their environment,

In this study, fluorescence *in situ* hybridization (FISH) with specific oligonucleotide probes targeting the dominant strains allowed the direct visualization of the community distribution by using confocal laser scanning microscope. Figure 36 shows that the anaerobic microorganisms distributed uniformly at the surface of fiber biofilm, whereas microbes such as archaea are specifically distributed at the inner part of biofilm. The results so far have already validated that manure fiber could be used as an effective biofilm support material.

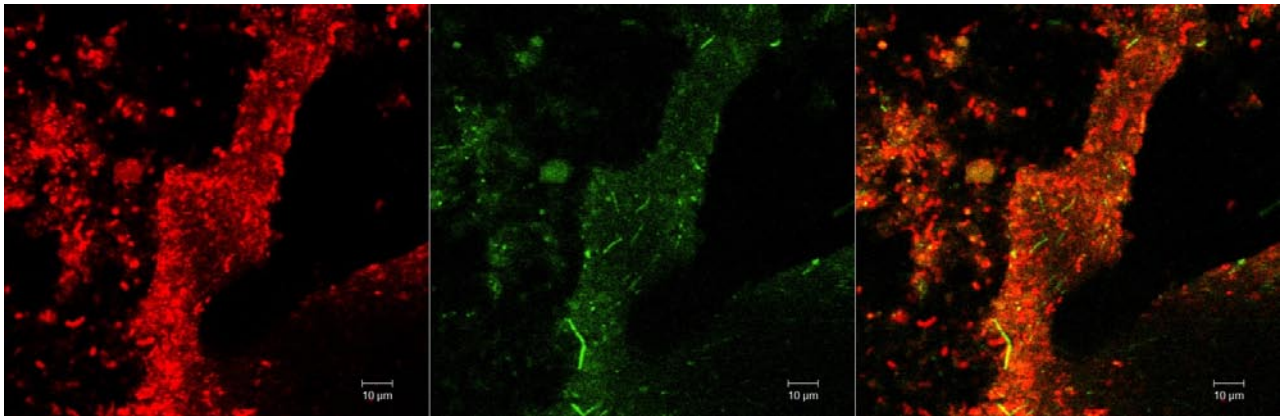

Figure 36 In situ hybridization of biofilm from a digested manure fiber at 15 ^{o}C viewed by confocal laser scanning microsope. Left: View of the fiber biofilm which was hybridized with FITC-labeled bacteria-domain probe (EUB338) (red); Middle: View of the fiber biofilm which was hybridized with TRITC-labeled archaeal-domain probe (green); Right: Simultaneous distribution of archae and bacteria in the fiber biofilm

Studying the novel biofilm enhanced hydrolysis technology by enzyme immobilization and interspecies synergywill advance the knowledge and understanding of the mechanisms in the little understood microbialhydrolysis processes. According to this, innovative approaches can be proposed to increase the enzyme production capability of the hydrolytic organisms so that complex biofilms can be useful for the efficient biodegradation process on insoluble substrates. This novel biofilm-based hydrolysis enhancement technology can be directly incorporated with most existing anaerobic digestion processes treating high solid substrates in a cost-effective manner. Furthermore, this technology can be also readily extended to any other hydrolysis rate-limiting bioprocess, such as bioethanol and biodiesel production.

4.4. Objective 4: Develop mixing strategies and models

4.4.1. Selection of mixing type for the HSAD system

Based on the modeling results in section 3.6, about 75% of HSAD cost is related to solids mixing. Therefore, selection of a proper mixing scheme is essential. Mechanical mixing was previously shown to be more effective than sludge recirculation or biogas injection. A review of the literature suggests that biogas recirculation plays an ineffective role in HSAD systems. Moreover, the biogas systems need regular maintenance, and high pressure systems can be potentially dangerous. In the design this system, gas recirculation will not be taken into account.

Computational Fluid Dynamics technology was used in the selection of mixing type for this system. Figure 37 is a comparison of velocity distribution with slurry recirculation and mechanical mixing (A-310 Impeller) in low viscosity fluid. Total solids are set at 2.5%. It is shown that slurry recirculation has relatively poor mixing performance because the proportion of

dead zone to mixing zone is large. The digester with impeller has symmetrical distribution which can give microorganisms and substrates more opportunities for contact. If the digester was equipped with a longer tank length, then more impellers would be required to realize complete mix. Several studies have shown that above 4% TS manure becomes non-Newtonian (like pudding), mostly due to the presence of the fibrous particles. Figure 38 shows a velocity distribution with a single impeller (A-310) in high viscosity fluid (12.1% TS). The flow pattern has been changed into a spindle-shape. A zone of significant motion around impellers is formed. This phenomenon is called a cavern and results in mixing performance for the impeller A-310 that is poor. It indicates that ordinary impellers cannot play an effective role in HSAD.

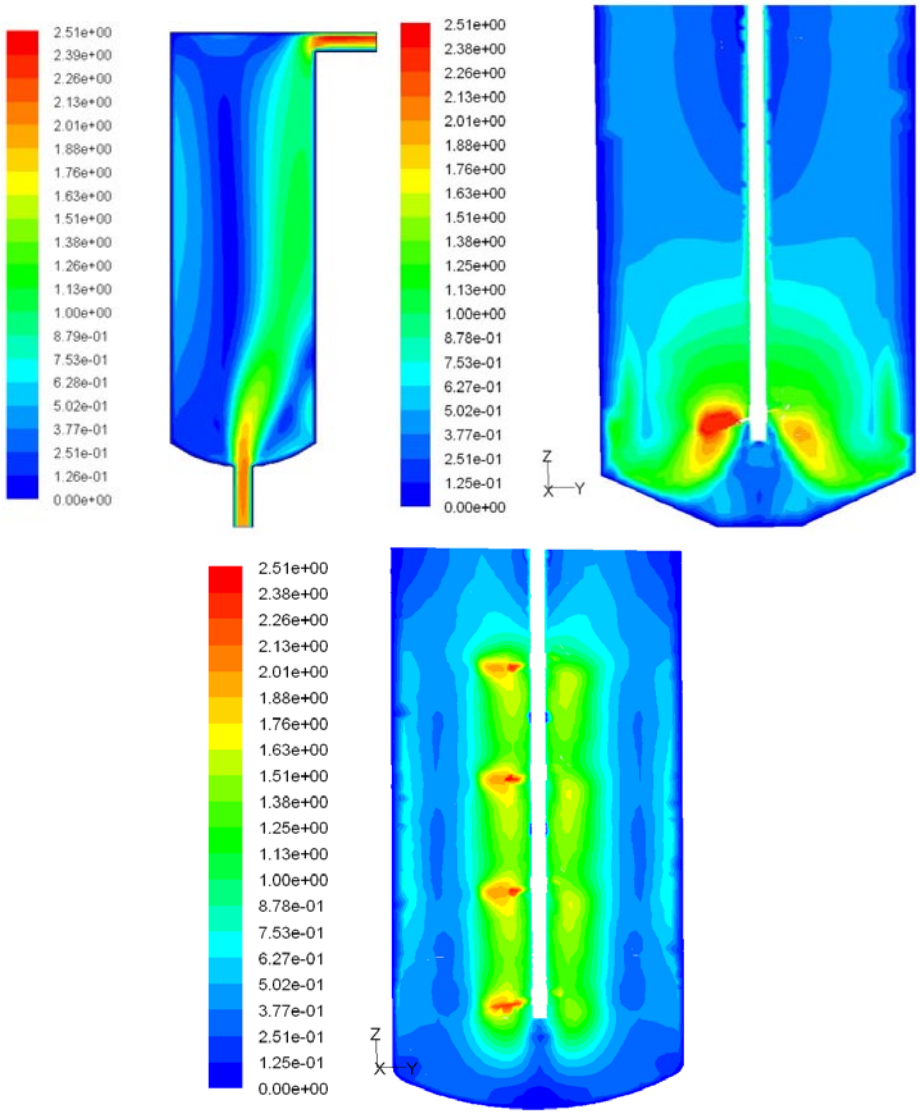

Figure 37 Comparison of velocity distribution with slurry recirculation and mechanical mixing (A-310 Impeller) in low viscosity fluid (2.5% TS)

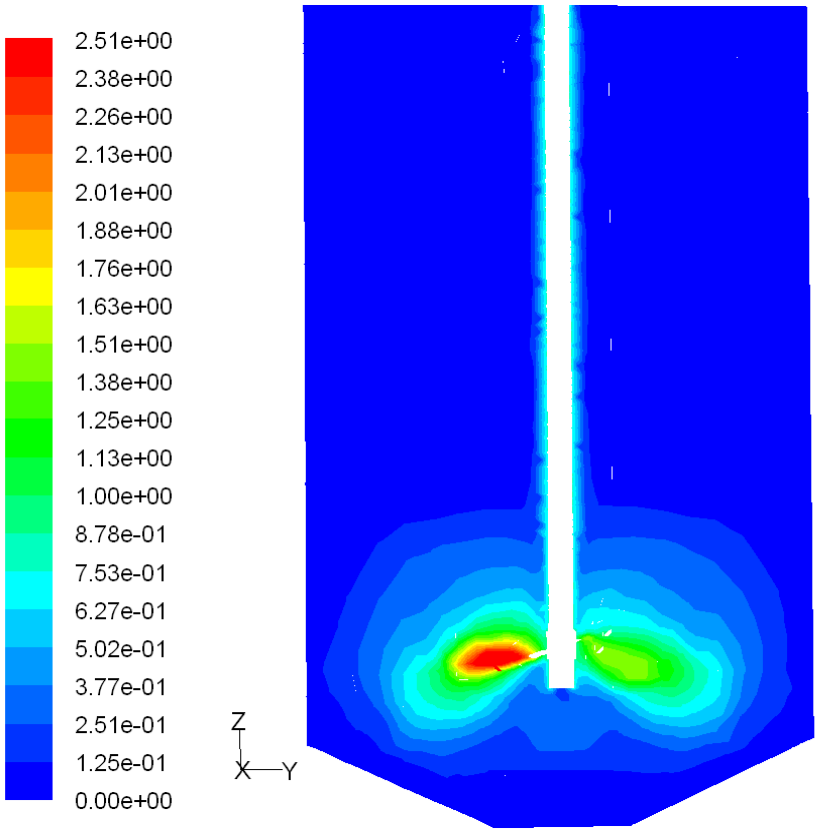

Figure 38 Velocity distribution with single impeller A-310 in high viscosity fluid (12.1% TS)

Figure 39 further compares the velocity distribution of a Multi-A310 Impeller with that of a Helical Ribbon and Auger in high viscosity fluid (12.1% TS). It shows that there are dead zones around the multi-impellers while the helical ribbon and auger are effective in limiting dead zones. Therefore, helical ribbon and auger are shown to be the best selection to deal with HSAD environments.

A batch ribbon blender is depicted in Figure 40. It is capable of effectively performing a wide range of mixing processes including liquid, solid, and liquid–solid blending. Common industrial applications of these blenders include mixing the powder components of pharmaceutical tablets, blending oils and shortenings into dry ingredients to form a cake batter, and combining gravel and asphalt (Paul, Atiemo-Obeng et al. 2004). Although the helical ribbon and auger have good qualities in high solids mixing, high energy consumption may put them at a disadvantage. According to the varying characteristics of HSAD, a combination of mixing strategies is needed to solve the conflict between mixing efficiency and energy consumption.

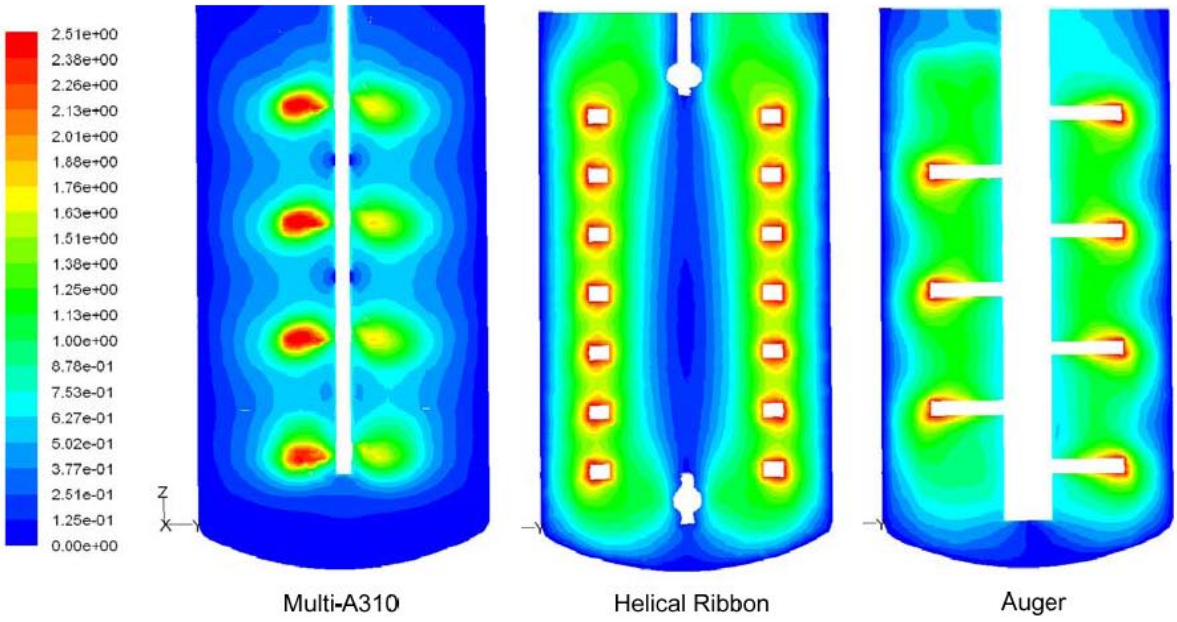

Figure 39 Comparison of velocity distribution with Multi-A310 Impeller, Helical Ribbon and Auger in high viscosity fluid (12.1% TS)

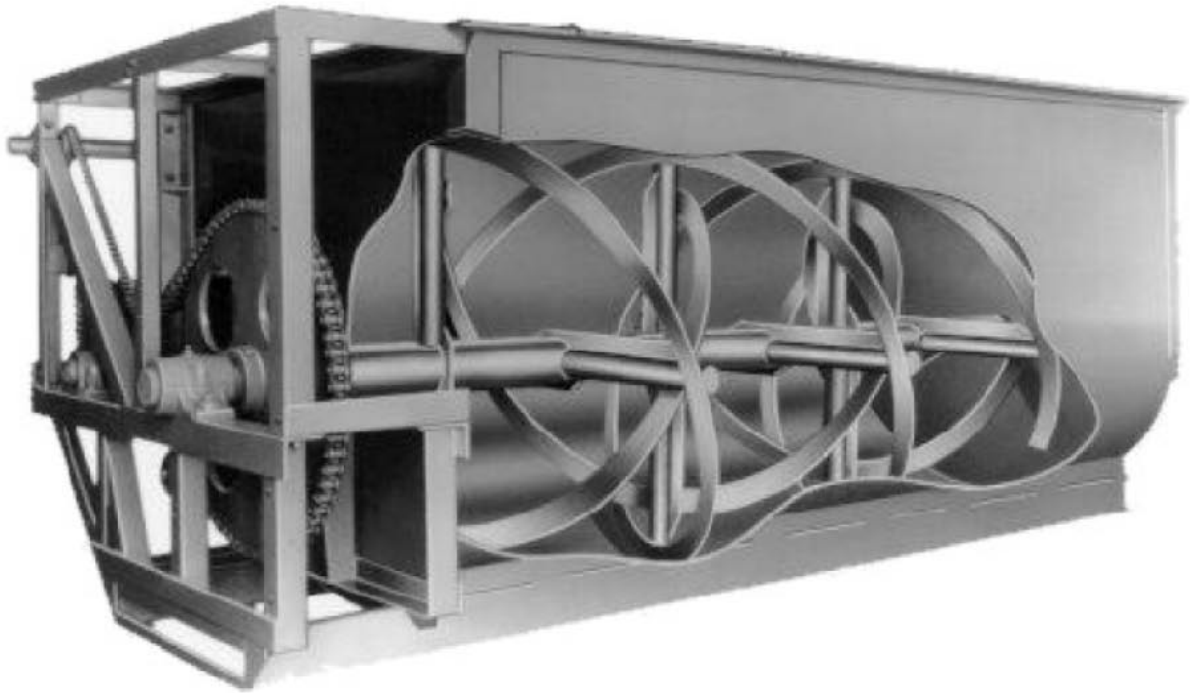

Figure 40 Schematic of a ribbon blender

Mixing of fluids requires the input of mechanical equipment, such as an impeller, or impellers, attached to a rotating shaft. An alternative method for getting energy into the fluid is to generate a high velocity jet of fluid in the vessel. The jet entrains and mixes the surrounding fluid and the mechanical energy is supplied from a pump. Jet mixers are commonly used in large storage tanks, such as crude oil tanks, where the liquid viscosity is higher than water, but the required blend time can be on the order of hours rather than minutes or seconds. When used in large storage tanks the jet usually enters from the side of the vessel close to the base and is directed toward the opposite top corner (Figure 41).

A jet mixer can be designed to deliver a concentrated horizontal force on the tank floor to dislodge settled sludge. This jet must, however, be rotated to cover the entire floor. The jet can be energized by the liquid flow during receipt or by pumping around the tank. Although a single rotating jet can be operated, a mixer with two diametrically opposite nozzles can produce a better balance of forces on the mixer body, which is called impinging streams—currently a hot topic among mixing researchers.

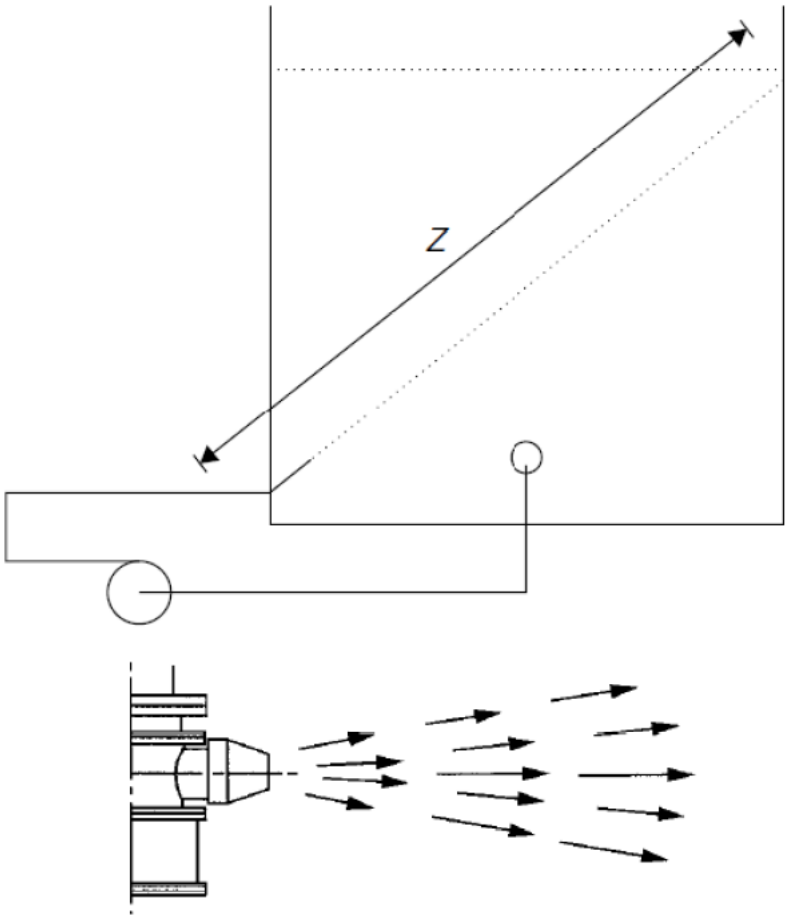

Figure 41 Jet mixer configuration for blending operation

Jet mixers are driven by pumps that can be located on the ground next to the vessel, giving easy access for maintenance. The vessel will often need a pump for filling and emptying, and this pump can also be used for the jet mixer, thus reducing the capital investment needed, especially if an agitator is being considered. Based on the above discussion of the close-clearance impellers (helical ribbon and auger) and jet mixing, we can further apply this combination technology into the design of this system.

Figure 42 presents the proposed mixing scheme for this system. The red line represents a pipeline newly added to provide jet mixing. The liquid pumped from the seed chamber is injected into the high solids chamber at the bottom. The settled sludge is forced to suspend to contact with the new feedstock. Jet mixing can play an effective role due to the operational characteristics in the new design of this project. There is a wide range of total solids (8~15% TS) at different stages in the high solids chamber. When the injected liquid is mixed with substrate and large organic polymers are broken down into smaller molecules, the slurry viscosity decreases. Jet mixing will then provide an effective replacement to the traditional impeller. Furthermore, the high solids chamber also has the capacity to handle high solids materials up to 45% TS.

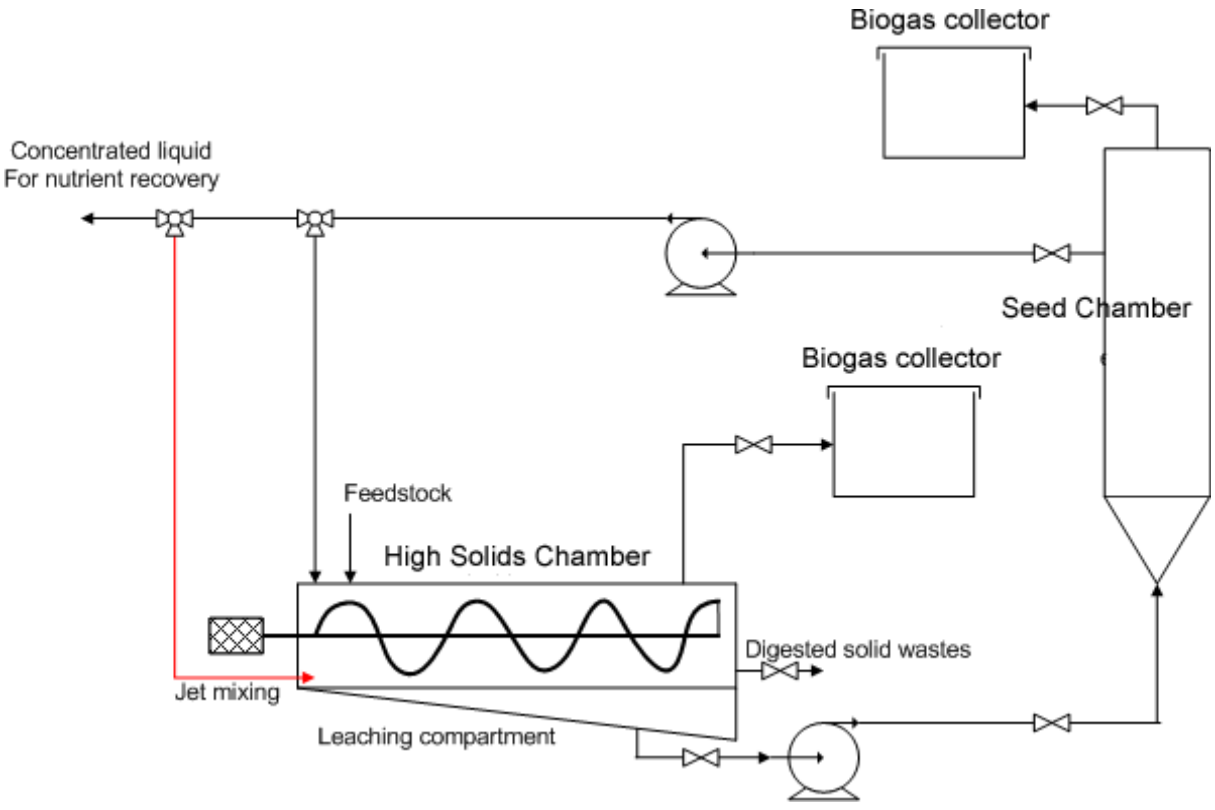

Figure 42 HSAD Process Flow diagram

4.4.2. Design of Mixing Strategies

Two very important aspects of digester mixing are the intensity and duration. Several studies indicate that a lack of sufficient mixing in low solids digesters resulted in a floating layer of solids similar to what was observed during experimental trials of this system (James, Wiles et al. 1980; Stenstrom, Ng et al. 1983). In these studies, the mixing level was increased to prevent formation of the solids layer. Chen et al. (1990) also observed the development of a floating layer of solids in a non-mixed digester. They compared the performance of a non-mixed (downward flow) and a continuously mixed digester at mesophilic conditions. The digesters were fed a mixture of refuse-derived fuel and primary sludge at relatively low solids levels. The non-mixed digester exhibited a higher methane yield than the continuously mixed digester, though the authors attributed this to the longer effective solids retention time in the non-mixed digester. This longer solids retention time was accomplished because solids accumulated near the top of the reactor. This study demonstrated the possibility of operating a co-digestion system under non-mixed conditions.

James et al. (1980) evaluated the feasibility of co-digestion with feed at three solids levels (4, 7, and 10% TS) and two mixing mechanisms (gas mixing and mechanical rotor). Operational problems were experienced when feed with the higher TS level was used. A scum layer consisting mostly of cellulosic fibrous material accumulated at the surface. The fibrous material interfered with the mechanical mixing apparatus, and mixing was not uniform with either mixing mechanism. The authors concluded that more energy would be required to ensure complete mixing making the process economically unfeasible. However, they did not consider the effects of mixing on the biological conversion processes and the types of impeller for mechanical mixing apparatus.

Rivard et al. (1990) did not observe a significant difference in performance between agitator speeds of 1 and 25 rpm in digesters fed MSW for which the solids levels were gradually increased from 5 to 30–35%. However, no detailed performance data were presented to thoroughly compare the effect of mixing rates. It was concluded that the lowest mixing rate was preferable, presumably because energy requirements were minimized.

The importance of spatial juxtaposition was investigated experimentally by Conrad et al. (1985) by monitoring gas metabolism and interspecies electron transfer in sewage sludge and anoxic sediments. They presented a theoretical diagram that emphasized the structure of the microbia matrix or floc, and how it enabled the effective transfer of hydrogen/formate and acetate from syntrophic acetogens to neighboring methanogens. Whitmore et al. (1987) suggested that very rapid mixing disrupts the structure of flocs in completely mixed reactors, thereby disturbing the syntrophic relationships between organisms.

Dolfing (1992) provided a similar argument within the context of high-rate treatment systems. Biofilms and granules represent ideal conditions for close physical associations between electron-producing and electron-consuming organisms. Appropriate spatial juxtaposition allows for high hydrogen fluxes at relatively low hydrogen concentrations, by minimizing the

development of electron gradients. In vigorously mixed systems, spatial associations are likely continuously disrupted, leading to a state of instability. Based on the research in macro-scale (digester performance) and micro-scale (microbial population dynamics), Stroot and Mcmahon et al. (McMahon, Stroot et al. 2001; 2001) suggest that vigorous, continuous mixing may prevent good performance of high solids digesters. Minimal mixing was provided to distribute the feed adequately and may have allowed the formation of new spatial associations. The results obtained indicate that mixing may play a detrimental role in the turnover of propionate, possibly because of the destruction of syntrophic interactions that require a defined juxtaposition between microorganisms in anaerobic consortia. ***In summation, it can be concluded that mixing intensity is not required to be vigorous and mixing duration is not required to be continuous in high solids digesters due to the production of inhibitory VFA.***

Vavilin et al. (2005) give us a clearer picture about mixing in high solids digesters. Different waste-to-biomass ratios and intensity of mixing were studied theoretically and experimentally. The experiments showed that when organic loading was high, intensive mixing resulted in acidification and failure of the process, while low mixing intensity was crucial for successful digestion. Others also agree that intensive mixing resulted in acidification (Stroot, McMahon et al. 2001; Vavilin, Lokshina et al. 2004; Vavilin and Angelidaki 2005). However, when loading was low, mixing intensity had no significant effect on the process. They hypothesized that mixing was preventing establishment of methanogenic zones in the reactor space due to enhancing VFA inhibition. But they do not analyze how mixing acted on establishment of methanogenic zones without VFA inhibition or add more methanogens to promote the process of VFA consumption. These issues should be further research for the design of a high rate digester.

Finally, Vavilin et al. suggested that spatial separation of the initial methanogenic zones from active acidogenic zones is the key factor for efficient anaerobic decomposition of high solids waste at high organic loading rates. If methanogenesis is the rate-limiting step during the start-up period, it is better to avoid vigorous mixing that may suppress growth and propagation of methanogenic centers over the reactor volume. If hydrolysis becomes the rate limiting step, a high rate of mixing may enhance methane production and solids degradation. Referred from the literature and prior experimentation, the mixing intensity and duration for high solids systems are discussed as follows.

a. Intensity

In the systems design of HSAD, the high solids chamber was expected to be mixed homogeneously so that the substrate would adequately contact enzymes and anaerobic microorganisms. The properties of the feedstock are one of the most important factors to determine mixing intensity and duration. The feedstock assessment is included in Appendix 1. The experimental validation of this system was performed with feedstock of highest potential biogas production, based on the annual production quantities (Q > 1000 ton/year), organic content (OC > 80%) and potential biogas production (PBP > 1 ft^3/lb). The easily degradable solid waste such as the food waste was the major feedstock introduced to the high solids chamber.

The hydrolysis of solid waste moves forward easily because seeding a high concentration of anaerobic microorganisms with the influent waste produced enzymes for hydrolysis and increased the biological rate of reaction. The HSAD design maximizes the biological driving force of the hydrolysis step. However, methanogenesis will become the rate-limiting step due to high VFA production. It is better to reduce mixing intensity and duration and promote establishment of methanogenic zones in the high solids chamber. Considering the requirement of mass and heat transfer, the mixing intensity cannot be reduced to such a low value that the stratification will be formed. Figure 43 gives us the relationship between diffusion mass transfer coefficient and stirred speed. It shows that diffusion mass transfer coefficient increases with increasing stirred speed. There is a peak value where the stirred speed has no impact on the diffusion mass transfer coefficient. It would be better to select the velocity N_{js} which keeps the solids just suspended and not in full suspension, which corresponds to the optimized mixing intensity because there is no significant difference between the diffusion mass transfer coefficients in just suspension and in full suspension.

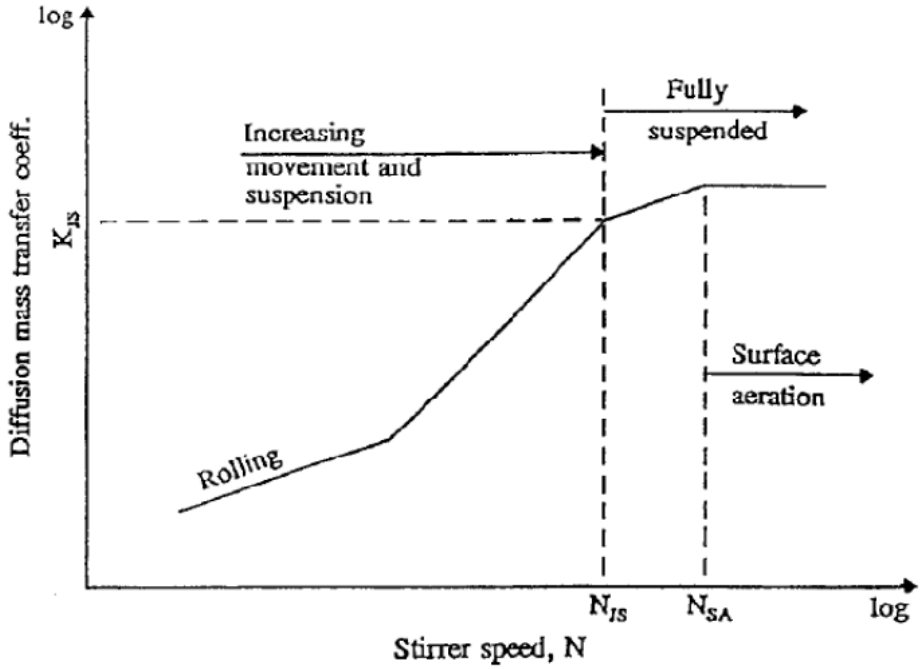

Figure 43 Solid-liquid mass transfer coefficient over a range of impeller speeds

There have been many experimental studies and theoretical analyses on minimum impeller speeds for "solids just suspended." Zwietering (2004) derived the following correlation from dimensional analysis and estimated the exponents by fitting to data for this just suspended impeller speed.

$$\mathrm{Re}_{\mathrm{imp}}^{0.1}\,\mathrm{Fr}^{0.45}\left(\frac{D}{d_p}\right)^{0.2} X^{0.13} = S \qquad \textbf{(6)}$$

The correlation is often expressed in dimensional form as

$$N_{js} = Sv^{0.1}\left[\frac{g_c(\rho_s - \rho_l)}{\rho_l}\right]^{0.45} X^{0.13} d_p^{0.2} D^{-0.85} \quad \textbf{(7)}$$

Where Re_{imp} is the impeller Reynolds number, $Re_{imp} = \frac{ND_{js}^2}{\nu}$;

Fr the Froude number, $Fr = \frac{\rho_l N^2 D}{(\rho_s - \rho_l)g}$;

D the impeller diameter (m);
d_p the mass-mean particle diameter, $(d_p)_{43}$ (m);
X the mass ratio of suspended solids to liquid × 100 (kg solid/kg liquid);
S the dimensionless number which is a function of impeller type, as well as of D/T and C/T;
N_{js} the impeller speed for "just suspended" (rps);
ν the kinematic viscosity of the liquid (m^2/s);
g_c the gravitational acceleration constant, 9.81 m/s^2;
ρ_s and ρ_l the density of particle and the density of liquid (kg/m^3).

With the exception of the density difference, the influence of fluid and particle properties on N_{js} is not large, as indicated by the small exponents on the kinematic viscosity, ν, the particle diameter, d_p, and the solid loading parameter, X, in equations 6 and 7. The density difference is the property with the largest influence on N_{js}. Its exponent reflects the effect of the terminal settling velocity of the particles. The exponent on the impeller diameter, D, represents the effect of scale. Note that an exponent of −0.67 on D would imply a scaling rule based on power per volume. The suitable range of solid loading for Zwietering correlation is 2~15% total solids (by liquid volume), and the ratio of particle diameter to tank diameter cannot be too high.

b. Duration

Walker Process Equipment has traditionally used turnover rate as a method of quantifying mixing performance. They recommend a 20 minute turnover for thickened sludge, and 30minute turnover for non-thickenend sludge. Their operational experience has shown that the Walker GasLifter at a 20minute turnover can be run on an intermittent basis.

The average time required for all high solid slurry in a digester to be turned over once is (NIENOW, Harnby et al. 1997)

$$t_T = \frac{M_{slurry}}{R_m} \quad \textbf{(8)}$$

Where t_T is turnover time, M_{slurry} is mass of slurry in digester and R_m is mixing rate.

c. Energy benefits from appropriate mixing method

An economic analysis of HSAD compared to current technology was presented in section 4.2.3. Compared to using other conventional systems for the solid waste utilization for biogas and power production, the savings from this system are significant. There are three kinds of public benefits from the new system developed in this research project. The first is the potential annual savings for operational costs of solid waste treatment using this system compared to other existing systems. Second, the developed system is more environmentally-friendly since the treatment is in a completely closed system. Therefore, the emissions of odors or toxic gases are almost eliminated. The third is that this system produces biogas of >50% methane that can be utilized as a renewable source for energy production.

d. Benefit/cost ratio

The energy demand for high solids mixing was reviewed in the literature. Angelidaki et al. (2003) think slow moving, top mounted central mixers with a freely suspended shaft with two propellers have become the preferred solution for digester mixing. The mixers usually work continuously with a mixing power input of 3-4 W/m^3. The mixing energy input is often discontinuous (high power for a short period) and average mixing power input typically varies from 10 W/m^3 in prestorage/mixing tanks to 1 W/m^3 in after storage tanks. The position and type of mixers in combination with tank geometry have proven to be very critical. Hydrodynamic favorable solutions, allowing the material to flow to the mixers, generally work best in combination with mixing at different depths. The US EPA (1979) recommends a power input of 0.20~0.30 HP/1000 cu ft (5.26~7.91 W/m^3) used for proper digester mixing. Karim et al. (2005) used 8W/m^3 as the power input per unit volume of the slurry treated to mix 5% and 10% manure slurry.

In the new design of this system, the combination of the close-clearance impellers (Helical ribbon and auger) and jet mixing is suggested to provide adequate mixing for HSAD. The close-clearance impellers have similar capacity to handle the high viscosity materials. The ribbon blend was a case to be optimized as follow.

Using the data of http://aaronprocess.com/ribbonMixersBlendersNR.asp, the power input per unit volume can be estimated. If the ribbon blend is running at a high speed of 15~40 RPM, the power input volume also will be very high (about 8 kW/m^3). However, according to Rivard et al.'s research on HSAD, no significant difference in fermentation performance was observed between agitator speeds of 1 and 25 RPM. Therefore, we can take 1 RPM to optimize the power input per unit volume of ribbon blends. It has been shown through experimental data that the power consumption (P) of an impeller is proportional to the cube of the rotational speed of the impeller. It is defined as follow:

$$P = N_P \rho N^3 D^5 \qquad \textbf{(9)}$$

Where N is rotational speed, D is diameter of the impeller, and N_P is the power number.

$$P_2 = \frac{P_1 N_2^3}{N_1^3} \quad \textbf{(10)}$$

Figure 44 shows the relationship between driven power and reactor working capacity. The power input per unit volume is estimated at the range of 0.15~2.34W/m^3. It is well satisfied the requirement of the conventional mixing energy input. Therefore, it indicates it is possible to reduce energy demand for high-solids mixing to the standard level through optimization.

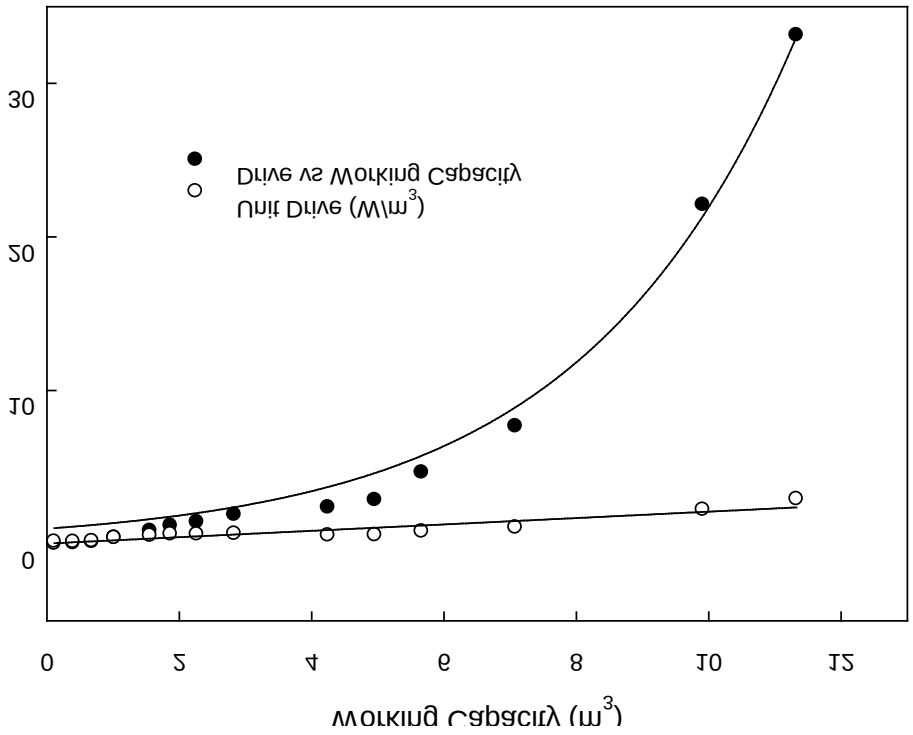

Figure 44 Ribbon blenders driven power vs. working capacity (1RPM)

The proposed cost of ribbon blend was given in the ORBIT technology report of HSAD (Williams 2004). The feedstock up to 3 tons/day needed to be agitated adequately on a farm. Table 6 is the costs that were related to fixed investment in ribbon blender. These costs only can be offset by the benefits gained from this system from the potential 31% savings over existing technologies. Table 7 shows the operating costs for the ribbon blender and centrifugal pump. These costs will significantly decrease if the mixing strategy is correctly selected. In this table, two mixing strategies are compared. One is ORBIT mixing which only applies the ribbon blend to agitate the high solids digester while the slurry is recirculated by centrifugal pump. Although the slurry recirculation has some impact on mixing, poor design will weaken mixing intensity and strength. Therefore, the new design integrates jet mixing with ribbon blender to save the

running time of ribbon blender (Table 7). This kind of mixing strategy is designed because the total solids in digester always change with liquid entering and hydrolysis occurring, and jet mixing can be used over a wide range of viscosity compared to conventional slurry recirculation. Moreover, no extra investment is needed because the centrifugal pump can provide the driving force to jet mixing. Therefore, the usage hours per day for the new mixing design at least can be reduced by half.

Table 6 Proposed Costs of Installing ORBIT as a Stand-Alone HSAD Technology on a Farm

Unit Process	Cost($)
Ribbon blender	
Purchase price	72000
Installation cost	1000
Electrical installation	5000
Total	78000

Table 7 Summary of Operating Costs for Proposed HSAD System Installed on a Farm

Unit Process			
	ORBIT	This system (Integrate jet mixing)	Percentage %
Ribbon blender			
Kilowatts-hours	34.02	34.02	
Usage hours/day	4	2	
Kilowatts-hours/day	136.07	68.04	
Centrifugal pump			
Kilowatts-hours	1.28	1.28	
Usage hours/day	24	24	
Kilowatts-hours/day	30.62	30.62	
Totals	166.69	98.66	59.19%
Electricity fee ($ per kilowatt-hour)	0.08	0.08	
Daily Oper. Cost	13.3352	7.8928	59.19%
Yearly Oper. Cost	4867.348	2880.872	59.19%

4.4.3. Summary of mixing recommendations

Close-clearance impellers (helical ribbon and auger) are designed to apply direct mechanical force to physically turnover digester content because viscous high solids concentration liquids are difficult to pump. These impellers are typically large in size, nearly the same size as the tank

diameter, and provide gentle macro-scale blending of liquids at low shear. The selection of close-clearance impellers permits higher total solids (up to 45% TS) to be handled in the solids reactor of the new design. Although they are the most effective to generate homogeneous flow field, the high cost of energy consumption will put this kind of mixing at a disadvantage. A combination of close-clearance impellers with jet mixing can offset the negative effects caused by only impellers. This combination has an opportunity to be optimized because there is a wide range of total solids (8~15 %) at different stages in the solids reactor. The optimization of impeller structure, assembly and rotational speed can significantly reduce the mixing cost. After optimization, the power input per unit of ribbon blend is estimated at the range of 0.15~2.34 W/m^3 at the speed of 1 RPM. It fits well to the standard that the US EPA recommends--a power input of 0.20~0.30 HP/1000 cu ft (5.26~7.91 W/m^3) used for proper digester mixing. The savings to utilization of food waste is significant. This economic estimate will increase the potential savings to 24% compared to the original design without mixing optimization. The feedstock assessment for Washington State shows the easily degradable solid waste such as food waste and animal waste will be the major feedstock in the high solids chamber. It indicates that methanogenesis is the rate-limiting step during the start-up period. It is better to avoid vigorous mixing that suppresses growth and propagation of methanogenic centers over the digester volume. The mixing strategy should be low mixing intensity and long duration.

4.5. Objective 5: Scientific publications developed as a result of this project

The project results so far are disseminated through scientific publications and conference presentations in addition to the project deliverables:

Zaher U., Ewing T. and Chen S. (2008) Biochemical and spatial based selection of anaerobic digestion feedstock: California and Washington case study, The 23rd International Conference on Solid Waste Technology and Management, Philadelphia, PA, U.S.A. March 30 - April 2, 2008.

Zaher U. Buffiere P., Steyer J.-P., Rosen C., Jeppsson U. and Chen S. (2008) Integrated modeling tool to optimize co-digestion of solid wastes, The 23rd International Conference on Solid Waste Technology and Management, Philadelphia, PA, U.S.A. March 30 - April 2, 2008.

Zaher U. and Chen S. (2007) Identifying state of the art in biological treatment of municipal solids waste, Middle East Waste & Water Congress, May 28-29th 2007, Hyatt Regency Dubai, UAE.

Zaher U., Paramod P. and Chen S. *in press*. A simple elemental continuity based model to study the anaerobic microbial activity: Application to dairy manure, *Applied Mathematical modelling*. Accepted November 2008.

Zaher U., Buffiere P., Steyer J-P. and Chen S. *in press*. A procedure to estimate proximate analysis of mixed organic wastes, *Water Environment Research*. (Accepted, June, 2008)

Zaher U., Cheong D.Y., Wu B., and Chen S. (2007) Review and model based comparison of high solids digestion - producing energy and fertilizer from organic municipal solid

waste, project report no.1, Center for Bioproducts and Bioenergy, Washington State University, Pullman, Washington, USA, PP 95.
Zaher U., Pandey P., Rongping L., Frear C. and Chen S. (2006) An innovative model based approach to plan anaerobic digester start up and operation, Pacific Northwest Clean Water Association, Coeur d'Alene, Idaho, USA, October 1-4, 2006.

5. Conclusions

Preliminary modeling from bench-scale experimental results has indicated that the HSAD design compares favorably to the reported performance of current HSAD technologies. Based on the bench-scale results, this system is capable of supporting a solids loading rate of 0.06 ton/m^3/day, corresponding to an organic loading rate of 78 kg-COD/m^3/day. This compares quite favorablyto 0.04 ton/m^3/day and 0.026 ton/m^3/day reported for two leading existing technologies. The biogas production rate for this system was determined to be 4.62 m^3/m^3/day, with a methane yield of 50-70%, which compares favorably to 3.0 m^3/m^3/day and 2.8 m^3/m^3/day reported for two leading existing technologies. The HSAD design demonstrates 47% chemical oxygen demand (COD) removal and 70% total solids (TS) reduction, which compares favorably to the 50-70% removal/reduction range reported for existing technologies. In addition to the waste treatment benefits of this system, the potential to integrate a nutrient removal and recovery system increases the overall economic value of the system. It is estimated that integrating the leachate recycle loop into a nutrient removal and recovery system would produce 2.1 kg/ton of nitrogen and 3.72 kg/ton of phosphorous from food waste.

Based on the bench-scale results, the cost of treating organic waste with this system is estimated to be $1.08/kWh, which compares favorably to $1.55/kWh calculated for an existing technology. These values account for capital and operational costs amortized over the predicted operating life of the facility. The HSAD system has the potential to lower capital and operational costs compared to existing technologies.

The HSAD design was tested, optimized, and compared with current technology. Process augmentation was the main innovation developed in the HSAD design system. An advanced research approach based on bench-scale experimentation and mathematical modeling was used to test, optimize, and evaluate the economics of this system. The HSAD design consists of two components: the seed chamber and the high solids chamber. The seed chamber treated liquid leachate contacted with solid waste and grew anaerobic seed to continuously inoculate the high solids chamber.

To maximize the economic benefits from HSAD, feedstocks were selected on the basis of a detailed assessment of the Washington State biomass inventory. Potential biogas, and equated power andproduction were evaluated from each digestible feedstock. The food waste and animal wastes were the largest digestible quantities that are produced year-round and have the highest potential biogas and power production. Therefore, food waste and manure were selected as the feedstocks to test this system. In addition, approximately 420 thousand dry ton/year of yard non-wood biomass (grass and green waste) is underutilized. With proper pretreatment this biomass

can be fully exploited as a co-substrate with food waste, yellow and brown grease, and other organics for the production of renewable biogas and the recovery of nutrients with this system.
The seed chamber was validated with two experiments using leachate from dairy manure and from food waste. The seed production in the project proposal was set to a target of 1% VS. The seed production in the seed chamber overflow was 0.7% VS from food waste leachate and 2% from dairy manure leachate. The integrated bench-scale experimental apparatus was tested for the digestion of food waste by connecting the seed chamber with the high solids chamber. The overflow from the seed chamber was recycled to the high solids chamber, which was continuously leached. The target for the high solids chamber effective volume was set to 90% in the project proposal. The high solids chamber effective volume was 97% as estimated with the developed process model by fitting the biogas results data from the integrated system experiment. For manure, the seed chamber alone is enough for the treatment of dairy manure since leaching the fresh manure washed out the biodegradable fecal material and left only non-easily degradable fibers.

A set of mathematical models were developed to define the process kinetics and understand the treatment mechanism of this system. The mathematical models were calibrated from separate bench-scale experiments digesting selected feedstock. The models were then validated on the seed chamber and the integrated apparatus. The validated models were useful for optimizing this system and for evaluating economics compared to existing systems.

This system reduces the high solids chamber volume, eliminates solids recycle, and reduces solids mixing due to process augmentation. These improvements lead to a savings on capital and operation costs compared to existing systems.

6. Recommendations

The potential economic benefits from the continued development and ultimate deployment of the HSAD system are significant. Compared to an existing technology and using only the food fraction of MSW, the estimated annual savings of treating organic waste is greater than $75 million. The cost of the HSAD system for generated power is estimated at $1.08//kWh where 75% of this cost is related to solids mixing; therefore, a mixing study was undertaken to detail strategies to minimize expensive solids mixing and highlight the benefit of using the dual-chamber design with the more economical leachate recycle loop. The results of the mixing study comprise CFD (computational fluid dynamics) models developed to give numerical and visual indication of mixing effectiveness. These models will be refined and optimized during pilot-scale trials in order to give effective output for scale-up and design of industrial-scale facilities. The scaled design will incorporate other materials especially grass and green waste. The study on this feedstock is not included in this report and will be presented independently in a separate report.

Prior to developing a pilot-scale design, further development of the HSAD system is warranted at the large bench-scale. A small demonstration system treating 10 kg/day of food fraction would be suitable for validating CFD and thermodynamic models and to expand the validation of the process models. Increasing the volume of the high solids chamber would also call for the design

and testing of industrial (auger type) mixing and conveying to maintain efficient distribution of the solids over the entire SRT. Increasing the leachate chamber volume would allow for the installation of a variable speed pump with automated control valves for efficiently and effectively controlling anaerobic seed washout. Ultimately, an automated small pilot-scale facility will need to be built to demonstrate this system and to validate the full design to prospective industrial partners.

7. Public Benefits to Washington State

There are three main ways in which the tax payers of Washington State will benefit from further development and ultimate deployment of this system. First, there is the potential to lower capital and operational costs for the treatment of organic waste using this system compared to existing technologies. Second, this new system significantly reduces the emissions of odors and waste gases emitted by utilizing a closed leachate recycle loop, thus it is more environmentally friendly compared to existing technologies.

The benefits can be listed as follows:

1. Biogas recovery from AD which replaces fossil fuels. The HSAD system developed produces biogas containing 50-70% methane. After the biogas has been scrubbed (please contact the authors concerning biogas scrubbing technology) this methane can be utilized as a renewable source of combined heat and power (CHP) or compressed and utilized as an alternative vehicle fuel.
2. Nutrient recovery saves fossil fuels. The leachate recycle loop, nitrogen and phosphorus based nutrients can be removed and recovered for use as fertilizers instead of being sequestered in landfills or being released in a saturated form during land application. From the food fraction of MSW, it is estimated that 2.1 kg/ton of nitrogen and 3.72 kg/ton of phosphorus can be recovered in mineralized form.
3. Anaerobic digestion can be used to balance carbon and energy.

These points can be broken down and shown to directly benefit three specific sectors of the Washington State economy. First, the upfront capital and annual operating savings of implementing this system along with the reduced emissions of GHG can benefit tax payers by reducing the cost burden associated with the treatment of organic waste. Second, the removal and recovery of nitrogen and phosphorus based nutrients can provide a local and renewable source of organic fertilizer to Washington State farmers. Third, energy producers will have a local renewable source of biogas to use for the production of electricity, heat, and alternative vehicle fuel.

References

Angelidaki, I., L. Ellegaard, et al. (2003). "Applications of the Anaerobic Digestion Process." Advances in Biochemical Engineering/Biotechnology **82**: 1-33.

Angenent, L. T. (2007). "Energy biotechnology: beyond the general lignocelluloses-to-ethanol pathway." Current Opinion in Biotechnology **18**: 191-192.

Asgher M., Asad M. J., et al. (2006). "Enhanced lignin peroxidase synthesis by Phanerochaete Chrysosporium in solid state bioprocessing of a lignocellulosic substrate." World Journal of Microbiology and Biotechnology **22**: 449-453.

Barnes, S. P. and J. Keller (2003). "Cellulosic waste degradation by rumen-enhanced anaerobic digestion." Water Science and Technology **48**(4): 155-162.

Chen, T. H., P. Chynoweth, et al. (1990). ANAEROBIC-DIGESTION OF MUNICIPAL SOLID-WASTE IN A NONMIXED SOLIDS CONCENTRATING DIGESTER, Humana Press Inc.

Choate C. E., Sherman P. A., et al. (2008). Organic waste material treatment system. U. S. P. a. T. Office. USA.

Conrad, R., T. J. Phelps, et al. (1985). "GAS METABOLISM EVIDENCE IN SUPPORT OF THE JUXTAPOSITION OF HYDROGEN-PRODUCING AND METHANOGENIC BACTERIA IN SEWAGE-SLUDGE AND LAKE-SEDIMENTS." Applied and Environmental Microbiology **50**(3): 595-601.

Costerton, J. W. (1992). "Pivotal role of biofilms in the focused attack of bacteria on insoluble substrate." International Biodeterioration and Biodegradation **30**: 123-133.

Curreli, N., M. Agelli, et al. (2002). "Complete and efficient enzymic hydrolysis of pretreated wheat straw." Process Biochemistry **37**: 937-941.

Dar, H. G. and S. M. Tandon (1987). "Biogas production from pretreated wheat straw, lantana residue, apple and peach leaf litter with cattle dung." Biol Wastes **21**: 75-83.

De Baere, L. (2000). "Aanerobic digestion of solid waste: state-of-the-art." Water Science and Technology **41**(3): 283-290.

Dolfing, J. (1992). "THE ENERGETIC CONSEQUENCES OF HYDROGEN GRADIENTS IN METHANOGENIC ECOSYSTEMS." Fems Microbiology Ecology **101**(3): 183-187.

Duff, S. and W. Murray (1996). "Bioconversion of forest products industry waste cellulosics to fuel ethanol: a review." Bioresource Technology **55**: 1-33.

Fan, L. T., M. M. Gharpuray, et al. (1981). "Evaluation of pretreatment for enzymatic conversion of agricultural residues." Biotechnology & Bioengineering Symposium **11**: 29-45.

Fan, Y. T., Y. H. Zhang, et al. (2006). "Efficient conversion of wheat straw wastes into biohydrogen gas by cow dung compost." Bioresource Technology **91**: 500-505.

Fang, H. H. P. and Y. Liu (2001). Anaerobic wastewater treatment in (sub-) tropical regions. Advances in Water and Wastewater Treatment Technology, Elsevier Science**:** 285-294.

Frear, C., B. Zhao, et al. (2005). Biomass Inventory and Bioenergy Assessment: An Evaluation of Organic Material Resources for Bioenergy Production in Washington State, Department of Ecology Publications Distributions Office, PO Box 47600, Olympia WA 98504-7600.

Gabriel, B. (1999). Waster Microbiology. New York, John Wiley &Sons, Inc.

Glenn, J. K., L. Akileswaran, et al. (1986). "Mn(II) oxidation is the principal function of the extracellular Mn-peroxidase from Phanerochaete chrysosporium." Archives of Biochemistry and Biophysics **251**: 688-696.

Gusakov, A. V., T. N. Salanovich, et al. (2007). "Design of highly efficient cellulase mixtures for enzymatic hydrolysis of cellulose." Biotechnology and Bioengineering **97**: 1028-1038.

Himmel, M. E., S. Y. Ding, et al. (2007). "Biomass Recalcitrance: engineering plants and enzymes for biofuels production." Science **315**: 149-174.

Hobson, P. N. and A. D. Wheatley (1993). Pretreatment of feedstocks. Anaerobic digestion : modern theory and practice. London and New York, Elsevier Applied Science**:** 149-174.

Hoffmann, R. A., M. L. Garcia, et al. (2008). "Effect of shear on performance and microbial ecology of continuously stirred anaerobic digesters treating animal manure." Biotechnology and Bioengineering **100**(1): 38-48.

James, S. C., C. C. Wiles, et al. (1980). "MIXING IN LARGE-SCALE MUNICIPAL SOLID WASTE SEWAGE SLUDGE ANAEROBIC DIGESTERS." Biotechnology and Bioengineering **22**: 259-272.

Karim, K., R. Hoffmann, et al. (2005). "Anaerobic digestion of animal waste: Effect of mode of mixing." Water Research **39**(15): 3597-3606.

Karim, K., R. Hoffmann, et al. (2005). "Anaerobic digestion of animal waste: Waste strength versus impact of mixing." Bioresource Technology **96**(16): 1771-1781.

Karim, K., K. T. Klasson, et al. (2005). "Anaerobic digestion of animal waste: Effect of mixing." Bioresource Technology **96**(14): 1607-1612.

Macfarlane, A. and G. T. Macfarlane (2006). "Composition and Metabolic Activities of Bacterial Biofilms Colonizing Food Residues in the Human Gut." Applied and Environmental Microbiology **72**(9): 6204-6211.

Mata-Alvarez, J., S. Mace, et al. (2000). "Anaerobic digestion of organic solid wastes. An overview of research achievements and perspectives." Bioresource Technology **74**: 3-16.

McMahon, K. D., P. G. Stroot, et al. (2001). "Anaerobic codigestion of municipal solid waste and biosolids under various mixing conditions-II: microbial population dynamics." Water Research **35**(7): 1817-1827.

McMillan, J. D. (1994). Pretreatment of lignocellulosic biomass. Enzymatic conversion of biomass for fuels production. B. J. Himmel ME, Overend RP. (Eds.). Washington DC, American Chemical Society**:** 292-324.

Mosier, N., C. E. Wyman, et al. (2005). "Features of promising technologies for pretreatment of lignocellulosic biomass." Bioresource Technology **96**: 673-686.

Nagata, S. (1975). Mixing Principles and Applications. New York, Halsted Press.

NIENOW, A. W., N. Harnby, et al. (1997). Mixing in the Process Industries: Second Edition. Oxford, Butterworth-Heinemann.

Nijaguna, B. T. (2002). Biogas Technology. New Delhi, India, New Age International.

Patel, V., M. Desai, et al. (1993). "Thermochemical pretreatment of water hyacinth for improved biomethanation." Applied Microbiology and Biotechnology **42**(1): 67-75.

Paul E. L., Atiemo-Obeng V. A., et al. (2004). Handbook of industrial mixing. New Jersey, John Wiley & Sons, Inc.

Paul, E. L., V. A. Atiemo-Obeng, et al., Eds. (2004). HANDBOOK OF INDUSTRIAL MIXING. New Jersey, John Wiley & Sons.

Rivard, C. J. (1993). Anaerobic Bioconversion of Municipal Solid-Wastes Using a Novel High-Solids Reactor Design - Maximum Organic Loading Rate and Comparison with Low-Solids Reactor Systems, Humana Press Inc.

Rivard, C. J., B. W. Duff, et al. (1998). Demonstration-scale evaluation of a novel high-solids anaerobic digestion process for converting organic wastes to fuel gas and compost, Humana Press Inc.

Rivard, C. J., M. E. Himmel, et al. (1990). "ANAEROBIC-DIGESTION OF PROCESSED MUNICIPAL SOLID-WASTE USING A NOVEL HIGH SOLIDS REACTOR - MAXIMUM SOLIDS LEVELS AND MIXING REQUIREMENTS." Biotechnology Letters **12**(3): 235-240.

Rivard, C. J., B. D. Kay, et al. (1995). "HORSEPOWER REQUIREMENTS FOR HIGH-SOLIDS ANAEROBIC-DIGESTION." Applied Biochemistry and Biotechnology **51-2**: 155-162.

Seok, J. and S. J. Komisar (2003). "Integrated modeling of anaerobic fluidized bed bioreactor for deicing waste treatment. II: Simulation and experimental studies." Journal of Environmental Engineering-Asce **129**(2): 110-122.

Shinkai, T. and Y. Kobayashi (2007). "Localization of ruminal cellulolytic bacteria on plant fibrous materials as determined by fluorescence in situ hybridization and real-time polymerase chain reaction." Applied and Environmental Microbiology **73**(5): 1646-1652.

Smith, S. R., N. L. Lang, et al. (2005). "Factors controlling pathogen destruction during anaerobic digestion of biowastes." Waste Management **25**(4): 417-425.

Stenstrom, M. K., A. S. Ng, et al. (1983). "ANAEROBIC-DIGESTION OF MUNICIPAL SOLID-WASTE." Journal of Environmental Engineering-Asce **109**(5): 1148-1158.

Stephanopoulos, G. (2007). "Challenges in engineering microbes for biofuel production." Science **315**: 801-804.

Stroot, P. G., K. D. McMahon, et al. (2001). "Anaerobic codigestion of municipal solid waste and biosolids under various mixing conditions-I. digester performance." Water Research **35**(7): 1804-1816.

Sun, Y. and J. Y. Cheng (2002). "Hydrolysis of lignocellulosic materials for ethanol production: a review." Bioresource Technology **83**(1): 1-11.

US and EPA (1979). Process Design Manual for Sludge Treatment and Disposal. Cincinnati, Ohio, EPA 625/1-79-011.

van Lier, J. B., A. Tilche, et al. (2001). "New perspectives in anaerobic digestion." Water Science and Technology **43**(1): 1-18.

Vandeviviere, P. L., D. Baere, et al. (2002). Types of anaerobic digester for solid wastes. Biomethanization of the Organic Fraction of Municipal Solid Wastes. J. Mata-Alvarez. London, IWA Publishing**:** 111-137.

Vavilin, V. A. and I. Angelidaki (2005). "Anaerobic degradation of solid material: Importance of initiation centers for methanogenesis, mixing intensity, and 2D distributed model." Biotechnology and Bioengineering **89**(1): 113-122.

Vavilin, V. A., L. Y. Lokshina, et al. (2004). "Modeling solid waste decomposition." Bioresource Technology **94**(1): 69-81.

Verma, S. (2002). Anaerobic Digestion of Biodegradable Organics in Municipal Solid Wastes. Department of Earth & Environmental Engineering. New York, Columbia University. **Master**.

Verstraete, W., D. de Beer, et al. (1996). "Anaerobic bioprocessing of organic wastes." World Journal of Microbiology and Biotechnology **12**: 221-238.

Wang, Q., M. Kuninobu, et al. (1999). "Upgrading of anaerobic digestion of waste activated sludge by ultrasonic pretreatment." Bioresource Technology **68**(3): 309-313.

Whitmore, T. N., D. Lloyd, et al. (1987). "HYDROGEN-DEPENDENT CONTROL OF THE CONTINUOUS ANAEROBIC-DIGESTION PROCESS." Applied Microbiology and Biotechnology **26**(4): 383-388.

Williams, C. M. (2004). Technology Report: High Solids Anaerobic Digester (HSAD). Raleigh, NC, USA, North Carolina State University.

Wilson K. C., Addie G. R., et al. (2006). Slurry transport using centrifugal pumps. New York, Springer Science.

Wyman, C. E., B. E. Dale, et al. (2005). "Coordinated development of leading biomass pretreatment technologies." Bioresource Technology **96**: 1959-1966.

Zabranska, J., M. Dohanyos, et al. (2002). "The contribution of thermophilic anaerobic digestion to the stable operation of wastewater sludge treatment." Water Science and Technology **46**(4-5): 447-453.

Zaher, U., D.-Y. Cheong, et al. (2007). Producing Energy and Fertilizer From Organic Municipal Solid Waste. Pullman, WA, USA, Washington State University.

Zaher U., Cheong D. Y., et al. (2007). Review and model based comparison of high solids digestion - producing energy and fertilizer from organic municipal solid waste. Pullman, Center for bioproducts and Bioenergy. **Project report no.1**.

Appendices

Appendix 1: Feedstock characterization and selection
Appendix 2: The Simple ADM2 model and Dairy Manure Degradation Analysis
Appendix 3: Transformer model procedure
Appendix 4: GISCOD model and Experimental Analysis of Food Waste Co-digestion
Appendix 5: ADM1 Process model parameters

Appendix 1: Feedstock characterization and selection

Zaher U., Ewing T., Johnson R., and Chen S. (2008) Biomass assessment for potential bio-fuels production: simple methodology and case study, Journal of Solid Waste Technology and Management (in review)

BIOMASS ASSESSMENT FOR POTENTIAL BIO-FUELS PRODUCTION: SIMPLE METHODOLOGY AND CASE STUDY

U. Zaher, T. Ewing, R. Johnson and S. Chen

Department of Biological Systems Engineering, Washington State University, P.O. Box 646120, Pullman, WA 99164-6120, USA zaheru@wsu.edu; chens@wsu.edu

Abstract

United States is experiencing increasing interests in fermentation and anaerobic digestion processes for the production of biofuels. A simple methodology of spatial biomass assessment is presented in this paper to evaluate biofuel production and support the first decisions about the conversion technology applications. The methodology was applied to evaluate the potential biogas and ethanol production from biomass in California and Washington states. Solid waste databases were filtered to a short list of digestible and fermentable wastes in both states. Maximum methane and ethanol production rates were estimated from biochemical and ultimate analysis of each waste and projected on a GIS database. Accordingly, the optimal locations for methane and ethanol production plants were approximately determined. The available net power for transportation and electricity generation was evaluated considering three process efficiency factors in the waste to power life cycle. The net power from methane and ethanol would ultimately cover ~ 6-8% of the transportation needs for motor gasoline or cover ~ 3% - 4% of the electrical power consumption in each state.

Keywords anaerobic digestion, biomass, bio-energy, fermentation, GIS database

1. Introduction

With the multiple challenges of decreasing fossil fuel reserves and global warming caused by increased man-made greenhouse gas (GHG) emmisions, the US government has proposed to triple the production and use of renewable bio-energy over the next ten years (Demirbas, 2007). Renewable bio-energy is an end product of the sun powered carbon cycle, building organic carbon through photosynthesis. During the growth phase of a plant, carbon is utilized from the environment and stored as biomass (Gunaseelan, 1997). The natural decay of the abundant biomass releases large quantities of carbon dioxide (CO_2) and methane (CH_4), both are GHGs, into the atmosphere. Although CO_2 and CH_4 can be ultimately reincorporated into new biomass, an effective method to short-circuit the carbon cycle is needed (van Wyk, 2007). The controlled use of anaerobic digestion (AD) and fermentation technologies to process biomass or organic solid wastes into renewable biofuels (e.g., methane and ethanol) are considered carbon cycle short circuit solutions (Ward et al., 2008). Optimally, such technologies would be further upgraded for the recovery of macronutrients for inclusion in fertilizers and other value-added products (Ma et al., 2005).

Biomass feedstock for use in AD systems is available from a diverse number of waste streams such as manure, organic fraction of municipal solid waste (OFMSW), sewage sludge, organic fraction of industrial waste (OFIW), and agricultural byproducts (Faaij, 2006). Whereas plant residues are rich in lingocellulose. Proper pretreatment would render lingocellulose susceptible to enzymatic/chemical hydrolysis (Schacht et al., 2008). Moreover, Wang et al. (2008) tested the production of ethanol from kitchen waste using open and closed fermentation. In addition to waste streams, agricultural crop sources are available for AD and fermentation processes (Bungay, 2004) provided that the crop use does not economically affect food resources (Foo et al., 2008; Nonhebel, 2005). Whereas the direct production of feedstock for such processes is nominally a function of economics, the use of agricultural

waste streams enables the reduction of environmentally damaging air, water, and land use application (Matteson and Jenkins, 2007).

California and Washington produce 82 million and 17 million dry ton/year of biomass, respectively (BFRS, 2005; PRBEP, 2005) from municipal solid waste (MSW) and agricultural and food processing residues. Transportation fuel consumption is 3,290 and 614 TBtu/year in California and Washington, respectively (U.S.EIA, 2005) motor gasoline consumption represents 50–60% of this transportation fuel consumption which can be replaced or augmented with methane or ethanol. California and Washington consume 272 TWh and 80 TWh of electrical power (CTED, 2007; CEC, 2007) of which only 0.7% and 0.3%, respectively, are derived from biomass. This paper is aimed at evaluating the feedstock in both California and Washington and to estimating the ultimate contribution of methane and ethanol to transportation and electrical power requirements of both states. In the process of achieving this goal:

1. The maximum potential methane and ethanol production was evaluated from biochemical and ultimate analysis of each waste.
2. The results were projected on a GIS database for each county in both states

The maximum potential of such bio-fuel production and its spatial distribution would be a powerful tool to benchmark different systems and select the optimal technology and location of future biofuel plants in both states.

2. Methods

Selecting anaerobic digestion and fermentation as targeted bioconversion technologies for California and Washington, a simple biomass assessment methodology for methane and ethanol bio-fuels production takes the chronological order of the following sections. The first two steps, sections 2.1 and 2.2 lead to a short list of the optimal feedstock to achieve the highest bio-fuel production and, therefore, focus the future development of the conversion processes on the utilization of the sort-listed biomass.

The next two steps, sections 2.3 and 2.4 evaluate the maximum potential of bio-fuels production and, therefore, provide useful information to benchmark different designs and technologies in converting the selected feedstock's to biofuel. Mapping potential biofuel production, section 2.5, determines the optimal areas for location of biomass processing plants. Finally, evaluation of the potential power generation, section 2.6 supports high-level decisions based on the biomass contribution to power needs. The last step determines whether biofuel production should be considered on a large scale (e.g. national or state levels) or focused and planned at the local level (e.g. county or catchment levels).

2.1 Data collection

The biomass inventories of California and Washington states were filtered to determine digestible, fermentable, and year-round available wastes. The biomass databases, as recorded for each county in California (BFRS, 2005) and Washington (PRBEP, 2005) were sorted according to yearly biomass (waste) production at the state level. Each biomass type was classified into four categories: wet, dry, tilled, and seasonal. The databases were filtered to exclude:

1) agricultural residuals that are tilled within soils to maintain their fertility
2) seasonal wastes that are not available for year-round feed of reactors as the sole feedstock
3) solid wastes that are mainly inert; and

Accordingly, wastes consisting of more than 30% dry content and that were mainly cellulosic were selected for ethanol production. Other wastes containing higher moisture content were selected for methane production.

2.2 Evaluation of degradable fractions

The biodegradable fraction was determined for the wastes that passed the previous filtering step. The biochemical composition of these wastes was collected from reported biomass characteristics (Liao et al., 2007; Jiménez et al., 2007; Yuan et al., 2007). The evaluated total state production, dry fraction,

and the biochemical analysis of each waste are listed in Table 1. The biodegradable fractions were determined as the sum of the starch, sugars, cellulose, hemicelluloses, protein, and lipid fractions. The remaining non-degradable fractions corresponded to the ash content.

Table 1 Biochemical analysis for the biodegradable fraction of the short listed wastes

Waste	California total Dry tons/year	Washington total Dry tons/year	Dry mater %	Starch and sugars % dry	Cellulose % dry	Hemi-celluloses % dry	Crude protein % dry	Lipids % dry	Degradable fraction % dry
AD feedstock									
Milk Cow Manure	3,857,800	446,537	14		22	12	14		48
Other Cattle Manure	3,652,400	--	14		22	12	14		48
MSW Food Waste	1,920,700	246,011		40	9	22	14	4	89
Horse Manure	997,900	407,160	30		37.8	32.4	7.5		77.7
Beef Cow Manure	868,600	242,404	15		22	12	16		50
Biosolids Generation	800,000	94,820	26	20			20	25	65
Poultry Manure	746,700	39,659	26		11.1	20.2	18.3		49.6
Meat Processing	79,490	31,828	5.5	17			45	20	82
Swine	49,400	6,592	10		14.6	10.4	25	5	55
Cull Potatoes	48,360	90,747	15	70	5	9.6	10.6		95.2
Cull Apples	--	40,262	11	85	13		0.1	0.5	98.6
Fermentation feedstock									
Paper/card board	8,300,000	2,428,084	90		White 65 Board 35	15			50 - 80
Wood /Lumber	3,700,000	834,057	94		47	21			68
Rice	1,676,300				41	24			65
Cotton	973,580				58	14			72
Wheat Straw	776,870	1,609,486	91		39	23			62
Grass /leaves	740,000	35,826	91		30	11			41
Corn Stover	508,870	45,637	80		35	28			63
Barley Straw	88,240	311,521	90		44	26			70

2.3 Evaluation of potential methane production

The maximum theoretical biogas production for each waste using the ultimate analysis is listed in Table 2. The potential gas production was evaluated according to NCEES (2005) assuming complete stabilization of the wastes using the Buswell equation (1):

$$C_nH_aO_bN_d + (n + a/4 - b/2 - 3d/4)\ H_2O \rightarrow (n/2 + a/8 - b/4 - 3d/8)\ CH_4 + (n/2 - a/8 + b/4 + 3d/8)\ CO_2 + d\ NH_3 \quad (1)$$

The CH_4, CO_2, and ammonia fractions from each waste were estimated. Sulfur and phosphorus contents were very small compared to other elemental fractions, but they are also listed to assist other studies estimating the potential hydrogen sulfide in the produced biogas or potential mineralized phosphorus in the stabilized waste.

Table 2 Ultimate analysis and potential biogas production for the shortlisted digestible wastes

Waste	C %	H %	N %	O %	P %	S %	Ash %	CH_4 m^3/dry ton	CO_2 m^3/dry ton	NH_3 m^3/dry ton
Milk Cow Manure	44.70	5.90	2.24	38.20	0.48	0.30	8.42	435.26	399.14	1.600
MSW Food Waste	45.40	5.94	0.89	35.90	0.40	0.53	11.00	459.06	388.40	0.635
Horse Manure	46.90	4.20	1.20	26.30	0.22	1.50	17.78	456.08	419.38	0.857
Beef Cow Manure	45.40	5.40	2.56	31.00	0.48	0.29	14.90	451.07	396.39	1.829
Biosolids Generation	40.40	6.20	0.80	20.40	2.30	0.80	28.10	474.46	279.66	0.571
Poultry Manure	39.57	5.11	2.93	48.27	3.40	0.77	13.02	325.87	412.76	2.093
Meat Processing	50.50	7.70	13.80	25.50	0.15	0.50	1.85	514.88	427.78	9.857
Swine	45.70	6.45	3.45	21.30	2.45	0.38	20.27	511.88	341.18	2.464
Cull fruits / vegetables*	45.00	6.50	1.70	42.00			4.80	444.80	395.20	1.214

** assumed according to the ultimate analysis of cull potatoes*

2.4 Evaluation of potential ethanol production

The maximum theoretical ethanol production was calculated assuming a perfect lignin extraction and hydrolysis of cellulose and hemi-cellulose to glucose and xylose, respectively. The maximum theoretical ethanol production was evaluated from the stoichiometric reactions equation (2) and (3) for glucose and xylose, respectively. The theoretical yield of ethanol is 0.511 g ethanol/g sugar.

$$C_6H_{12}O_6 \rightarrow 2C_2H_5OH + 2CO_2 \qquad \textbf{(2)}$$

$$3C_5H_{10}O_5 \rightarrow 5C_2H_5OH + 5CO_2 \qquad \textbf{(3)}$$

2.5 Mapping per county

The potential methane production was evaluated for each county and waste according to equation(4), number of counties,

$$Q_{i,j,k} = q_{j,k} \cdot f_j \cdot Q_{W,i,j} \qquad \begin{array}{l} i = 1 \text{ to number of counties} \\ j = 1 \text{ to number of wastes} \\ k = \{\text{Methane, Ethanol}\} \end{array} \qquad (4)$$

Where:

$Q_{i,j,k}$: maximum theoretical yearly production of bio-fuel k for county i from waste j

f_j : biodegradable fraction of waste j

$q_{j,k}$: maximum theoretical production of bio-fuel k per dry ton of waste ,

$Q_{W,i,j}$: annual production of waste j from county i

Accordingly, the maximum methane and ethanol production rates were built on a spatial database for both California and Washington states, using ESRI® ArcMap 9.2 (ESRI, 2005).

2.6 Potential power generation

The maximum theoretical production of methane and ethanol was estimated stoichiometrically from biochemical and ultimate analysis to reflect the bio-energy content of each waste as a resource. The energy content of each waste resource E_j (MWh/year) was estimated from equation (5) from the evaluated yearly production $Q_{i,j,k}$ of methane (*k=1*) and ethanol (*k=2*). The net standard enthalpy of methane and ethanol are 0.8026E+9 and 1.235E+9J/kmol, respectively (Perry and Green, 1997). Accordingly, the heating values are W_1=35.8 MJ/m^3 of methane at standard conditions and W_2 =26.85E+3 MJ/ton of ethanol.

$$E_j = \frac{\sum_{i=1}^{m} \sum_{k=1}^{2} Q_{i,j,k} \cdot W_k}{3600}, \qquad m = \text{number of counties in each state} \qquad (5)$$

The waste resources to electricity life-cycle consists of three main processes: bioconversion process (e.g., anaerobic digestion or fermentation), operation and handling, and power generation. Each process has efficiency h_i, i=1:3 that depends on the applied technology. For each state, net biofuel for transportation $E_{\text{transportation}}$ TBtu/year and net electrical power $E_{\text{electricity}}$ TWh/year were evaluated according to equations (6) and (7) using the following reported efficiency factors. The bioconversion process efficiency is h_1=75% for methane production, according to Mata-Alvarez et al. (2000), assuming co-digestion of different solid wastes, and 65% for ethanol, as typically reported for fermentation of wheat straw (Börjesson and Mattiasson, 2008). Studying biomass conversion, Berglund and Börjesson (2006) reported that average energy input into large-scale biogas plants was approximately 30% of the energy content in the biogas produced. Accordingly, handling and operation efficiency was h_2 = 70%. Power generation efficiency or engine-generator efficiency was h =30% (Matteson and Jenkins 2007).

$$E_{\text{transportation}} = \sum_{j=1}^{n} E_j \cdot \frac{\prod_{i=1}^{2} h_i}{292.8} \qquad ,n = \text{number of wastes} \qquad (6)$$

$$E_{\text{electricity}} = \sum_{j=1}^{n} E_j \cdot \frac{\prod_{i=1}^{3} h_i}{1000} \qquad ,n = \text{number of wastes} \qquad (7)$$

3. Results and Discussion

3.1 Feedstock selection

The maximum methane production rates for California and Washington are listed in Table 3. The table shows the rank of each feedstock according to its annual mass and CH_4 production. In California, dairy manure and landfilled OFMSW (mainly food) had the highest potential biogas production. The result for Washington was similar although horse manure had the highest potential for biogas production since it is more concentrated as compared to dairy manure. However, spatial investigation showed that horse manure production is scattered all over the state and therefore transportation to treatment plants may increase costs. Also, horse manure is 30% TS and requires additional dilution with water before treatment, even with high solids digestion applications which normally handle a maximum of 20% solids. Therefore, further spatial investigation in this paper will focus on dairy manure and OFMSW in both California and Washington.

The maximum ethanol production for both California and Washington, provided that a pre-treatment for lignin separation is successful, is listed in Table 4. Paper from MSW represents the maximum source for ethanol production in both states. Wheat straw and lumber are the next ranked wastes for ethanol production in Washington. In California, lumber and rice straw are the next ranked wastes for ethanol production. Also, agricultural residues of cotton, wheat straw, and corn are considered sources for ethanol production in California

Table 3 Sorting wastes for maximum methane production in California and Washington states

Waste	California State				Washington State			
	total Q_W Dry tons/y	Rank/ Q_W	Total Q_{CH_4} M^3/y	Rank/ Q_{CH_4}	total Q_W Dry tons/y	Rank/ Q_W	Total Q_{CH_4} M^3/y	Rank/ Q_{CH_4}
Milk Cow Manure	3,857,800	1	805,990,093	1	446,537	1	117,058,058	2
MSW Food Waste Landfilled	1,920,700	3	784,733,420	2	246,011	3	102,529,321	3
Other Cattle Manure	3,652,400	2	763,076,940	3	-	-	-	-
Horse Manure	997,900	4	353,632,559	4	407,160	2	147,037,292	1
Biosolids Generation	800,000	6	246,722,667	5	94,820	5	29,242,804	6
Beef Cow Manure	868,600	5	195,901,149	6	242,404	4	5,8721,403	4
Poultry Manure	746,700	7	91,145,413	7	39,659	8	6,410,243	9
Meat Processing	79,490	8	3,3561,022	8	31,828	9	13,437,920	8
Cull potatoes	48,360	10	19,131,453	9	90,747	6	38,426,781	5
Sweet potatoes	12,990	11	5,496,376	10	-	-	-	-
Swine	49,400	9	3,322,123	11	6,592	10	1,855,884	11
Cull apples	-	-	-	-	40,262	7	17,657,818	7
Poultry meat	-	-	-	-	5,480	11	2,313,680	10
Pork meat	-	-	-	-	248	12	104,707	12

Table 4 Sorting wastes for maximum ethanol production in California and Washington states

Waste	California State				Washington State			
	total Q_W Dry tons/y	Rank/ Q_W	Total $Q_{Ethanol}$ ton/y	Rank/ $Q_{Ethanol}$	total Q_W Dry tons/y	Rank/ Q_W	Total $Q_{Ethanol}$ ton/y	Rank/ $Q_{Ethanol}$
Paper/card board	8,300,000	1	2,752,394	1	2,428,084	1	806,488	1
Wood /Lumber	3,700,000	3	1,287,135	2	834,057	3	289,818	3
Rice	1,676,300	2	556,783	3	-	-		
Cotton	973,580	4	358,200	4	-	-		
Wheat Straw	776,870	6	246,127	5	1,609,486	2	509,917	2
Grass /leaves	740,000	5	154,325	7	35,826	6	7,505	6
Corn Stover	508,870	7	163,820	6	45,637	5	14,691	5
Barley Straw	88,240	8	31,563	8	311,521	4	111,431	4

3.2 Spatial distribution

Most of the feedstock and potential methane and ethanol production in both states are collocated in cross-boundary counties. The next sections will describe the counties, their most suitable feedstock, and the corresponding maximum methane and ethanol production. It should be noted that the estimated methane and ethanol production rates are the maximum theoretical values. These rates are useful for future studies to benchmark different conversion technologies.

3.2.1 California State

3.2.1.1 *Methane*

The potential gas production in California from dairy manure only is shown in Figure 1. Most of this CH_4 could be generated by treating the dairy manure produced in Tulare, Merced, Stanislaus, Kings, Fresno, Madera, and San Joaquin counties. Yearly methane production potential, assuming complete degradation, is 207, 110, 85, 71, 51, 31, and 4.8 million m^3 CH_4/year, respectively, evaluated at standard temperature and pressure. The potential methane production from these 7 counties is 560 million m^3 CH_4/year that comprises 70% of the CH_4 production potential by digesting all manure produced from the state. These counties are in close proximity. Therefore, central anaerobic digester plants constructed and utilized for commercial energy production from manure are best located in these counties to minimize transportation costs.

Considering other animal and poultry manure types, the potential CH_4 production was mainly concentrated in the same counties. It is possible to co-digest different animal manures in these counties because of the close geographical location of the waste. In addition, Imperial County has a potential CH_4 production of 125 million m^3 CH_4/year from cattle manure, which would be

processed by other digestion plants due to its remote location compared to the other counties. Accordingly, the potential methane production, assuming complete anaerobic degradation of animal wastes in Tulare, Merced, Stanislaus, Kings, Fresno, Madera, San Joaquin and Imperial counties, is 1,250 million m^3 CH_4/year, which constitutes 67% of the CH_4 potential if digesting all the animal waste from the entire state of California. It is therefore worthwhile to build central digester plants for CH_4 and energy production in these eight counties, but more detailed cost and tipping fees analysis is required (Matteson and Jenkins, 2007).

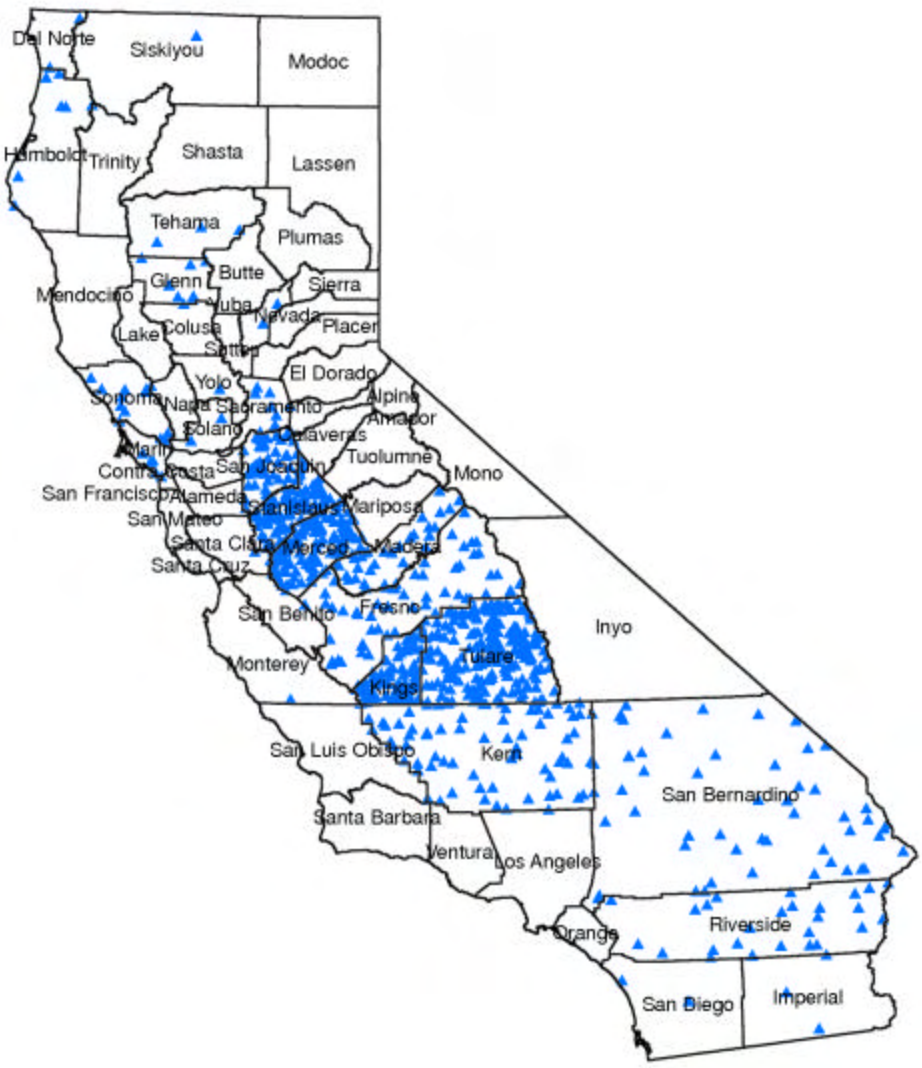

Figure 1 Potential methane production in California from dairy manure alone: each dot represents million m^3 methane/year

OFMSW is the second highest waste for biological CH_4 production in California. For the entire state 785 million m^3 CH_4/year are theoretically available if the OFMSW is completely stabilized. As highlighted in Figure 2, two AD centers in San Francisco and Los Angeles source 67% of all estimated CH_4 production in California, utilizing OFMSW. The indicated counties of San Francisco, Orange, Los Angeles, Alameda, Sacramento, San Mateo, Contra Costa, Santa Clara, San Diego, and Ventura constitute 8.5 % of the state area, and therefore central processing plants close to San Francisco and Los Angeles merit further investigation.

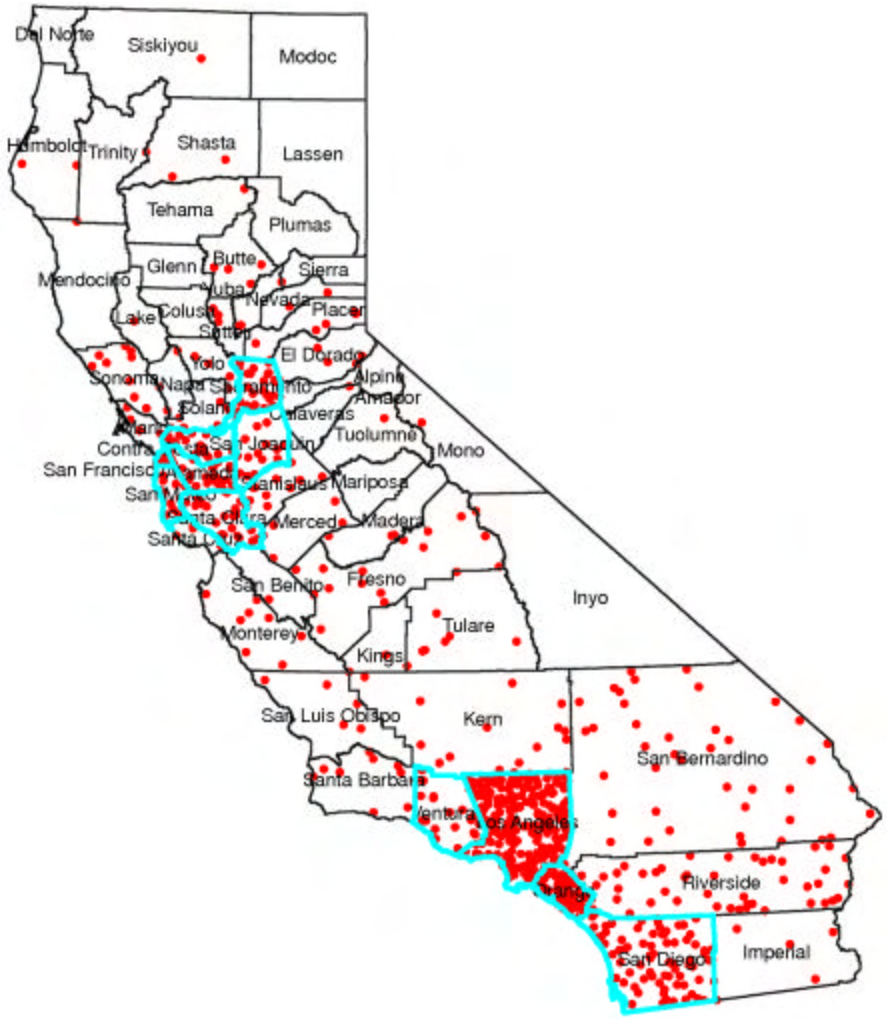

Figure 2: Potential methane production in California from MSW (land filled food waste fraction), each dot represents million m3 methane/year

3.2.1.2 *Ethanol*

The indicated counties for maximum methane production from manure are also best located for production of ethanol from cellulosic wastes, as shown in Figure 3.

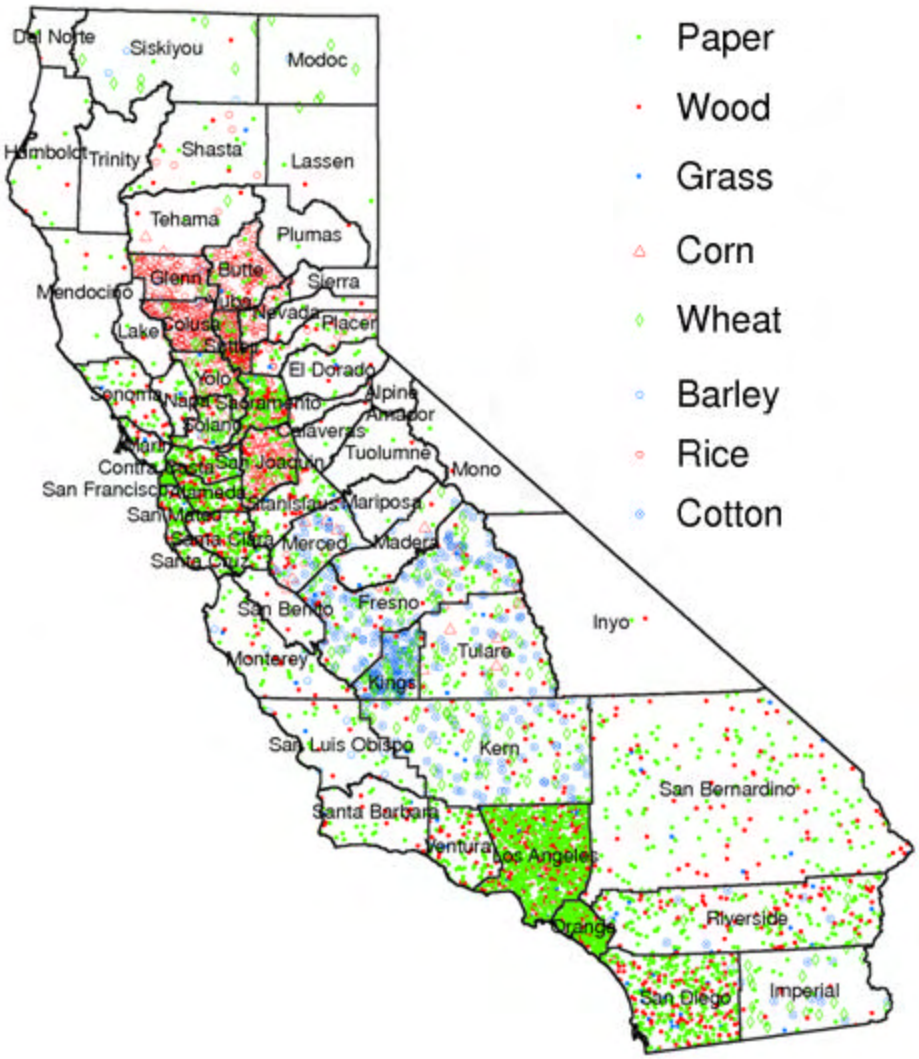

Figure 3 : Potential ethanol production in California from municipal and agricultural solid wates, each dot represents thousand ton ethanol/year

The four counties of Kings, Fresno, Kern, and Merced provide 85% and 40% of the state's total cotton stalk and wheat straw feedstock, respectively. San Joaquin and Sacramento counties provide 60% of the state's total corn stover feedstock. Moreover, the counties Colusa, Sutter, Butte, Glenn, Yuba and Yolo counties provide 90% of the state's rice straw

feedstock. The aforementioned feedstock portions and in the listed collocated counties would feed ethanol production plants with a maximum capacity of million tons of ethanol per year, assuming full conversion of cellulose and hemi-cellulose contents. Wood and paper feedstock are part of the MSW and can be found in the same locations as defined for CH_4 generation from OFMSW. The previously defined two central areas around San Francisco and Los Angeles produce 85% of the state's total wood and paper feed stock. The maximum potential ethanol production from these areas is ~ 3.4 million ton/year.

3.2.2 Washington State

3.2.2.1 *Methane*

Similar to the situation in California, the potential CH_4 production from OFMSW in Washington was concentrated in the most populated counties, while CH_4 potential was high in counties that are actively farmed, Figure 4. King, Pierce, Spokane, Snohomish, Cowlitz, and Clark counties generate 70% of Washington's potential CH_4 production from OFMS. The theoretical CH_4 production from these six counties was estimated to be 72 million m^3 CH_4/year with 27 million m^3 CH_4/year ultimately generated by digesting the OFMS from King county alone.

Yakima, Whatcom, Snohomish, Skagit, and Grant counties can generate 71% of Washington's potential CH_4 production from dairy manure. The theoretical CH_4 production from these five counties was estimated to be 67 million m^3 CH_4/year with 24 million m^3 CH_4/year ultimately generated digesting the dairy manure from Yakima county alone. Snohomish county also has a potential of CH_4 production from both OFMS and dairy manure that could be co-digested to ultimately produce 15.5 million m^3 CH_4/year.

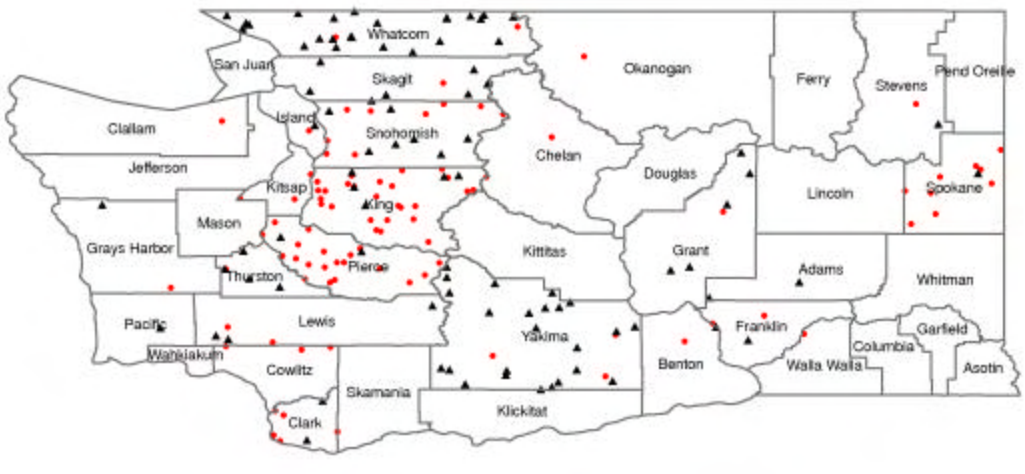

Figure 4 Potential methane production in Washington from MSW-food fraction (●) and manure (▲) each symbol represents million m3 methane/year

3.2.2.2 *Ethanol*

The maximum ethanol production from MSW paper and wood and agricultural crop residuals is shown in Figure 5. The counties of King, Pierce, Snohomish, and Spokane provide 60% of the state's total paper and wood feedstock for ethanol. The area for this feedstock portion has two centers, one in Spokane county and the other in King county. Instead of transporting from these centers to landfill and disposal sites, processing plants for ethanol production would be optimally located nearby these centers. The wood and paper wastes in these counties have a maximum potential for producing 670 thousand tons/year of ethanol.

Most of the cellulosic agricultural residuals are located in the southern and eastern counties. Corn stover is mainly located in Grant, Yakima, Franklin, and Adams counties with maximum potential of ethanol production of 15 thousand tons/year. Franklin, Whitman, Lincoln, Walla Walla, and Adams counties provide 75% of the wheat straw feed stock with maximum potential production of 380 thousand tons/year of ethanol. Whitman, Lincoln, Spokane, Garfield,

Columbia and Walla Walla counties provide more than 90% of the barley feed stock with maximum potential production of ethanol of 100 thousand tons/year.

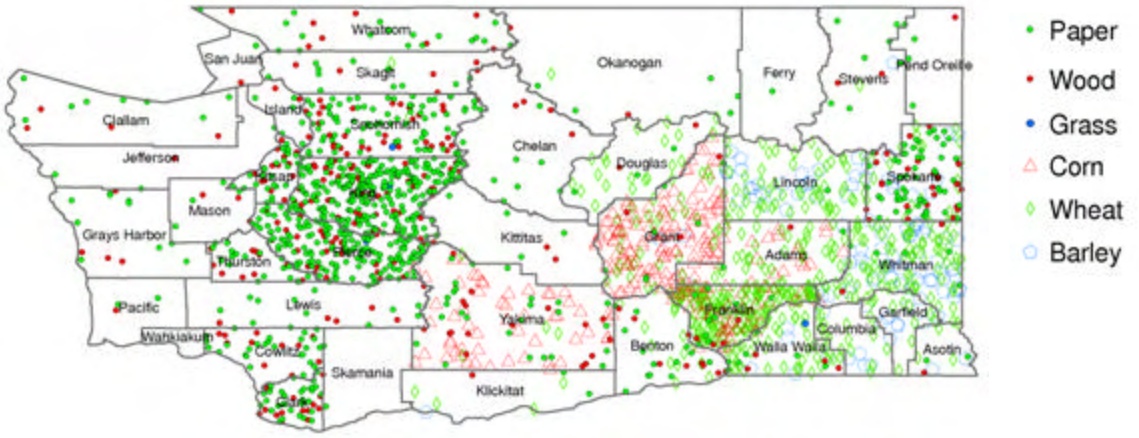

Figure 5 Potential ethanol production in Washington from municipal and agricultural solid wastes, each dot represents thousand ton ethanol/year

3.3 Maximum power potential

The distribution of electrical power from the solid wastes bioconversion to biogas and ethanol then to electricity in California and Washington is shown in Figure 6. It is clear that manures and OFMSW are the main wastes for power generation from CH_4 while MSW paper and MSW wood, and wheat straw (Washington) and rice straw(California) are the main wastes for power generation from ethanol. The total electrical consumption in 2005 for Washington was 80 TWh/year (CTED, 2007). The estimated net electrical power production utilizing methane and ethanol from the short-listed solid wastes was 2,6 TWh/year which represents 3.2% of the electrical requirement for the state of Washington. As transportation fuel (i.e. without accounting for engine-generator efficiency h =30%) the net methane and ethanol production is 29 TBtu/year which would source 4.7% of the total transportation fuel consumption in Washington. This

renewable fuel would therefore source more than three times the state natural gas consumption for transportation or would replace about 8.7% of the state distillate fuel from petroleum.

For California, the total electrical power consumption in 2005 was 272 TWh/year (CEC, 2005) and the estimated electrical power from ethanol and methane is 10.7 TWh/year, which represents 4% of the state electrical power requirements. The corresponding value as transportation fuel is 123 TBtu/year that would cover 3.7% of the total state's needs for transportation fuel. This is about 6 times the California state consumption of natural gas and it is equivalent to 6.2% of the state's use of motor gasoline according to the reported consumption in 2005 (U.S.EIA, 2008).

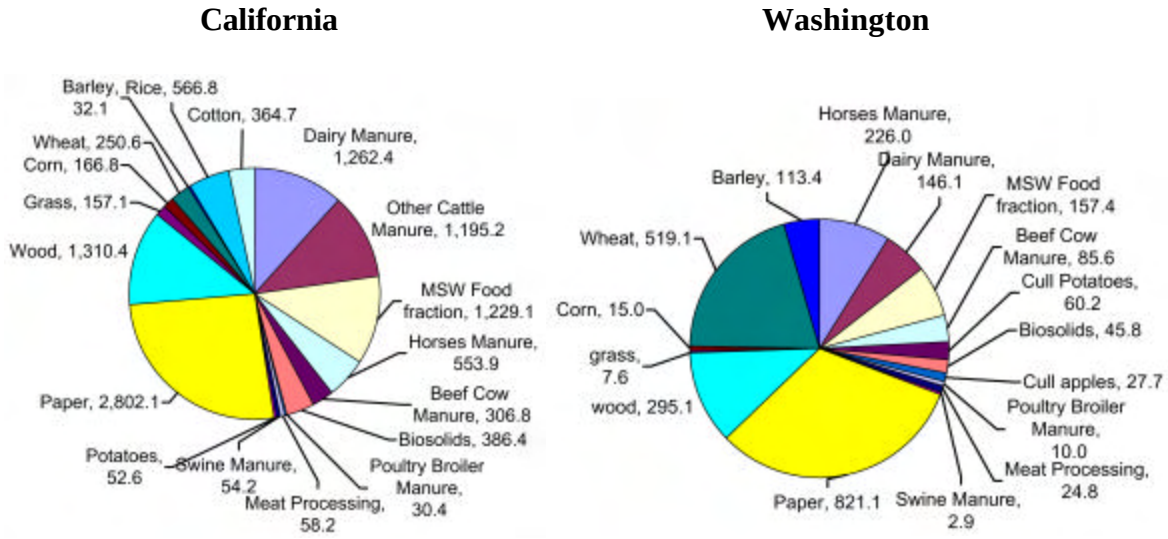

Figure 6 Distribution of estimated net power generation GWh/year from California and Washington solid wastes through ethanol and methane bio-production

The potential power generation is significant for some counties compared to their consumption which might encourage future local application of ethanol and methane production. For example, according to the consumption rates in 2005, Kings County in California would generate 17% of its electricity needs utilizing methane from dairy manure digestion and ethanol from corn stover fermentation. Detailed economic studies considering local county level power needs compared to the available feedstock would optimize such biofuel production.

4. Conclusions

A simple methodology was presented to assess the biomass inventories, to estimate potential bio-fuel production and to determine the location and scale for bio-fuel and bio-energy production. The presented case study of California and Washington states determined the potential feedstock for methane and ethanol production for each county and estimated the net power that can be recovered for transportation and electricity generation. The short listed wastes would replace ~ 6–8% of both state needs for motor gasoline for transportation. The estimated methane and ethanol production would increase both state's utilization of biomass as a renewable fuel for electricity production to 4 % and 3.2 % instead of the current utilization of 0.3 % and 0.7 % in California and Washington, respectively.

Cattle manure, rice straw, and MSW contain 80% of the potential methane and ethanol power production from solid wastes in California. Cattle manure, wheat straw, and MSW comprise 77% of the potential methane and ethanol power production from solid wastes in Washington. GIS mapping of the potential methane and ethanol production indicated some counties that would be optimal geographical location for treatment and processing plants of a particular feedstock or feedstock combinations. Accordingly, the evaluated GIS for maximum potential methane and ethanol production per feedstock per county in this paper is a useful tool for benchmarking different conversion systems/technologies and determining their optimal locations.

Acknowledgment

This work was partly funded by California Energy Commission and Washington State Department of Ecology.

References

Berglund, M., Börjesson, P., 2006. Assessment of energy performance in the life-cycle of biogas production. Biomass and Bioenergy, 30(3) , 254-266.

BFRS, California Biomass Facilities Reporting System, 2005. Resource Assessment, retrieved January 15, 2008 from http://cbc2.ucdavis.edu/cbc/biomassResource/resourceByCounty.asp

Börjesson, P., Mattiasson B. 2008. Biogas as a resource-efficient vehicle fuel. Trends in Biotechnology 26(1), 7-13.

Bungay, H. R., 2004. Confessions of a bioenergy advocate. TRENDS in Biotechnology. 22, 67-71.

CEC, California Energy Commission, 2005. California Electricity Consumption by County, retrieved January 15, 2008 from http://www.energy.ca.gov/electricity/electricity_by_county_2005.html

CTED, Washington State Department of Community, Trade and Economic Development (2007), Biennial Energy Report Issues and Analysis for the Washington State Legislature and Governor, retrieved June 19, 2008 from http://www.cted.wa.gov/

Demirbas, A., 2007. Progress and recent trends in biofuels. Progress in Energy and Combustion Science 33, 1-18.

ESRI, 2005. ArcMap Version 9.2. Environment Systems Research Institute Inc. Redlands, CA, USA

Faaij, A. P.C. (2006).Bio-energy in Europe: Changing technology choices. Energy Policy *34*, 322-344.

Foo, D.C.Y., Tan, R.R., Ng, D.K.S., 2008. Carbon and footprint-constrained energy planning using cascade analysis technique, Energy, In Press, Corrected

Gunaseelan, V. N., 1997. Anaerobic digestion of biomass for methane production: A review. Biomass and Bioenergy 13, 83-114.

Jiménez, L., Pérez, A., de la Torre, M.J., Moral, A., Serrano, L., 2007. Characterization of vine shoots, cotton stalks, Leucaena leucocephala and Chamaecytisus proliferus, and of their ethyleneglycol pulps. Bioresource Technology 98(18), 3487-3490.

Liao, W., Frear, C. and Chen, S., 2007. Biomass Inventory Technology and Economics Assessment, Report 1. Characteristics of Biomass, retrieved January 15, 2008 from http://www.ecy.wa.gov/biblio/0707025.html

Ma, J., Scott, N.R., DeGloria, S.D., Lembo, A.J., 2005. Siting analysis of farm-based centralized anaerobic digester systems for distributed generation using GIS. Biomass and Bioenergy 28, 591-600.

Mata-Alvarez, J., Mace, S., Llabres, P. 2000. Anaerobic digestion of organic solid wastes. An overview of research achievements and perspectives. Bioresource Technology 74(1), 3-16.

Matteson, G.C., Jenkins, B. M., 2007. Food and processing residues in California: Resource assessment and potential for power generation. Bioresource Technology 98, 3098-3105.

NCEES, National Council of Examiners for Engineering and Surveying, 2005. Fundamentals of engineering supplied-reference handbook, seventh edition, the National Council of Examiners for Engineering and Surveying, ISBN 1-932613-19-6.

Nonhebel S., 2005. Renewable energy and food supply: will there be enough land?. Renewable and Sustainable Energy Reviews. 9(2), 191-201.

Perry, R.H., Green, D.W., 1997. Perry's Chemical Engineers' Handbook (seventh ed.), McGraw-Hill, NY, USA.

PRBEP, Pacific Regional Biomass Energy Partnership, 2005. Washington State Biomass inventory by county, retrieved January 15, 2008 from http://www.pacificbiomass.org/Default.aspx?tabid=33.

Schacht, C., Zetzl, C., Brunner G., 2008. From plant materials to ethanol by means of supercritical fluid technology. The Journal of Supercritical Fluids, In Press, Corrected

U.S.EIA, Energy Information Administration – Official Energy Statistics from the U.S. government, 2008. Transportation Sector Energy Consumption Estimates, 2005. **http://www.eia.doe.gov/emeu/states/sep_sum/html/sum_btu_tra.html**

van Wyk, J. P.H., 2001. Biotechnology and the utilization of biowaste as a resource for bioproduct development. TRENDS in Biotechnology 19, 172-177.

Wang, Q., Ma, H., Xu, W., Gong, L., Zhang, W. Zou, D., 2008. Ethanol production from kitchen garbage using response surface methodology. Biochemical Engineering Journal 39(3) , 604-610.

Ward, A.J., Hobbs, P.J., Holliman, P.J., Jones, D.L., 2008. Optimisation of the anaerobic digestion of agricultural resources. Bioresource Technology, In Press, Corrected

Yuan, X.Z., Li, H., Zeng, G.M., Tong, J.Y., Xie, W., 2007. Sub- and supercritical liquefaction of rice straw in the presence of ethanol-water and 2-propanol-water mixture. Energy 32(11) , 2081-2088

Appendix 2: Simple ADM2 model and Dairy Manure Degradation Analysis

Zaher U., Pramod P., and Chen S. (2008) A simple elemental continuity based model to study the anaerobic microbial activity: Application to dairy manure, Applied Mathematical Modeling. (in press)

Applied Mathematical Modelling 33 (2009) 3553–3564

Contents lists available at ScienceDirect

Applied Mathematical Modelling

journal homepage: www.elsevier.com/locate/apm

A simple elemental continuity based model application to study the anaerobic microbial activity for the treatment of dairy manure

Usama Zaher *, Pramod Pandey, Shulin Chen

Department of Biological Systems Engineering, Washington State University, P.O. Box 646120, Pullman, WA 99164-6120, USA

ARTICLE INFO

Article history:
Received 18 August 2007
Received in revised form 3 November 2008
Accepted 14 November 2008
Available online 27 November 2008

Keywords:
Anaerobic digestion
Dairy manure
Elemental continuity
Nutrients recovery
Parameter identifiability
Process modeling

ABSTRACT

A simple anaerobic digestion (AD) model was formulated with emphasis on understanding the microbial activity during AD. The model was formulated according to two main rules that regulate the microbial growth. The first rule was maintaining the elemental continuity of macronutrients C, H, N, O, P, and S. The second rule satisfied the thermodynamics of the main AD catabolic reactions: acidogenesis and both acetotrophic and hydrogenotrophic methanogenesis. Accordingly, the stoichiometric parameters were evaluated as functions of the bacterial yield. The model also considered the enzymatic hydrolysis of solid waste. For a known solid waste composition, experimental data was utilized to estimate microbial initial concentrations, yields and kinetics, i.e., to achieve better understanding of the main AD microbial activity. The model was applied to three sets of batch experiments focusing on anaerobic dairy manure degradation. The model predicted the degradation dynamics, estimated the bacterial concentration in different inoculums, and evaluated the effect of inoculum ratios in speeding up the degradation. Elemental continuity based formulation of the model evaluated additional components that are necessary for future studies of macronutrients recovery, limitation/toxic effects, and chemical equilibrium.

1. Introduction

The anaerobic digestion (AD) process has been applied to treatment of wastes and biosolids for decades [1]. Recently, AD has received added attention since it produces biogas and releases nutrients that can be recycled to agriculture as natural fertilizers [2]. While more substrates, including wastes and crops for which the average composition is known, are being considered as a feedstock to AD [3], dairy manure is commonly used as a feedstock to AD for nutrient recovery [4] and biogas production [5].

This paper formulates a simple elemental continuity based AD model and applies it to dairy manure digestion. The objectives of this model application are: (1) to estimate bacterial concentrations and kinetics that are necessary to achieve anaerobic degradation and (2) to evaluate the corresponding biogas production. Furthermore, nutrients' release and uptake were considered in the model to define its stoichiometric parameters and to assess future studies of nutrients' recovery.

Several models have been developed to study the AD process and they can be classified into two categories – complex and simple [6]. On one hand, complex models consider most of the AD pathways to understand the process behavior. Hence, complex models have many parameters that are not identifiable from practical measurements. Simple AD models, on the other hand, consider the limiting process steps only, and therefore, can be applied to experimentation and parameter esti-

* Corresponding author. Tel.: +1 509 335 3743; fax: +1 509 335 2722.
E-mail addresses: zaheru@wsu.edu (U. Zaher), chens@wsu.edu (S. Chen).

0307-904X/$ - see front matter © 2008 Elsevier Inc. All rights reserved.
doi:10.1016/j.apm.2008.11.019

mation. In the case of soluble substrates (a simple model), the acidogenesis and methanogenesis steps are considered [7]. When solid substrates form a considerable part of the digester, the feed hydrolysis step is also considered [8–11].

Even with simple AD models there are parameter identifiability problems in that not all bioprocess model parameters (i.e., stoichiometry, kinetic parameters, and initial concentrations) are practically identifiable from available data [12]. Estimating stoichiometry of simple models by regression may require extension of model reactions to reproduce observed variability [13]. Extension of the model reactions introduces more kinetic parameters and complicates their estimation. When utilizing experimental data for estimation of stoichiometry, reduced information content is left to identify microbial activity in terms of their initial concentrations and kinetics. Therefore, other simple AD model formulations define the stoichiometry during the model formulation and spare the experimental data for the estimation of kinetic and initial concentration parameters. Assuming a fixed biomass (bacteria) yield per adenosine triphosphate (ATP) yield of limiting reactions as in [10] determines the model stoichiometry by summing anabolic and catabolic reactions. Although all model stoichiometry is defined this way, the model application is limited to optimal conditions. These models assume only CHNO elemental composition of the biomass and substrate. Thus, these models are suitable for estimating process kinetics assuming that other growth macronutrients, i.e., P and S, are redundant and other environmental conditions are optimal for the assumed ATP production.

Therefore, the new model in this paper was formulated to estimate process kinetics during optimal conditions as well as suboptimal conditions of nutrient limitations and inhibiting environmental factors. Elemental continuity was exploited to balance all macronutrients, including P and S. To extend the applicability of the model during inhibiting environmental factors, values of biomass yield were estimated from measurements and were not fixed in proportion to the theoretical ATP production. The stoichiometric parameters of the model were defined *a priori* as functions of the microbial yield satisfying the thermodynamics of the catabolic reactions and considering the carbon sourcing for bacterial anabolism. The model was calibrated and validated with three sets of batch experiments. Microbial initial concentrations and kinetics were estimated to predict the general behavior of anaerobic degradation of dairy manure.

2. Methods

2.1. General model

2.1.1. Model structure

Fig. 1 shows schematically the modeled biological reactions. Four main steps in the AD process were considered: (1) hydrolysis, (2) acidogenesis, (3) hydrogenotrophic methanogenesis, and (4) acetotrophic methanogenesis. Hydrolysis breaks down the particulate substrate (X_0) to soluble substrates such as sugars. Hydrolysis is typically assumed to be driven by extra-cellular enzymes. The next three steps were related to the observed main pathways of the AD process. In the second step, the hydrolysis products (S_1) are smaller molecules that are ingested by the first bacterial group, acidogens (X_1), to produce volatile fatty acids (S_2) and gases (CO_2 and H_2). Then two pathways are followed to produce methane (CH_4). In the acetotrophic methanogenesis pathway, the second bacterial group (X_2) converts (S_2) to CH_4 and CO_2. In the other pathway of hydrogenotrophic methanogenesis, the third bacterial group (X_3) utilizes CO_2 and H_2 to produce CH_4. Through elemental mass balance of C, H, N, O, P, and S, nutrient release was considered during the hydrolysis step. Nutrient uptake was evaluated according to the net growth of the three bacterial groups presented in the model.

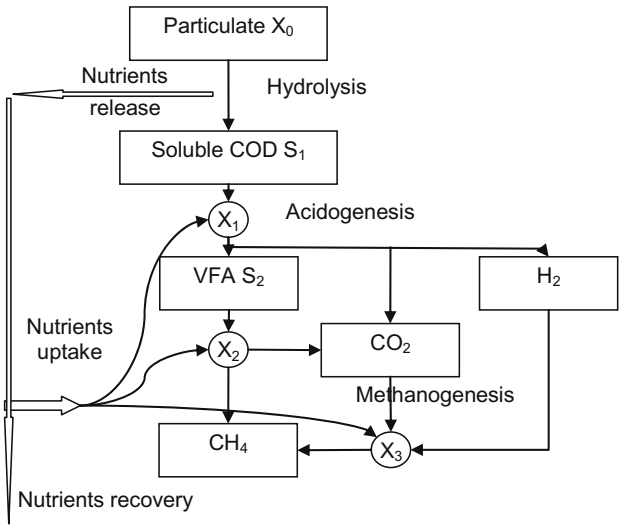

Fig. 1. Proposed model structure and nutrient release/uptake mechanisms.

2.1.2. Biological reaction rates

Hydrolysis of particulates X_0 was considered in this model as a first order reaction as shown in Eq. (1). The particular application in this paper applied low solids to biomass ratios due to initial bacterial concentrations in manure and added inoculums. Complex hydrolysis models such as the Contois model [14] are needed if biomass concentrations are low compared to X_0 [15]. The Contois model is equivalent to first order kinetics for low solids to biomass ratio [14]. Acidogenesis was modeled using Monod kinetics as shown in Eq. (2). Haldane kinetics in Eq. (3) was assumed for the volatile fatty acids (VFA) uptake by acetoclastic methanogenesis according to [7]. Haldane kinetics accounts for substrate inhibition. So, acetoclastic methanogenesis inhibition due to VFA accumulation [16] was considered. Hydrogenotrophic methanogens were considered to follow Monod kinetics as shown in Eq. (4):

$$r_0 = k_{\text{hyd}} X_0, \tag{1}$$

$$r_1 = k_{m,S_1} X_1 = \frac{k_{\max,S_1} S_1}{k_{s,S_1} + S_1} X_1, \tag{2}$$

$$r_2 = k_{m,S_2} X_2 = \frac{k_{\max,S_2} S_2}{k_{s,S_2} + S_2 + \frac{S_2^2}{k_{I,S_2}}} X_2, \tag{3}$$

$$r_3 = k_{m,h_2} X_3 = \frac{k_{\max,h_2} h_2}{k_{s,h_2} + h_2} X_3, \tag{4}$$

where r_{0-3} are rates of the four reactions considered in the model; k_{hyd} is the first order hydrolysis rate; $k_{m,i}$ ($i = \{S_1, S_2, h_2\}$) are the specific uptake rates of soluble substrates and hydrogen; $k_{\max,i}$ are the maximum specific uptake rates; $k_{s,i}$ are the Monod affinity (half-saturation) constants; and k_{I,S_2} is inhibition constant for S_2 uptake.

2.1.3. Model matrix

The general model is presented by the Petersen matrix format in Table 1. The rows of the matrix present the four modeled reactions followed by the composition matrix of the theoretical chemical oxygen demand (ThOD) and elemental composition of all model variables. The columns of the matrix present the metabolites of the biological reactions, the bacterial groups and nutrient components. In addition to the enzymatic hydrolysis, the three biological steps were considered according to the following catabolic reactions:

$$C_6H_{12}O_6 + 2H_2O \rightarrow 2CH_3COOH + 2CO_2 + 4H_2, \tag{5}$$

$$CH_3COOH \rightarrow CH_4 + CO_2, \tag{6}$$

$$4H_2 + CO_2 \rightarrow CH_4 + 2H_2O. \tag{7}$$

These reactions produce the highest free energies to maintain the bacterial catabolism. Parallel to these catabolic reactions, anabolism was considered by evaluating the model stoichiometry as functions of the yield of each bacterial group Y_{1-3} using the elemental mass balance of nutrients. The composition of all model components and elemental mass balances were evaluated according to elemental continuity transformation methods illustrated in [17]. The stoichiometric parameters were evaluated as functions of the bacterial yield and the composition of model components. The inorganic carbon (IC), inorganic nitrogen (IN), inorganic phosphorous (IP), hydrogen sulfide (H_2S), water (H_2O), protons H^+ and cations components were added to the model to account for nutrient release and uptake. Those components were used to close the elemental mass balance of C, N, P, S, O, H, and charge, respectively. The added components are buffers that enable accurate pH evaluation and future model extension with chemical equilibrium modeling.

Easily degradable substrates (mainly sugars) S_1 produced from hydrolysis are acidified according to the catabolic reaction (5), as reported in [18]. Parallel to the catabolic reaction, some S_1 is utilized for anabolism [10]. Thus, the final conversion stoichiometry was calculated from the theoretical chemical oxygen demand COD (ThOD) and carbon balances while maintaining the molar ratio of the catabolic reaction products. Eq. (8) specifies the stoichiometry of VFA as acetate (k_2) from the ThOD balance. Eq. (9) specifies the CO_2 stoichiometric coefficient (k_4) from the carbon balance. Eq. (10) specifies the stoichiometry of hydrogen (k_{10}) such that 2 moles of hydrogen are produced for each mole of acetate produced

$$k_2 = -\frac{1}{\text{ThOD}_{S_2}} \sum_{\forall i \neq \text{CO}_2} \text{ThOD}_i v_{i,r_1}, \tag{8}$$

$$k_4 = -\frac{1}{C_{\text{CO}_2}} \sum_{\forall i \neq \text{CO}_2} C_i v_{i,r_1}, \tag{9}$$

$$k_{10} = 32/60 k_2. \tag{10}$$

The acetotrophic methanogens follow the catabolic reaction (6), as reported in [18]. The methane stoichiometric coefficient (k_6) was calculated from the ThOD balance, as in Eq. (11). According to the catabolic reaction (6), the CO_2 stoichiometric coefficient was evaluated by Eq. (12)

Table 1
General Petersen matrix presentation of the high solids anaerobic digestion model.

Component (i)	Degradable substrate (as sugars) (S_1)	VFA (as acetate) (S_2)	Hydrogen (H_2)	Carbon dioxide (CO_2)	Methane (CH_4)	Biosolids (X_6)	Bacteria			Bicarbonate (IC)	Ammonium (IN)	Phosphates (IP)	Hydrogen sulphide (H_2S)	Moisture (H_2O)	Protons (H^+)	Cations (Cat^+)	Specific process rate (concentration/d)
							X_1	X_2	X_3								
Process (r)	kg COD/m^3	kg/m^3	kg COD/m^3	kmol/m^3	kg COD/m^3	kg/m^3	kg COD/m^3	kg COD/m^3	kg COD/m^3	kmol C/m^3	kmol N/m^3	kmol P/m^3	kmol S/m^3	kmol/m^3	kmol/m^3	kmol/m^3	
Hydrolysis	$(\mathrm{ThOD}_{X_0} - 2 * S_{X_0})/1000$					-1				$\sum_{\forall i \neq \mathrm{IC}} C_i \nu_{i,r_0}$	$\mathrm{N}_{X_0}/14{,}000$	$\mathrm{P}_{X_0}/30{,}973$	$\mathrm{S}_{X_0}/32{,}000$	$-\sum \mathrm{O}_{i,r_0}/16{,}000$	$-\sum \mathrm{H}_{i,r_0}/1000$	$-\sum \mathrm{Ch}_{i,r_0}/1000$	r_0
Acidogenesis	-1	k_2	k_{10}	k_4			Y_1			0	$Y_1 * \mathrm{N}_{X_i}/14{,}000$	$-Y_1 * \mathrm{P}_{X_i}/30{,}973$	$-Y_1 * \mathrm{S}_{X_i}/32{,}000$	$-\sum \mathrm{O}_{i,r_1}/16{,}000$	$-\sum \mathrm{H}_{i,r_1}/1000$	$-\sum \mathrm{Ch}_{i,r_1}/1000$	r_1
Ac-methanogenesis		-1		k_5	k_6			Y_2		$\sum_{\forall i \neq \mathrm{IC}} C_i \nu_{i,r_2}$	$Y_2 * \mathrm{N}_{X_i}/14{,}000$	$-Y_2 * \mathrm{P}_{X_i}/30{,}973$	$-Y_2 * \mathrm{S}_{X_i}/32{,}000$	$-\sum \mathrm{O}_{i,r_2}/16{,}000$	$-\sum \mathrm{H}_{i,r_2}/1000$	$-\sum \mathrm{Ch}_{i,r_2}/1000$	r_2
H-methanogenesis			-1	k_8	k_7				Y_3	$\sum_{\forall i \neq \mathrm{IC}} C_i \nu_{i,r_3}$	$Y_3 * \mathrm{N}_{X_i}/14{,}000$	$Y_3 * \mathrm{P}_{X_i}/30{,}973$	$-Y_3 * \mathrm{S}_{X_i}/32{,}000$	$-\sum \mathrm{O}_{i,r_3}/16{,}000$	$-\sum \mathrm{H}_{i,r_3}/1000$	$-\sum \mathrm{Ch}_{i,r_3}/1000$	r_3
ThOD (gCOD)	1000.0	1066.7	1000.0	0.0	1000.0	ThOD_{X_0}	ThOD_{X_i}	ThOD_{X_i}	ThOD_{X_i}				64000.0				
C (g)	375.0	400.0		12000.0	187.5	C_{X_0}	C_{X_i}	C_{X_i}	C_{X_i}	12000.0							
H (g)	62.5	66.7	125.0		62.5	H_{X_0}	H_{X_i}	H_{X_i}	H_{X_i}	1000.0	4000.0		2000.0	2000.0	1000.0		
N (g)						N_{X_0}	N_{X_i}	N_{X_i}	N_{X_i}		14000.0						
O (g)	500.0	533.3		32000.0		O_{X_0}	O_{X_i}	O_{X_i}	O_{X_i}	36000.0		64000.0		16000.0			
P (g)						P_{X_0}	P_{X_i}	P_{X_i}	P_{X_i}			30973.0					
S (g)						S_{X_0}	S_{X_i}	S_{X_i}	S_{X_i}				32000.0				
Ch (Equ.)						Ch_{X_0}	Ch_{X_i}	Ch_{X_i}	Ch_{X_i}	-1000.0	1000.0	-3000.0		0.0	1000.0	1000.0	

$$k_6 = -\frac{1}{\mathrm{ThOD}_{CH_4}} \sum_{\forall i \neq CH_4} \mathrm{ThOD}_i v_{i,r_2}, \tag{11}$$

$$k_5 = -\frac{1/64}{\mathrm{ThOD}_{CH_4}} \sum_{\forall i \neq CH_4} \mathrm{ThOD}_i v_{i,r_2}. \tag{12}$$

Hydrogenotrophic methanogens follow the catabolic reaction (7), also as reported in [18]. The methane stoichiometric coefficient (k_7) was calculated from the ThOD balance Eq. (13). The CO_2 stoichiometric coefficient was calculated according to the catabolic reaction by Eq. (14)

$$k_7 = -\frac{1}{\mathrm{ThOD}_{CH_4}} \sum_{\forall i \neq CH_4} \mathrm{ThOD}_i v_{i,r_3}, \tag{13}$$

$$k_8 = \frac{1/64}{\mathrm{ThOD}_{CH_4}} \sum_{\forall i \neq CH_4} \mathrm{ThOD}_i v_{i,r_2}. \tag{14}$$

2.2. Validation and calibration experiments

Three sets of batch experiments were used to calibrate and validate the model. In each batch reactor, dairy manure was incubated both with and without external inoculums in 100 ml serum bottles at 35 °C. Continuous mixing was maintained in all batch experiments using a shaker. The produced gas was evacuated and collected daily using a syringe. In addition to the common practice of measuring initial and final concentrations of incubated serum bottles, several measurements were performed daily for replicate bottles or for extracted and diluted samples. Daily samples were analyzed for total solid (TS), total volatile solids (TVS), volatile fatty acids (VFA), and total chemical oxygen demand CODt using standard methods. Each set of experiments was configured differently, i.e., by changing the manure source, inoculation source/ratio, and incubation time, as described in the following paragraphs, to test microbial activity in degrading dairy manure and to use different model calibration strategies.

2.2.1. Different inoculums

Dairy manure (Washington State University, Dairy Center) was collected and screened on 0.0331 in. mesh size and diluted with tap water to about 1.7% TS and stored at 5 °C for 30 days. The manure was homogenized and mixed with different inoculum sources at 1:4 inoculum to manure volume ratio. A control batch experiment was done for manure only (a). Other experiments used inoculums of granular sludge from an industrial upflow anaerobic sludge bed (UASB) reactor (b), sludge from anaerobic lagoon treating the same manure (c), and decanting water from a secondary anaerobic digester treating domestic sludge (d) (City of Pullman Wastewater Treatment Plant, WA, USA). Incubation time was set to 10 days, and each experiment was done in 10 replicates where one replicate reactor was discarded each day after analyzing its liquid content. Thus, gas measurements were averaged among the replicates with a reduced number toward the end of the experiment. Averaging the gas measurements with the larger number of samples toward the start of each experiment was designed to test the adequacy of replicates and gas collection accuracy.

2.2.2. Different inoculum ratios

One set of batch experiments was designed to test the effects of different granular sludge inoculum ratios on flush dairy manure degradation. Dairy manure waste was collected from the influent to Washington State University pilot digesters at the University Dairy Center. The manure originates from a flush system using lagoon water, and was collected after fiber screening that reduces solids to an average of approximately 2% TS. The collected manure was homogenized and then mixed with homogenized granule inoculum from the industrial UASB with inoculum ratios of 0%, 7%, 9%, 12%, 15%, 18%, and 20%. Each mixture was incubated in the serum bottles for 60 days.

2.2.3. Validation experiment

A batch experiment utilizing a different source of flush dairy manure was performed to validate the model. A sample was collected from the influent to a pilot fixed bed digester (JUB Engineers Inc., Kennewick, WA). The influent was collected after fiber screening of flush dairy manure (from 5-D Farms, Pasco, WA) during a period of using groundwater instead of lagoon water in the flush system. The sample was immediately incubated without inoculation for 60 days. The simulation results were compared statistically to measurements. Excluding the data outliers, the correlation coefficient, R, of the measured values to the corresponding simulation values was determined. The probability of no correlation hypothesis, P, was evaluated using the t-statistic with a 95% confidence interval ($\alpha = 0.05$).

2.3. Model implementation and calibration

The model matrix was evaluated for dairy manure, Table 2. The stoichiometric formula of bacteria is assumed to be $C_5H_7NO_2P_{0.06}S_{0.1}$ according to [19]. The model was implemented in AQUASIM [20]. Simplex algorithm [21] was used for

Table 2
model matrix for dairy manure measured composition and biomass stoichiometric formula of $C_5H_7NO_2P_{0.06}S_{0.1}$.

Component (i)	Degradable substrate (as sugars) (S_1)	VFA (as acetate) (S_2)	Hydrogen (H_2)	Carbon dioxide (CO_2)	Methane (CH_4)	Biosolids (X_6)	Bacteria			Bicarbonate (IC)	Ammonium (IN)	Phosphates (IP)	Hydrogen sulphide (H_2S)	Moisture (H_2O)	Protons (H^+)	Cations (Cat^+)	Specific process rate (concentration/d)
							X_1	X_2	X_3								
Process (r)	kg COD/m^3	kg/m^3	kg COD/m^3	kmol/m^3	kg COD/m^3	kg/m^3	kg COD/m^3	kg COD/m^3	kg COD/m^3	kmol C/m^3	kmol N/m^3	kmol P/m^3	kmol S/m^3	kmol/m^3	kmol00/m^3	kmol/m^3	
Hydrolysis	1.1587					−1				1.2919E−3	1.8786E−3	1.5497E−4	1.5312E−4	−6.25E−5 $\sum O_{i,r_0}$	−1E−3 $\sum H_{i,r_0}$	−1E−3 $\sum Ch_{i,r_0}$	r_0
Acidogenesis	−1	$-0.6Y_1 + 0.625$	32/60($-0.6Y_1$ + 0.625)	$-0.01Y_1 + 0.0104$			Y_1			0	$-5.9786E{-}3Y_1$	$-3.5838E{-}4Y_1$	$-0.6E{-}3Y_1$	−6.25E−5 $\sum O_{i,r_1}$	−1E−3 $\sum H_{i,r_1}$	−1E−3 $\sum Ch_{i,r_1}$	r_1
Ac-methanogenesis		−1		$(-0.9616Y_2 + 1.0667)/64$	$-0.9616Y_2 + 1.0667$			Y_2		$-1.4883E{-}2Y_2$	$-5.9786E{-}3Y_2$	$-3.5838E{-}4Y_2$	$-0.6E{-}3Y_2$	−6.25E−5 $\sum O_{i,r_2}$	−1E−3 $\sum H_{i,r_2}$	−1E−3 $\sum Ch_{i,r_2}$	r_2
H-methanogenesis			−1	$(-0.9616Y_3 + 1)/64$	$-0.9616Y_3 + 1$				Y_3	$-1.4883E{-}2Y_3$	$-5.9786E{-}3Y_3$	$-3.5838E{-}4Y_3$	$-0.6E{-}3Y_3$	−6.25E−5 $\sum O_{i,r_3}$	−1E−3 $\sum H_{i,r_3}$	−1E−3 $\sum Ch_{i,r_3}$	r_3
ThOD (gCOD)	1000.0	1066.7	1000.0	0.0	1000.0	1168.4578	1000	1000	1000				64000.0				
C (g)	375.0	400.0		12000.0	187.5	450.0	358 9	358.9	358.9	12000.0							
H (g)	62.5	66.7	125.0		62.5	62.5	41.9	41.9	41.9	1000.0	4000.0		2000.0	2000.0	1000.0		
N (g)						26.3	83.7	83.7	83.7		14000.0						
O g	500.0	533.3		32000.0		500.0	191.4	191.4	191.4	36000.0		64000.0		16000.0			
P (g)						4.8	11.1	11.1	11.1			30973.0					
S (g)						4.9	19.2	19.2	19.2				32000.0				
Ch (Equ.)										−1000.0	1000.0	−3000.0		0.0	1000.0	1000.0	

all model calibrations. Measured variables were simulated by adding the corresponding model state variables after adjusting their stoichiometric units. For example, TS (g/l) was simulated by adding all particulate components after converting their stoichiometric units to g/l according to the assumed composition in Table 2, i.e., $TS = X_0 + 0.7\sum_{i=1:3} X_3$.

For experiments testing different inoculums, kinetics for the acidogensis and methanogenesis steps were set to the values given in [7], since they estimated the kinetic parameters using the same Monod and Haldane kinetics in a two step acidogensis–methanogensis model. Accordingly, for these experiments, only two biomass populations were considered in the present model, assuming that both hydrogenotrophic and acetotrophic methanogens are carried out by X_2. The TS, VFA, and gas production measurements were used to estimate the hydrolysis first order rate constant k_{hyd}, and the initial biomass populations for each inoculum. Measured variables were simulated by adding the corresponding model state variables after adjusting their stoichiometric units. For example, TS was simulated by adding all particulate components after converting their stoichiometric units to g/l according to the assumed composition in Table 2, i.e., $TS = X_0 + 0.7\sum_{i=1:3} X_3$.

An advanced technique was then used to calibrate the model parameters for flush dairy manure. The model was calibrated using the whole set of batch experiments for testing different inoculum ratios at the same time. Initial concentration of biomass species was assumed for both manure and granular inoculum. Then the initial values for each experiment were set proportional to the inoculum to waste ratios. Accordingly, the initial concentrations of the three biomass groups of the model were reduced to six parameters instead of 21 for the seven experiments. The model was calibrated running the simplex minimization algorithm twice. The first time all model parameters were estimated to obtain the best fit achieved in a maximum of 10,000 simulations, and the same hydrolysis rate estimated from the previous set of batch experiments since the solid substrate is almost the same, i.e., originating from dairy manure. The second calibration was to improve the estimated values of the acidogens' and methanogens' initial concentrations for flush dairy manure and granule inoculums using the entire set of batch experiments.

The model was then validated using the batch experiment of the other flush dairy manure source, as defined above in the validation experiment. All model parameters were used from the previous calibration experiment, except the acidogens' and acetotrophic methanogens' initial concentrations that were calibrated first using the gas measurements only. Other measurements were used for validation.

3. Results

For measured manure composition and assumed biomass formula, the model stoichiometry was explicitly determined for the hydrolysis step. For the acidogensis and methanogenesis steps the stoichiometric parameters were determined as functions of the biomass yield. Evaluating the model stoichiometric parameters *a priori* allowed the utilization of measurements for estimation of the kinetic and initial concentration parameters, as illustrated in the following results.

3.1. Simulating different inoculum effects

Batch experiments with 10 days incubation time were used to estimate the initial concentrations of biomass and the hydrolysis constant using TS, VFA, and gas production measurements. Estimated initial acidogens concentrations were 1.43, 1.20, 1.51, and 1.30 gCOD/l for manure alone, manure with granules, anaerobic lagoon sludge, and decanting water from a secondary digester, respectively. Estimated initial methanogens were, respectively, 0.24, 0.77, 1.53, and 0.99 gCOD/l. With these estimated parameters, the model could simulate main experiment dynamics as shown in Fig. 2. The figure presents the TS that is related to the model hydrolysis step, VFA that is related to the model acidogenesis step and gas flow that is related to methanogenesis. These results are presented for different experimental data sets using the different sources of bacterial inoculum. Slow hydrolysis was indicated by the estimated small value of the hydrolysis constant, $k_{hyd} = 0.0035\ d^{-1}$, that was presented by the gentle slope of the simulated TS for all types of inoculums. Additional degradation dynamics were simulated for the VFA and gas flow. A VFA peak occurred at different times for different inoculums. Also, maximum gas flow was reached at different times for different inoculums. The standard deviation of the gas flow measurements was relatively small which indicates the validity of replicates.

3.2. Model calibration varying inoculum ratio

Model kinetic parameters were estimated by fitting a set of experiments with variable experiment ratios. However, optimization criteria were not met after the first optimization run for 10,000 simulations. Parameter values for the best fit model are listed in Table 3, in comparison to the literature values that were used in the previous simulations using different inoculums. Using the best fit values of the kinetic parameters, the second optimization run converged to the initial acidogens X_1 and acetotrophic methanogens X_2 concentrations of both flush dairy manure and granular sludge as if they were separate. Flush manure was initially rich in acidogens (initial $X_1 = 2.06$ gCOD/l) compared to acetotrophic methanogens (initial $X_2 = 0.68$ gCOD/l). On the contrary, granular sludge inoculum was richer in acetotrophic methanogens (initial $X_2 = 2.79$ gCOD/l), compared to acidogens (initial $X_1 = 0.00056$ gCOD/l).

The effect of the inoculum ratio was therefore evident from the gas flow simulation of the seven batch experiments, as shown in Fig. 3. The figure shows the biogas production along the 60 day incubation period and for different inoculum ratios

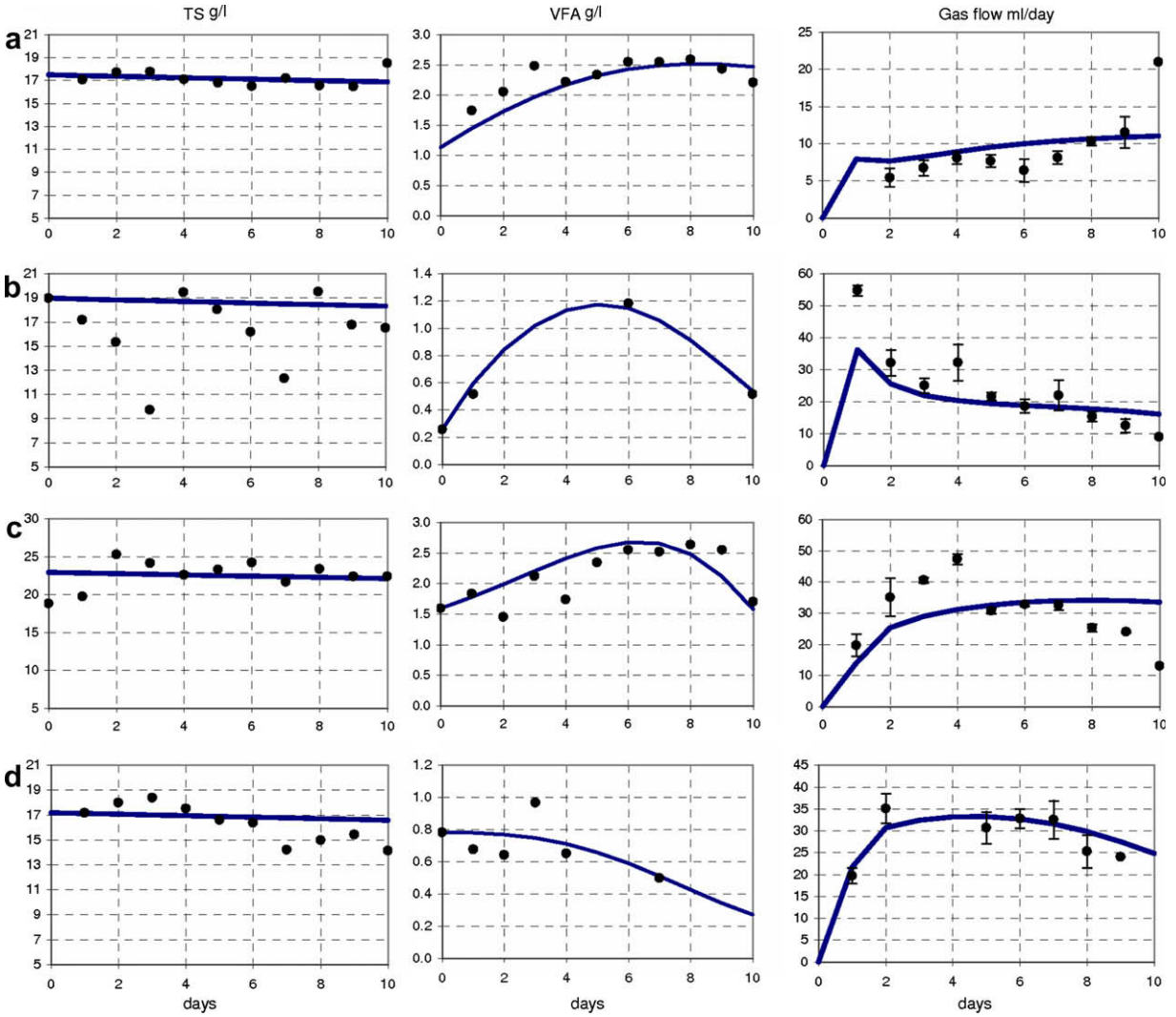

Fig. 2. Batch experiment results testing different inoculums for flush dairy manure digestion: (a) manure only, (b) manure + granular sludge, (c) manure + lagoon inoculum, and (d) manure + domestic anaerobic sludge from a secondary digester. Continuous lines are simulations and dots are experimental data.

Table 3
Best fit estimate of the model parameters.

Parameter	Unit	Symbol	Estimated value	Literature value[a]
Hydrolysis rate constant	d^{-1}	k_{hyd}	0.0036	–
Maximum specific uptake rate of S_1	d^{-1}	k_{max,S_1}	2.11	1.2
Half-saturation constant of S_1	gCOD/l	k_{s,S_1}	4.66	7.1
Yield of acidogens X_1	–	Y_1	0.15	0.14
Maximum specific uptake rate of S_2	d^{-1}	k_{max,S_2}	0.26	0.74
Half-saturation constant of S_2	g/l	k_{s,S_2}	0.22	0.56
Inhibition constant for S_2 uptake	g/l	k_{I,S_2}	5.7	15.36
Yield of acetotrophic methanogens X_2	gCOD/g	Y_2	0.10	0.07
Maximum specific uptake rate of H_2	d^{-1}	k_{max,h_2}	25.97	–
Half-saturation constant of H_2	gCOD/l	k_{s,h_2}	0.75	–
Yield of hydrogenotrophic methanogens X_3	–	Y_3	0.01	–

[a] Obtained from [7] after unit adjustment.

applied to the seven batch experiments. The biogas production reached an initial maximum within the first two days independent of the inoculum ratio. The initial peak was followed by a decrease in the biogas production, and the decrease

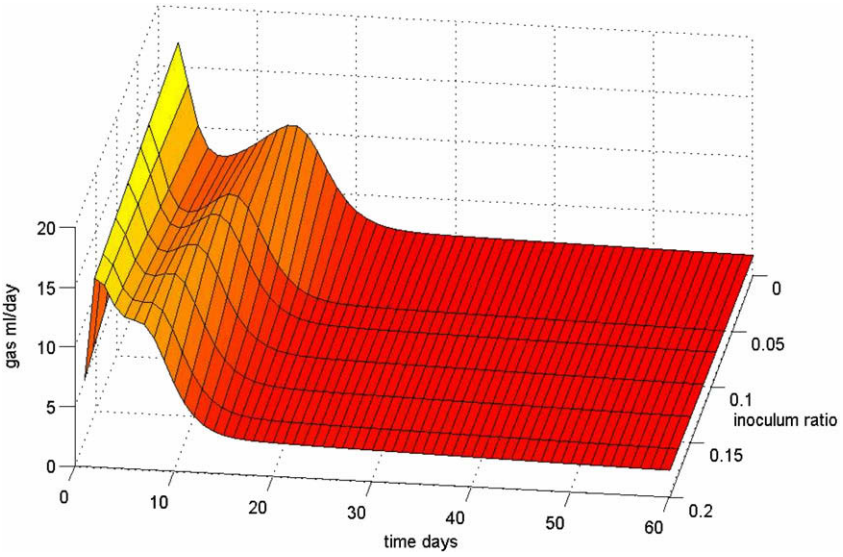

Fig. 3. Effect of granular sludge inoculum ratio on the degradation and biogas production from flush dairy manure.

was followed by a second peak. The biogas production dropped again to a minimum and continued until the end of the experiment. The duration between the two biogas peaks was shorter with the increase of the inoculum ratio. The ultimate minimum of biogas production was reached in a shorter time with the increase of the inoculum ratio.

3.3. Model validation using another manure source

Using the estimated parameters in Table 3, the model was validated by simulating a 60-day batch experiment after estimation of initial biomass concentration. The initial acidogens and methanogens concentrations were different. Initial acidogens concentration was 0.031 gCOD/l while acetotrophic and hydrogenotrophic methanogens were 0.404 and 0.014 gCOD/l, respectively. The simulated dynamics were in agreement with the measurements, as shown in Fig. 4. The figure compares the model predictions of TS, total COD, VFA (S_2) and gas flow against measured data. Using the intial concentrations of these components as the model inputs the model predicted the TS and COD by the end of the experiment and showed the dynamic evolutions of VFA and biogas production without using the measurements for regression or calibration. Slow hydrolysis was represented by the gentle slope of TS dynamics, while CODt slope was comparably steeper. The VFA was initially decreasing, then increased to a peak as observed at 25 days. A peak was observed in the gas flow at 20 days, i.e., just before the VFA peak at 25 days. Another small peak occurred in the biogas production at 45 days.

Statistically, the correlation between simulation and measurement was significant. The correlation coefficients were 0.76, 0.9, 0.9, and 0.83 for the TS, VFA, CODt, and gas production, respectively. The probabilities of no correlation between measurements and simulation results were, respectively, 0.025, 0.006, 0.005, and 0.0. The probabilities were less than $\alpha = 0.05$. So, the hypothesis of no correlation is rejected with 95% confidence.

4. Discussion

4.1. Advantages of elemental continuity

Formulation of the simple AD model utilizing the continuity of all elemental macronutrients, COD, and charge leads to several advantages. The model stoichiometric coefficients are determined *a priori* as functions of biomass yield parameters. In one class of simple AD models, stoichiometric coefficients are estimated from experimental data and, therefore, only ratios between the stoichiometric parameters are practically identifiable [7]. The stoichiometric coefficients are correlated. These simple models, however, have an advantage in that they can be applied to any waste type since they do not assume the main substrate composition. The model developed in this paper solves the identifiability problem of such simple models' stoichiometry and defines the correlations as functions of the yield coefficients. For instance, the stoichiometric coefficient of VFA in the acidogenesis step is a function of the yield Y_1, Table 2. General model applications of unknown waste compositions are shown in Table 1. The waste composition must be estimated from data rather than from the stoichiometry. Measuring the model variables IC, IN, IP, and (H_2S) that were added to quantify nutrients' release and uptake will be helpful to estimate such waste compositions, with an additional advantage of evaluating the possible nutrients' recovery.

In another class of simple models [10,11], stoichiometric parameters are determined assuming a certain biomass yield per ATP of standard catabolic reactions. Such an assumption is not valid if the environmental conditions are not optimal for the

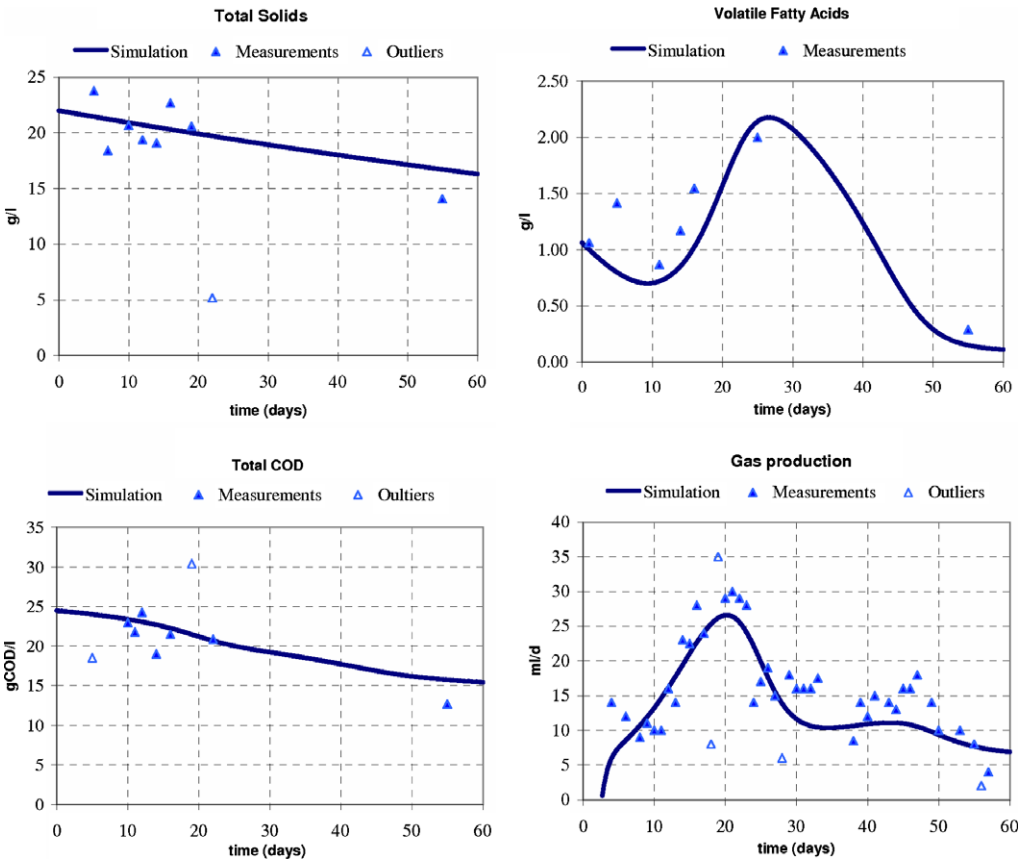

Fig. 4. Model validation using a batch experiment degrading dairy manure that was diluted and flushed with groundwater.

assumed metabolism. On one hand, such a formulation assumes only the balance of C, H, N, and O, and does not consider other macronutrients (P and S). If such macronutrients are not sufficiently available, biomass anabolism will not proceed at the assumed yield. On the other hand, inhibitory effects are due to an excess of N or S in terms of ammonia toxicity [18,22] or sulfate reducing bacteria competition with methanogens [23]. Also, deviation of pH from the optimal process range (6.5–7.5) will inhibit the assumed catabolic reactions or the metabolism in general [18]. The developed model follows the catabolic reactions by maintaining the ratios between their metabolic products according to Eqs. (10), (12), and (14). So, the thermodynamics of the catabolic reactions are maintained and the extent of the substrate conversion through the catabolism and anabolism are determined through the elemental mass balance. The model considers all macronutrients' balance, estimates the inhibitory forms, and evaluates all buffering components that are necessary for pH evaluation. The developed model can check levels of nutrient limitations and inhibitory effects, and, if they are critical, the model's kinetic reactions can be updated by the appropriate inhibitory terms.

4.2. Estimation of acidogenic and methanogenic activities

Using the model, initial acidogens (X_1) and methanogens (X_2) concentrations of inoculated dairy manure samples could be estimated from 10 day batch experiments. According to the model simulation of the first experiment set, Fig. 2, more dynamics were observed for VFA and gas production as compared to TS. For manure only, case (a), VFA was accumulating until the end of the experiment, while in cases of inoculated experiments, VFA declined after a certain time. These VFA dynamics can be related to the corresponding ratios of the initial (X_2) to (X_1) that were 0.1, 0.4, 0.6, and 0.5 for cases (a) through (d). The higher the ratio of methanogens to acidogens, the earlier the VFA accumulation declined; see cases (b) and (d). In case (c), VFA declined later than other inoculum cases although the X_2:X_1 ratio was the highest. In case (c), the organic load was increased since the inoculum was from the anaerobic lagoon. The acidogenesis was growing faster compared to methanogens [14] and, therefore, improved methanogens were needed to uptake the produced VFA simultaneously [15]. The gas production was increasing gradually in degrading manure without inoculum: see case (a). With inoculum, the gas production initially increased then gradually decreased and it was comparably higher than with manure alone. Accordingly, it can be concluded that improving the methanogens population by inoculation prevents VFA accumulation during manure digesters'

start-up, allowing early application of shorter retention time. Moreover, if the inoculum can be retained and grown in a certain reactor configuration the gas production will increase. However, for efficient TSS removal, longer retention time is needed due to the slow hydrolysis as indicated by TSS results, as shown in Fig. 2.

4.3. Effect of manure and water sources

Manure storage time influences the initial acidogens and methanogens concentrations. Before the start of the first set of experiments, manure was stored at 5 °C for 30 days. The second set of experiments was started with a fresh (unstored) sample. The estimated acidogens and methanogens were less in the first experiment as compared to the second experiment. Thus, storage of manure causes a drop in the biomass concentrations that are naturally available in fresh manure, and therefore, starting up a digester after a storage step may take a longer time than start-up after feeding the digester with fresh manure.

Also, flush water sources influence initial acidogens and methanogens concentrations. The manure collected for the second set of experiments was flushed on the farm by lagoon water. Groundwater was used in the flushing system from which the manure for the validation experiment was collected. The estimated acidogens and methanogens in the validation experiment were less than what was estimated in the second experiment. Lagoon water contains acidogens and methanogens populations as indicated by the increased initial biomass estimates from the first experiment case (c) which was inoculated with lagoon sludge.

4.4. Effect of inoculum ratio on gas production

In addition to obtaining reliable parameter estimates, useful process dynamics and gas production dynamics were generated from a set of batch experiments with variable inoculum ratio. The granular inoculum was rich in methanogens since it was collected from a UASB treating acidified waste. Thus, the inoculum ratio indicates mainly the improvement of methanogens concentration. Also, the manure sample was rich in methanogens since it was originally flushed by lagoon water. As shown in Fig. 3, two peaks of gas production can be distinguished along the degradation timeline for each inoculum ratio. The highest gas production is achievable during the first 2 to 3 days and further increase of methanogens does not lead to a significant improvement in the gas production during this initial period. Methanogenesis during this stage is mainly due to the availability of easily degradable substrates S_1 and S_2. The decrease in biogas production after 3 days can be explained by the substrate inhibition of methanogens due to faster acidogensis. This drop in gas production is shorter with improved methanogenesis by increased inoculum. Another peak appears after 5–15 days, depending on the inoculum ratio and when the VFA drops below the inhibitory level that is regulated in the model by k_{i,S_2}. After complete depletion of VFA, very low gas production continues due to the hydrolysis limitation of the whole process. Accordingly, the highest gas production from flush dairy manure digestion can be achieved at the short retention time of 2–3 days if the influent biomass concentration can be maintained. However, such an application will not lead to the complete degradation of substrates. For more complete degradation of easily degradable substrates, the retention time must be increased. Improved methanogens population will shorten the required retention times. As shown in Fig. 3, complete degradation of easily degradable substrates was achieved within 10 days at 20% inoculum ratio, while a period longer than 20 days was required at 0% inoculum. In practice, methanogens concentration can be improved by proper reactor design to maintain longer solids retention time (SRT) or attached growth. Longer SRT is also needed to enhance solids hydrolysis and removal. In the validation experiment, methanogens were very low and the initial gas peak was delayed. Therefore, a high rate reactor that can maintain long SRT is needed for the manure tested in the validation experiment.

4.5. Improved parameter identifiability

In general, *a priori* definition of the model stoichiometry and extension of its state variables contributed more information to the identification of the microbial activity in terms of their initial concentration and kinetic parameters and improved their practical identifiability. From all presented experiments the model was useful to estimate initial acidogenic and methanogenic population. Proper estimates of the model parameters were obtained by optimizing several experiments in the same time frame, i.e., as applied to experiments testing different inoculum ratios. With the estimated parameters, this model was found to be valid to simulate the degradation of dairy manure since simulation of another experiment, as shown in Fig. 4, was correlated with data and the hypothesis of no correlation was rejected.

More studies are needed to further improve the model identifiability using nutrients measurements and fitting IC, IN, IP, and IS state variables. These measurements may also be linked in the future to studies regarding nutrient recovery and biomass improvement or build-up in high rate reactors.

5. Conclusions

The slow dynamics of a complex biological process could be simulated by a simple model of the main limiting steps of the process by applying the elemental continuity of macronutrients and the most energetically favorable catabolic reactions.

A simple model was developed for the anaerobic digestion process of solid wastes considering the hydrolysis, acidogenesis and hydrogenotrophic and acetotrophic methanogenesis. The model stoichiometry was evaluated as functions of the bacterial yield considering the anabolism and catabolism of the main bacterial groups. The microbial anabolism was maintained by the continuity of the bacterial macronutrients. The main reactions that yield high energies at the limiting steps were considered as they maintain the bacterial catabolism.

Accordingly, the model was easily calibrated and validated using batch experiments digesting dairy manure with different inoculum sources. The model was used to quantify the main bacterial populations fitting the dynamic changes of their reaction products. The model was used also to study the effect of substrate and inoculum sources and ratios on the digestion process.

Acknowledgement

This work was partly funded by the Washington State Department of Ecology, the California Energy Commission, and the Paul Allen Family Foundation.

References

[1] W. Verstraete, D. Beer, M. Pena, G. Lettinga, P. Lens, Anaerobic bioprocessing of organic wastes, World J. Microbiol. Biotechnol. 12 (3) (1996) 221–238.
[2] H. Ødegaard, B. Paulsrud, I. Karlsson, Wastewater sludge as a resource: sludge disposal strategies and corresponding treatment technologies aimed at sustainable handling of wastewater sludge, Water Sci. Technol. 46 (9) (2002) 295–303.
[3] D.P. Chynoweth, J.M. Owens, R. Legrand, Renewable methane from anaerobic digestion of biomass, Renew. Energy 22 (1–3) (2001) 1–8.
[4] H.H. Van Horn, A.C. Wilkie, W.J. Powers, R.A. Nordstedt, Components of dairy manure management systems, J. Dairy Sci. 77 (7) (1994) 2008–2030.
[5] A.C. Wilkie, Reducing dairy manure odor and producing energy, Biocycle 41 (9) (2000) 48–50.
[6] D. Batstone, Mathematical modelling of anaerobic reactors treating domestic wastewater: rational criteria for model use, Rev. Environ. Sci. Biotechnol. 5 (1) (2006) 57–71.
[7] O. Bernard, Z. Hadj-Sadok, D. Dochain, A. Genovesi, J.P. Steyer, Dynamical model development and parameter identification for an anaerobic wastewater treatment process, Biotechnol. Bioeng. 75 (4) (2001) 424–438.
[8] R. Borja, A. Martin, E. Sanchez, B. Rincon, F. Raposo, Kinetic modelling of the hydrolysis, acidogenic and methanogenic steps in the anaerobic digestion of two-phase olive pomace (TPOP), Process Biochem. 40 (5) (2005) 1841–1847.
[9] J.E. Haag, A. Vande Wouwer, I. Queinnec, Macroscopic modelling and identification of an anaerobic waste treatment process, Chem. Eng. Sci. 58 (19) (2003) 4307–4316.
[10] A. Nopharatana, P.C. Pullammanappallil, W.P. Clarke, Kinetics and dynamic modeling of batch anaerobic digestion of municipal solid waste in a stirred reactor, Waste Manage. 27 (5) (2007) 595–603.
[11] A. Nopharatana, P.C. Pullammanappallil, W.P. Clarke, A dynamic mathematical model for sequential leach bed anaerobic digestion of organic fraction of municipal solid waste, Biochem. Eng. J. 13 (1) (2003) 21–33.
[12] N. Noykova, T.G. Müller, M. Gyllenberg, J. Timmer, Quantitative analyses of anaerobic wastewater treatment processes: Identifiability and parameter estimation, Biotechnol. Bioeng. 78 (1) (2002) 89–103.
[13] O. Bernard, G. Bastin, On the estimation of the pseudo-stoichiometric matrix for macroscopic mass balance modelling of biotechnological processes, Math. Biosci. 193 (1) (2005) 51–77.
[14] V.A. Vavilin, S.V. Rytov, L.Y. Lokshina, J.A. Rintala, G. Lyberatos, Simplified hydrolysis models for the optimal design of two-stage anaerobic digestion, Water Res. 35 (17) (2001) 4247–4251.
[15] V.A. Vavilin, L.Y. Lokshina, J.P. Jokela, J.A. Rintala, Modeling solid waste decomposition, Biores. Technol. 94 (1) (2004) 69–81.
[16] L. Borzacconi, I. Lopez, C. Anido, Hydrolysis constant and VFA inhibition in acidogenic phase of MSW anaerobic degradation, Water Sci. Technol. 36 (6–7) (1997) 479–484.
[17] U. Zaher, P. Grau, L. Benedetti, E. Ayesa, P.A. Vanrolleghem, Transformers for interfacing anaerobic digestion models to pre- and post-treatment processes in a plant-wide modelling context, Environ. Modell. Software 22 (1) (2007) 40–58.
[18] D.J. Batstone, J. Keller, R.I. Angelidaki, S.V. Kalyuzhnyi, S.G. Pavlostathis, A. Rozzi, W.T.M. Sanders, H. Siegrist, V.A. Vavilin, Anaerobic Digestion Model No. 1, IWA Publishing, London, UK, 2002. p. 77.
[19] R.E. Speece, Anaerobic Biotechnology for Industrial Wastewaters, Archae Press, Nashville, TN, 1996.
[20] P. Reichert, Computer Program for the Identification and Simulation of Aquatic Systems, EAWAG, Switzerland, 1998. ISBN: 3-906484-16-5.
[21] J. Nelder, R. Mead, A simplex method for function minimization, Comput. J. 7 (1965) 308–313.
[22] S. Sung, T. Liu, Ammonia inhibition on thermophilic anaerobic digestion, Chemosphere 53 (1) (2003) 43–52.
[23] V. Fedorovich, P. Lens, S. Kalyuzhnyi, Extension of anaerobic digestion model no. 1 with processes of sulfate reduction, Appl. Biochem. Biotechnol. 109 (1–3) (2003) 33–45.

Appendix 3: Transformer model procedure

Zaher U., Buffiere P., Steyer J-P., and Chen S. (2008) A procedure to estimate proximate analysis of mixed organic wastes, Water Environment Research (accepted)

A Procedure to Estimate Proximate Analysis of Mixed Organic Wastes

U. Zaher[1]*, P. Buffiere[2], J.-P. Steyer[3], S. Chen[1]

ABSTRACT: In waste materials, proximate analysis measuring the total concentration of carbohydrate, protein, and lipid contents from solid wastes is challenging, as a result of the heterogeneous and solid nature of wastes. This paper presents a new procedure that was developed to estimate such complex chemical composition of the waste using conventional practical measurements, such as chemical oxygen demand (COD) and total organic carbon. The procedure is based on mass balance of macronutrient elements (carbon, hydrogen, nitrogen, oxygen, and phosphorus [CHNOP]) (i.e., elemental continuity), in addition to the balance of COD and charge intensity that are applied in mathematical modeling of biological processes. Knowing the composition of such a complex substrate is crucial to study solid waste anaerobic degradation. The procedure was formulated to generate the detailed input required for the International Water Association (London, United Kingdom) Anaerobic Digestion Model number 1 (IWA-ADM1). The complex particulate composition estimated by the procedure was validated with several types of food wastes and animal manures. To make proximate analysis feasible for validation, the wastes were classified into 19 types to allow accurate extraction and proximate analysis. The estimated carbohydrates, proteins, lipids, and inerts concentrations were highly correlated to the proximate analysis; correlation coefficients were 0.94, 0.88, 0.99, and 0.96, respectively. For most of the wastes, carbohydrate was the highest fraction and was estimated accurately by the procedure over an extended range with high linearity. For wastes that are rich in protein and fiber, the procedure was even more consistent compared with the proximate analysis. The new procedure can be used for waste characterization in solid waste treatment design and optimization. *Water Environ. Res.*, **81**, 407 (2009).

KEYWORDS: ADM1, anaerobic digestion, Continuity-Based Interfacing Methodology, elemental continuity, practical measurement, substrate composition.

doi:10.2175/106143008X370548

Introduction

Organic municipal solid wastes are typically very heterogeneous in nature (Holm-Nielsen et al., 2006). Their anaerobic degradability depends on their composition, in terms of carbohydrates, proteins, lipids, and slowly degradable fractions, such as lingo-cellulose (Buffiere et al., 2006; Garcia de Cortazar and Monzon, 2007). The composition of the particulate substrates is considered to be the bottleneck in a high-solids digestion system, as a result of their effect on hydrolysis process (Hartmann and Ahring, 2006; Johansen and Bakke, 2006), as hydrolysis rates differ significantly for different particulate components (i.e., carbohydrates, proteins, and lipids) (Mata-Alvarez et al., 2000). Subsequent biological degradation kinetics also differs with the substrate composition, because each of the successive hydrolysis products is degraded by different bacterial populations (Islam and Singhal, 2002).

During anaerobic digestion, solid wastes are generally monitored using typical "practical" parameters that are relatively easy to measure, such as total solids (TS), volatile solids, chemical oxygen demand (COD), volatile fatty acid (VFA), total Kjeldahl nitrogen (TKN), and total ammonia-nitrogen (TAN) (Holm-Nielsen et al., 2006). Such measurements are well-defined in *Standard Methods* (APHA et al., 2005) and are commonly practiced. In contrast, "proximate" analysis of carbohydrate, protein, lipid, and inert composition of complex solid wastes is atypical and is difficult to perform, as a result of the heterogenic nature of wastes.

The International Water Association (London, United Kingdom) (IWA) task group for anaerobic digestion developed the Anaerobic Digestion Model number 1 (ADM1) (Batstone et al., 2002), to study and evaluate anaerobic digestion of complex wastes. ADM1 considers the degradation pathways of carbohydrates, proteins, and lipids. Because these components are difficult to measure in complex wastes, such as activated sludge, several methods were developed (Copp et al., 2003; Vanrolleghem et al., 2005; Zaher et al., 2007) to estimate the ADM1 inputs by interfacing it to the Activated Sludge Model number 1 (ASM1) (Henze et al., 2000). Furthermore, Kleerebzem and Van Loosdrecht (2006) developed a method that evaluates a lumped composition of wastewater. From the lumped composition, fraction parameters of ADM1 were estimated to distribute the composite particulate component to carbohydrates, proteins, and lipids components. The objective of this paper was to combine the advantages of these methods and to develop a generalized procedure to

(1) Estimate substrate composition of high solids (concentrated) wastes from "practical" measurements, and use biomass and solid waste databases (U.S. Department of Agriculture, 1996, 2007a, 2007b; U.S. Department of Energy, 2007; Energy Research Centre of the Netherlands, 2007);
(2) Estimate the necessary inputs to ADM1 for simulating the solid waste anaerobic digestion process.

To provide the reader with the necessary background for the procedure in this paper, the previous procedures developed for estimating the ADM1 inputs are briefly reviewed in the following section. The procedure developed in this paper was based on considering an extended list of practical measurements that would be ideally available for estimation of particulate substrate

[1] Department of Biological Systems Engineering, Washington State University, Pullman, Washington.

[2] INSA LYON, Laboratory for Civil and Environmental Engineering, Villeurbanne Cedex, France.

[3] INRA, UR 50, Laboratoire de Biotechnologie de l'Environnement, Narbonne, France.

* Department of Biological Systems Engineering, Washington State University, P.O. Box 646120, Pullman, WA 99164-6120; e-mail: zaheru@wsu.edu.

composition. Consequently, anaerobic digestion of these substrates can be studied and modeled using ADM1. The method was then validated using less extended data sets to test its applicability. Validation was conducted using various manure and kitchen waste types. The substrate composition estimated by the developed procedure was comparable with the composition determined by "proximate" analysis. Additionally, soluble components, such as sugars, VFA, TAN, and alkalinity, were considered, as they will be necessary inputs to accurately simulate the anaerobic digestion process of solid wastes.

Review of ADM1 Interfacing Methods

For the purpose of estimating the input characteristics for ADM1, Kleerebzem and Van Loosdrecht (2006) proposed a method to estimate the lumped elemental composition (stoichiometric formula) of wastewater from a set of practical measurements using averaged values. It worth noting here that the solid waste characteristics vary over time (i.e., are dynamic). As explained below, averaging the practical measurements will limit ADM1 application to one feed instance only or to an experiment with one constant feed substrate. From the stoichiometric formula of the wastewater, the ADM1 fraction parameters of the composite particulates to carbohydrates, proteins, and lipids were calculated. The authors reported that estimation of the lipids fraction parameter was problematic, as a result of high correlations with the other fractions and between the assumed measurements. The problem may be caused by the fact that the estimated fraction parameters are constant over time as originally defined for ADM1. The ADM1 model structure begins with a disintegration step of the composite particulates, which are mainly considered as biomass (i.e., activated sludge or decayed anaerobic bacteria). Because the biomass composition in ADM1 is considered constant and similar to activated sludge, the composite particulate fractions to carbohydrates, proteins, lipids, and inerts also were considered to be constant parameters. Consequently, evaluation of these constant parameters instead of dynamic characteristics of solid wastes would cause two problems for ADM1 application, as follows:

(1) The solid waste composition is most likely different from that of decaying biomass. Solid waste feedstocks should not be assigned as an input to the same composite particulate variable of decaying biomass.
(2) The fraction parameters are constant over time and thus do not reflect the dynamic changes of the waste composition. Digesting mixed types of wastes implies a dynamic change in the composition.

Therefore, a waste feedstock is better defined as influxes to ADM1 variables of carbohydrates, proteins, lipids, and inerts to simulate the effect of such dynamics on the anaerobic digestion process. Previously, Vanrolleghem et al. (2005) developed the Continuity-Based Interfacing Methodology (CBIM) for interfacing (i.e., connecting) different biological models that can be represented in the Petersen matrix form. Zaher et al. (2007) illustrated the detailed application of the CBIM for connecting standard aerobic and anaerobic models, that is, ASM1 (Henze et al., 2000) and ADM1. The main advantage of CBIM is that it considers the continuity of major constituting macronutrient elements (carbon, hydrogen, nitrogen, oxygen, and phosphorus [CHNOP]) and the charge balance while converting the output of the first model (i.e., ASM1) to an input for the second model (i.e., ADM1). The calculations in CBIM are straightforward and performed by solving a set of algebraic equations that are based on the elemental continuity and the charge balance. In some situations, the algebraic solution may result in negative influxes to ADM1 (i.e., some components are calculated as outputs instead of as inputs to the second model) and therefore the solution must be constrained by some logic rules to avoid such negative influxes.

Separately, Copp et al. (2003) proposed an interface for ASM1 to ADM1, and vice versa. They maintained the balance of COD and nitrogen in all conversions from ASM1 to ADM1. They also introduced the concept of maximizing the conversion of ASM1 components to ADM1 components in a predefined order. The maximization was done by summing the COD and nitrogen contents of ASM1 output and applying logic rules to check that there is enough COD and nitrogen to estimate the ADM1 inputs. These logic rules were based on the predefined COD and nitrogen content per stoichiometric unit of ADM1 components. As such, this method avoids the negative influxes to ADM1.

Procedure

Procedure Innovations. For this method development, the following practical measurements were considered available: total COD (COD_t), soluble COD (COD_s), VFA, total carbon (TC), total inorganic carbon (TIC), TKN, TAN, total phosphorous, orthophosphate (orthoP), total alkalinity (S_{cat}), total solids, and total volatile solids (TVS). This list of practical measurements presents the ideal case for waste characterization and guarantees the most accurate estimation of the particulate composition by the developed procedure.

Using the above common measurement list, a new procedure was developed to estimate the concentrations of carbohydrates, proteins, lipids, and particulate inerts. Liquid fractions, such as TIC, VFA, TAN, and orthophosphate, are directly quantified, and only their measuring units are converted. These components will influence the anaerobic digestion process. The procedure considers their composition to complete the balance of elemental mass, COD, and charge. The method was upgraded from the CBIM, previously discussed by Vanrolleghem et al. (2005) and Zaher et al. (2007) and reviewed in the previous section, assuming unique correlations between practical measurements and the substrate composition, as shown in Table 1. A breakdown of the complex particulate molecules was assumed to consist of an amino-group, a phospho-group, and carbon atoms that connect to OH^- and H^+. The theoretical COD calculations (ThOD) from elemental composition and charge intensity were upgraded from Gujer et al. (1999) and Reichert et al. (2001) by considering ThOD for the carbon covalent bonds, as shown in Table 2. This upgraded CBIM procedure is presented by transformation and composition matrices in Table 3, following the Petersen matrix format. This upgraded composition matrix also includes the intensity of the broken carbon covalent bonds to present the practical measurements. An additional balance of the covalent bonds intensities was done over all conversions of practical measurements, as presented in Table 4. The transformation matrix and equations were developed by upgrading the CBIM with the maximization concept illustrated in Copp et al. (2003) and reviewed in the previous section, considering a different maximization order defined in step 4 of the next section.

Procedure Development and Application. For the purpose of consistent description and applicability of the procedure to interface ADM1 to solid waste practical characteristics, we follow the same sequence used for describing the CBIM interface to activated sludge and ASM1 (Zaher et al., 2007). Thus, the necessary CBIM upgrades for solids anaerobic digestion are highlighted in this context.

Table 1—Basic structures assumed for ADM1 complex organic components and related practical measurements composition.*

ADM1 complex organic components	Related practical measurements
Lipids:	COD, TOC and organic phosphorus
i.e., phospholipids $C_7H_{11}PO_8^-$	HPO_4^{-1b-1}: 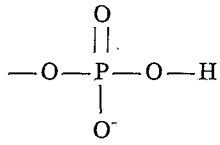
Proteins: $C_6H_{12}O_3N_2$	- COD, TOC and organic nitrogen (amino group NH_2^{-1b}): 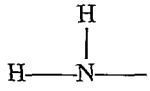
Carbohydrates: i.e., cellulose: $C_6H_{10}O_5$	- COD: $C_6H_{10}O_5$ and TOC: C^{+4b} 

* Note: superscript b is to count the assumed broken covalent bonds. It is positive if pointing out from C. Otherwise, it is negative.

Step 1—Elemental Mass Fractions and Charge Density. Elemental mass fractions of carbon, hydrogen, oxygen, nitrogen, and phosphorus and the corresponding charge density were defined according to Zaher et al. (2007), for both ADM1 components and practical measurements. Note that cationic elements, such as potassium (K), magnesium (Mg), and calcium (Ca) may also be considered for modeling precipitation and landfill leaching (Islam and Singhal, 2002). However, for simplicity, these cationic elements were not considered in the present procedure. The practical measurements were rearranged to represent unique components for which the elemental mass fractions can be assumed (i.e., Table 3 components 1 to 11). The COD_p presented the particulate COD and was calculated as $COD_t - COD_s$. The COD_s measurement was split into soluble substrate (COD_s – COD of VFA) and VFA. Total organic carbon (TOC) was calculated as TC – TIC. Similarly, organic nitrogen and phosphorous were calculated from the measured total less the inorganic portion. The cation concentration could be estimated from the total alkalinity measurement according to the charge balance (Bernard et al., 2001). Similarly, TIC is mainly bicarbonate that can be estimated from the titrimetric measurements of alkalinity (Moosbrugger et al., 1993; Zaher and Vanrolleghem, 2005). Fixed solids (FS) was calculated as TS – TVS. According to this rearrangement of practical measurements, their elemental mass fraction calculations were straightforward. The TOC consisted solely of the carbon fraction that sourced the carbon needed in the conversion to ADM1 organic components. The organic nitrogen (N_{org}) and organic phosphorous mass fractions will be determined according to the stoichiometric formulae of the amino- and phospho-groups, respectively. Table 1 shows the correlation between different measurements and the particulate components. The amino-group contains only hydrogen and nitrogen fractions. The phospho-group contains hydrogen, oxygen, and phosphorus fractions. Oxygen and hydrogen were initially assigned to COD_p, assuming the stoichiometric formula of starch or cellulose ($C_6H_{10}O_5$), as they are typically the largest portion of organic fraction in the solid waste. During the conversion, if part of the COD_p was assigned to proteins, extra hydrogen was sourced from the amino group (i.e., N_{org}). If part of the COD_p was converted to phospholipids, extra hydrogen and oxygen were sourced from the phospho-group. The COD_s was

Table 2—Theoretical COD per element, charge, and assumed covalent bond.

Element or charge *Z*		State of reference	Equivalent ThOD	
C	Carbon	CO_2	+ 32	g ThOD (mol C)$^{-1}$
H	Hydrogen	H_2O	+8	g ThOD (mol H)$^{-1}$
O	Oxygen	O_2	−16	g ThOD (mol O)$^{-1}$
N	Nitrogen	NH_4^+	−24	g ThOD (mol N)$^{-1}$
P	Phosphorous	PO_4^{3-}	+40	g ThOD (mol P)$^{-1}$
S	Sulfur	SO_4^{2-}	+48	g ThOD (mol S)$^{-1}$
−	Negative charge	Zero charge	+8	g ThOD (mol (−))$^{-1}$
+	Positive charge	Zero charge	−8	g ThOD (mol (+))$^{-1}$
	New rules	Example:		
−	Covalent bond to C	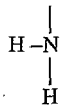	+8	g ThOD (covalent)$^{-1}$
		Example:		
+	Covalent bond to C		−8	g ThOD (covalent)$^{-1}$

Table 3—Calculated transformation and composition matrices of the ADM1 interface to practical measurements of manures and solid waste.

j ↓ / k →	Conversion to / components	1 CODp (gCOD m^-3)	2 CODs-VFA (gCOD m^-3)	3 VFA (gCOD m^-3)	4 TOC (gC m^-3)	5 Norg (gN m^-3)	6 TAN (gN m^-3)	7 TP-orthoP (gP m^-3)	8 orthoP (gP m^-3)	9 TIC (mol HCO3^- m^-3)	10 Scat (eq m^-3)	11 FS (g m^-3)	12 S_{su} (kgCOD m^-3)	18 S_{ac} (kgCOD m^-3)	21 X_I (kgCOD m^-3)	23 X_{ch} (kgCOD m^-3)	24 X_{pr} (kgCOD m^-3)	25 X_{li} (kgCOD m^-3)	33 S_{cat} (kmole m^-3)	34 S_{in} (kmoleN m^-3)	35 S_{ic} (kmoleC m^-3)	36 S_{ip} (kmoleP m^-3)	37 S_{OH-} (kmole m^-3)	38 S_{H+} kmole	39 S_{an} (kmole m^-3)
1	ammonia						-1													7.14E-05				-5.55E-20	-4.16E-20
2	bicarbonate									-1											1.00E-03				
3	ortho phosphate								-1													3.17E-05	5.43E-07	-3.23E-05	5.43E-07
4	cations										-1								0.001						
5	VFA			-1	-0.375001									0.001							1.00E-10		-7.50E-11	-2.60E-11	-5.00E-11
6	Sugars		-1		-0.375								0.001								-1.07E-18		8.07E-19	2.80E-19	5.47E-19
7	lipids	-0.457862			-2.712302			-1										0.006458					9.75E-08	-2.88E-05	-3.83E-05
8	proteins	-0.857143			-2.57143	-1											0.006857				1.00E-10		1.79E-05	5.36E-05	3.57E-05
9	carbohydrates	-1			-0.375											0.001					1.07E-18		-8.05E-19	-2.68E-19	-5.37E-19
10	organic inerts	-0.990616			-0.40403	-0.056021		-0.000388				-1			0.000901					-1.00E-07	2.85E-07	3.71E-12	-1.01E-06	-2.09E-12	8.18E-07
composition matrix	i_ThOD (gThOD/stoichunit)	1.000	1.000	1.0000									1000	1000.0000	1000	1000	1000	1000							
composition matrix	i_C (gC/stoichunit)				1.000					12.01			375	375.0000	403.073339	375	375	420			12000				
composition matrix	i_N (gN/stoichunit)					1.00	1.00								58.3753237		145.833333			14000					
composition matrix	i_O (gO/stoichunit)	0.417	0.500	0.5000				2.07	2.07	48.00			500	500.0000	481.150513	416.666667	250	840			48000	64000	64000		
composition matrix	i_H (gH/stoichunit)	0.052	0.063	0.0469		0.14	0.29	0.03		1.00			62.5	46.8750	61.5254[illegible]	52.0833333	62.5	60		4000	1000	1000	1000	1000	
composition matrix	i_P (gP/stoichunit)							1.00	1.00						0.44793374			151.85				31000			
composition matrix	i_Ch (Ch/stoichunit)			-0.0156			0.07	0.03	0.10	-1.00	1.00			-15.6250				-5	1000	1000	-1000	-2000	-1000	1000	-1000
	i_Covalent Bond (Bond/stoichunit)	-0.125	-0.125	-0.1250	0.333	0.07		-0.03																	
	Total mass/stoichunit											1			1009.47271			-							
													Source sink components of consequently:							N	C	P	O	H	Ch

assumed to originate mainly from sugars and VFA. Their oxygen and hydrogen fractions were calculated assuming the glucose and acetate stoichiometric formulae.

The elemental mass fractions of TAN, orthophosphate, and TIC were calculated assuming the stoichiometric formulae of ammonium, orthophosphate, and bicarbonate, respectively. For S_{cat}, only charge intensity was considered, as the corresponding cationic elements were not presented in the procedure for the sake of generality and simplicity. The fixed solids value was presented as total mass, as the elemental mass fractions were assumed unknown. The fixed solids composition is estimated in step 3.

Step 2—Composition Matrix. The composition matrix is listed in the lower pane of Table 3. It lists the mass of elemental composition per stoichiometric unit of each component. The COD_p, COD_s, and VFA were presented in COD units of grams COD per cubic meter. Thus, the ThOD per stoichiometric unit of these components was unity and was independent of their molecular structure. The VFA concentration was considered in COD units so that it accounted for the different VFA molecular structures (i.e., propionate, butyrate, and valerate). However, the present procedure considers only acetate estimation. Taking acetate ion (CH_3COO^-) as an example of composition matrix calculation, as shown in column 3 of Table 3, 1 mole is equivalent to 64 gCOD. It has 2 oxygen atoms. Its oxygen composition (i_O) is 32/64 = 0.5 gO/gCOD of acetate. Similarly, i_H = 3/64 = 0.0469 gH/gCOD of acetate and the charge intensity i_ch = −1/64 = −0.0156 Ch/gCOD. Acetate has 2 carbon atoms and 4 covalent bonds each. Its i_covalent bond = −2 × 4/64 = −0.125 bond/gCOD. The covalent carbon bonds have a negative sign, because carbon is sourced from the TOC measurement, as illustrated later. Other carbon, nitrogen, and phosphorus measurements were presented in grams of element per cubic meter, to conform to practical measurement units. The TIC and S_{cat} were considered in moles and equivalents, respectively, to consider titrimetric measurements of alkalinity and to allow future extension of the procedure to consider divalent and trivalent cations. The charge densities were considered for VFA, organic phosphorous, orthophosphate, TIC, and S_{cat}. In addition to the mass fractions and charge densities, a new line was added to the composition matrix, to account for the carbon covalent bonds, because the real molecular structure of the organic components was split among the practical measurements. Hence, new rules were added to the theoretical COD per element and charge, as shown in Table 3. Similar to charge, the covalent bond was assumed to be either positive, if it was pointing away from a carbon atom, or negative, if it was pointing toward a carbon atom. This helped to check that there was no free covalent bond when all conversions were done. As described in the next step, the balance of covalent bonds gave additional information to estimate the composition of inert particulates. By analogy to charge, a positive covalent bond was assumed to have -8 ThOD units, while a negative covalent bond was assumed to have +8 ThOD units. These assumptions resulted in correct ThOD calculations according to the assumed composition of the practical measurements. Also, the assumptions maintained the ThOD contents under the COD_p and COD_s components (main COD measurements) and nullified the ThOD of other measurements, so that no duplication of the COD assignment was considered during the estimation of the waste composition. The compositions of ADM1 components were calculated according to Zaher et al. (2007) using standard ADM1 units, and the assumed particulate stoichiometric formulae shown in Table 1.

Step 3—Transformation Matrix. The transformation matrix, as shown in the upper pane of Table 3, was designed to estimate the waste composition in 10 conversions ($j = 1{:}10$). The stoichiometric parameters $v_{j,k}$ were defined maintaining the continuity of ThOD, all elements, and charge intensity, according to eq 1, which was calculated at each conversion j for all components k. To solve these equations for $v_{j,k}$, source-sink components (S_{in}, S_{ic}, S_{ip}, S_{OH^-}, S_{H+}, and S_{an}) were considered to close the balance of nitrogen, carbon, phosphorus, oxygen, hydrogen, and charge (Ch), respectively. These calculations were performed by minimizing the stoichiometry under these source-sink components. Note that OH^- was used as the source-sink component for oxygen, and H^+ was used as the source-sink component for hydrogen. As a consequence, the least value of these two components will be moles of water. This water compensates for the differences that would occur if the particulate molecules were more complex than originally assumed (in step 1). Any difference between the OH^- and H^+ components will be compensating for extra oxygen or hydrogen compared with the assumed practical measurements composition. The difference between OH^- and H^+ introduces the charge difference that will be balanced by the difference between anions (S_{an}) and cations (S_{cat}).

$$\sum_k v_{j,k} i_{j,Comp} = 0 \quad \text{with } Comp = Thod, C, N, H, O, e \tag{1}$$

For each conversion j, the stoichiometric parameters were calculated by inserting a value of -1 under the most related measurement; then, the stoichiometric parameters under other correlated measurements and the composition components of ADM1 were calculated according to eq 1. This equation was calculated either directly by closing one of the elemental mass or ThOD balances, or indirectly by minimizing the stoichiometry under the source-sink components. The first four conversions were straightforward, as they comprised direct assignment of inorganic components (TAN, TIC, orthophosphate, and S_{cat}), and there were no other correlated measurements. The conversions (5 and 6) to VFA and sugar were correlated with TOC. Their stoichiometric parameters under TOC were calculated by minimizing the stoichiometry under S_{ic}. Their stoichiometry to the corresponding ADM1 components was calculated according to the COD balance. The most related measurement for lipids (conversion 7, assuming the form of phospho-lipids) was organic phosphorus (TP – orthoP) and, therefore, $v_{7,7} = -1$. Accordingly, the stoichiometric parameter for estimating lipids was calculated by imposing the continuity of phosphorous using eq 1. The other correlated measurements with the lipids were TOC and COD, for which $v_{7,4}$ and $v_{7,1}$ were calculated, respectively, by minimizing $v_{7,35}$ and imposing the ThOD balance. Taking the conversion to lipids as an example of the transformation matrix (Table 3, upper part) evaluation, 1 g of organic phosphorous in column 7 (TP – orthoP) is equivalent to 0.006458 kgCOD of lipids X_{li} in column 25, based on the phosphorus balance. This X_{li} also is equivalent to approximately 2.71 g TOC and 6.458 $gCOD_p$, which will be deducted from the corresponding practical measurements in columns 4 and 1, respectively. Similarly, the stoichiometry for protein estimation (conversion 8) was calculated by considering Norg as the most related measurement. The nitrogen balance was applied to calculate the stoichiometric parameter $v_{8,24}$ under proteins. The most related measurement to carbohydrate (conversion 9) was CODp and, therefore, $v_{9,1} = -1$. The stoichiometry under carbohydrates $v_{9,23}$ was calculated based on the COD balance. The second most correlated measurement to carbohydrates was TOC and, therefore, $v_{9,4}$ was calculated by minimizing $v_{9,35}$.

Table 4—Balance of carbon covalent bonds over all conversions.

Covalent bonds balance	Error
Conversion to VFA	−4.0E-07
Conversion to sugar	4.3E-15
Conversion to lipids	−6.5E-02
Conversion to proteins	7.1E-02
Conversion to carbohydrates	−4.3E-15
Conversion to inerts	−6.8E-03
Overall balance	0.00

Inert particulates (X_I) in conversion 10 were assumed to have carbon, nitrogen, and phosphorous fractions. In common practice, the inert fraction is quantified by fixed solids. Therefore, X_I was correlated with COD_p, TOC, N_{org}, organic phosphorus, and fixed solids. The stoichiometric parameters under these measurements and the composition of X_I were determined by constrained optimizations. Optimization was done to minimize the stoichiometric parameters under the source-sink components, that is, to maintain the continuity of elemental mass during the conversion. The following two constraints were applied to the optimization:

(1) The sum of covalent bonds over all conversions equals zero, as in Table 4; and
(2) Assume that the estimated composition of X_I as ThOD = 1000 g COD/g solids. Accordingly, the stoichiometry for conversion to X_I , except for $v_{10,1}$ and $v_{10,11}$, was evaluated. Also, the mass fractions of X_I were evaluated and, therefore, the corresponding total mass of X_I was estimated. The mass fractions of fixed solids were sourced by other measurements, and, because its unit is grams per cubic meters, its total mass is 1. Setting $v_{11,10} = -1$, because fixed solids is the most correlated measurement to X_I, the stoichiometry under X_I $v_{10,12}$ was determined by considering the total mass balance between fixed solids and X_I. The COD of X_I was sourced by COD_p. Thus, $v_{10,1}$ was calculated from the COD balance of COD_p and X_I.

Thus, all stoichiometric parameters were calculated, and the transformation matrix was complete in 10 conversions.

Step 4—Transformation Equations. The original transformation of CBIM was generated by eqs 2 and 3. A set of algebraic equations was generated by eq 2 to map the influxes to vector ρ_j, $j = 1{:}\ k$ and, where k is the number of conversions, using the stoichiometry in the left pane of the transformation matrix (i.e., for $k = 1{:}\ P$, where P is the number of practical measurements). Then, eq 3 calculates the outfluxes from ρ_j using the stoichiometry in the right pane of the transformation matrix (i.e., $k = P+1 : P+Q$, where Q is the number of the estimated composition components).

$$\sum_{j=1}^{n} v_{j,k}\rho_j = Influx_k \quad for\ k = 1{:}p \tag{2}$$

$$Outflux_k = \sum_{j=1}^{n} v_{j,k}\rho_j \quad for\ k = 1{:}\ p \tag{3}$$

In this paper, the elements of the vector ρ_j were maximized in a predefined order, to ensure that the elemental influxes sourced by

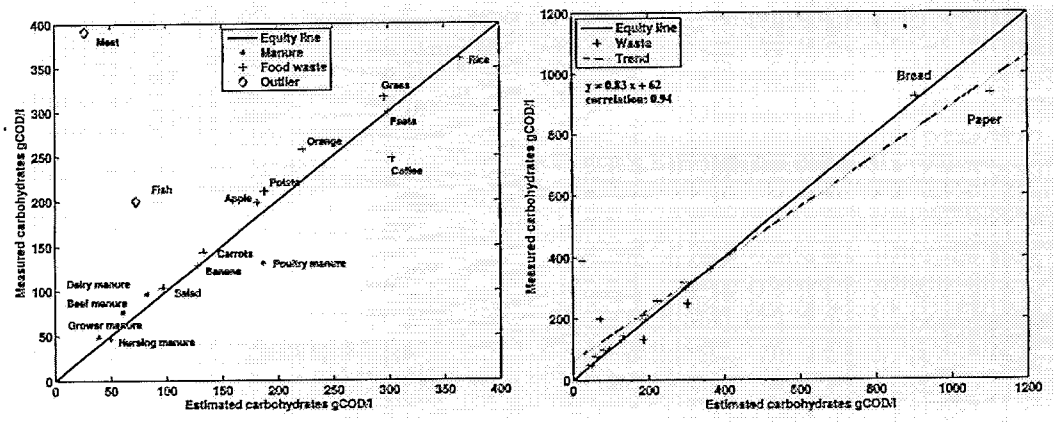

Figure 1—Comparison of the estimated and proximate analysis of carbohydrates for the different waste types: (left) concentrations up to 400 gCOD/L, (right) concentrations up to 1200 gCOD/L.

the input of practical measurements were sufficient before calculating the next element of ρ_j. A predefined order of ρ_z, $z = 1{:}10$, which corresponds to $j = (10, 5{:}9, 1{:}4)$, maximized the conversion to inert particulates, VFAs, sugars, lipids, proteins, carbohydrates, and then inorganic components. This maximization was done according to the following steps:

(1) ρ_z was calculated using eq 4 as a function of the influx of the most correlated measurement k (i.e., corresponding to the unique value of $v_{z,k} = -1$ at each conversion).
(2) ρ_z was verified using the conditions imposed by eq 5. If shown true, the next ρ_{z+1}, was calculated starting from step 1 above.
(3) If shown false, ρ_z was changed and calculated according to eq 6. The ρ_z calculation was then terminated, and other rates (ρ_i, $i = z + 1{:}n$) were assigned a value of 0.
(4) Any remaining fluxes were added to the relevant inorganic components.
(5) All practical measurements were mapped to the new vector ρ. The outflux of substrate composition was then calculated using eq 3.

$$\rho_z = \left[\frac{Influx_k - \sum_{i=1}^{z-1} v_{i,k}\rho_i}{v_{z,k}} \right] \quad (4)$$

$$\sum_{1}^{z} v_{z,k}\rho_z < Influx_k \quad for\ k = 1{:}p \quad (5)$$

$$\rho_z = \min \left| \frac{Influx_k - \sum_{i=1}^{z-1} v_{i,k}\rho_i}{v_{z,k}} \right| \quad for\ k = 1{:}p \quad (6)$$

Validation Analysis

Nineteen wastes, shown in Figure 1, were analyzed by proximate analysis for carbohydrates, proteins, and lipids to validate the procedure output. Processed and nonprocessed food wastes, waste office paper, and manure wastes were used for validation. These wastes had to be further classified into the 19 specific waste types in Figure 1 to allow accurate extraction, as required by the traditional proximate analysis. Also, practical characteristics were analyzed and collected from waste databases for the same wastes, to generate a practical input to the procedure. In preparation for proximate analysis, samples were freeze-dried, milled, and sieved with a 1-mm screen. The analyses were done after fractionation to soluble components, hemicellulose, cellulose, and lignin using the Fibrebag system (Gerhardt, Brackley, United Kingdom) and sequential extraction using neutral and acid detergents, followed by strong acid extraction. The soluble fraction was the amount of organic matter extracted with the neutral detergent. The hemicellulose fraction was the difference between the neutral detergent and the acid detergent residue. The cellulose fraction was extracted by 72% sulfuric acid. The lignin fraction was quantified by the volatile solids residue after 72% sulfuric acid treatment.

Carbohydrates. Different fiber fractions were quantified as the particulate carbohydrates content of hemicellulose, cellulose, and lignin, as determined above by the sequential extraction using neutral and acid detergents, followed by strong acid extraction for the cellulose content (Goering and Soest, 1970; Van Soest, 1963). Total sugars were measured with the Anthrone reduction method (Yemm and Willis, 1954).

Proteins. For different food and paper wastes, the extracted soluble fraction from the Fibrebag system was analyzed using the Lowry method (Lowry et al., 1951) calibrated on bovine serum albumin. For the different manure types, proteins were quantified by summing all amino acids, which were determined for each manure type using the Beckman 6300 analyzer (Beckman Coulter Inc., Fullerton, California) for amino acids following the *Official Methods of Analysis* (Association of Official Analytical Chemists, 1990).

Lipids. For food and paper wastes, lipids were estimated through conventional Soxhlet extraction with petroleum ether (40 to 60°C) as a solvent using the Soxtherm system (Gerhardt, United Kingdom). It worth mentioning that the Soxhlet method has been the most common method for lipid quantification since it was developed by Soxhlet in 1879 for quantifications of lipids in dairy products. It was not possible to extract the lipid contents of manures.

Inerts. The crude fiber obtained after boiling successively in sulfuric acid and sodium hydroxide was considered as the inert fraction. This method is known as the *Weende method* and has been commonly used for crud fiber determination (AOAC International, 2007).

Practical measurements were conducted using *Standard Methods* (APHA et al., 2005). The COD, total solids, and TVS were measured for all waste types. The TKN was also measured for all nonprocessed food wastes (i.e., salad and carrots). The TAN and

VFAs were measured for manures. Total phosphorus and TKN of processed foods (i.e., coffee, rice, pasta, and bread) and manures were determined from literature (American Society of Agricultural Engineers, 1998; Neitsch et al., 2001) and online solid waste and biomass databases (U.S. Department of Agriculture, 1996, 2007a, 2007b; U.S. Department of Energy, 2007; Energy Research Centre of the Netherlands, 2007). The TAN, total carbon, TIC, and orthophosphate were not measured.

The procedure output was estimated in ADM1 units. Proximate analysis was calculated in mass fractions, because these analyses were originally designed to report the composition of specific food types. For comparison between estimated and measured composition, proximate analysis results were converted to COD units according to the composition assumed for ADM1. The COD units were evaluated per unit of volume of waste (i.e., gCOD/L) and not per unit mass of dry matter (gCOD/g dry waste). The use of COD units avoids inconsistency in mass balance, whether resulting from water content in the complex substrate molecules or different moisture content. Water has zero COD; therefore, different moisture content will not have an influence on the used units, as long as the wet volume of waste is the same. For example, Kayhanian et al. (1996) illustrated the importance of including a mass correction parameter when modeling high solids digestion using mass units because of the considerable mass reduction and water evaporation.

Results and Discussion

The predicted composite analysis was highly correlated with the traditional extraction-based proximate analysis. Correlation coefficients were 0.94, 0.88, 0.99, and 0.96 for carbohydrates, proteins, lipids, and inerts, respectively. The hypothesis of no correlation or producing such correlations by random chance was tested. The probability (P) of such hypothesis was 0 for all 4 correlations, which is much less than the confidence level $\alpha = 0.05$. In other words, the correlations were statistically tested and observed with absolute confidence. Testing the linearity between the procedure and the proximate analysis, small drifts and few outliers were observed for each measurement.

Carbohydrates Estimation. Figure 1 shows the linearity between the estimated and measured carbohydrates for the 19 tested waste types. Figure 1 (left) shows the results up to 400 gCOD/L, and Figure 1 (right) shows the results up to 1200 gCOD/L of the high-carbohydrate wastes (i.e., bread and paper). Therefore, the procedure is applicable for an extended measurement range of carbohydrates, from as low as 50 gCOD/L (nursing manure) to 1000 gCOD/L (bread).

Some outliers could be observed. On one hand, proximate analysis of carbohydrates for fish and meat were very high (200 and 400 gCOD/L) compared with the estimated values (27 and 72 gCOD/L). On the other hand, carbohydrates were less detected in the proximate analysis of paper. Indeed, proximate analysis overestimated the carbohydrates for high-protein waste fractions while underestimating them for high-fiber waste fractions. The neutral detergent treatment was not enough to extract fish and meat proteins for subsequent quantification as amino acids; therefore, they were extracted by the subsequent acid treatment and quantified as carbohydrates. Also, it was not possible to extract all cellulose from paper fibers. These outliers affected the linear trend, as shown in Figure 1. Fibers present the main carbohydrate forms for most of the organic solid wastes. The developed procedure was more accurate when compared with the applied proximate analysis.

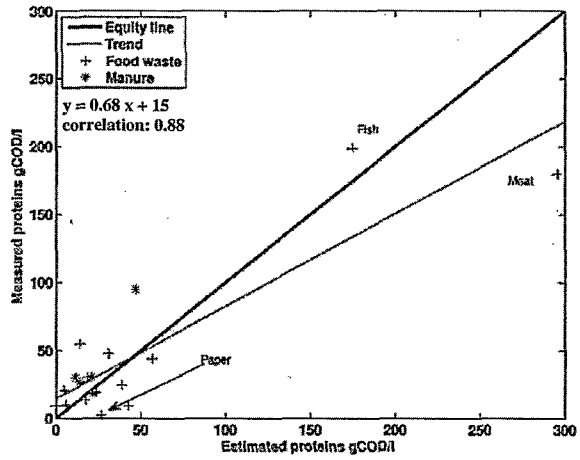

Figure 2—Comparison of the estimated and proximate analysis of proteins for the different waste types.

Protein Estimation. Figure 2 shows the comparison of protein results. Estimated and measured proteins were less correlated compared with the carbohydrates, with more noise around the equity and trend lines. The extracted proteins from each food waste were measured by a colorimetric method that is calibrated on a single type of soluble protein (i.e., bovine serum albumin), while proteins from each waste were composite particulates from different amino acids. For example, meat proteins were extremely underestimated by the proximate analysis compared with fish. Meat proteins were more complex and could not be completely extracted in a soluble form for colorimetric analysis. Comparing carbohydrate and protein results for both meat and fish, it can be seen that the estimated results using the developed procedure are more consistent. Estimated results show the reality that both fish and meat had more proteins than carbohydrates, while proximate analysis shows the reverse. This was explained by the effect of such outliers on regression and correlation parameters in Figure 2, with a lower slope and larger intercept of the regression (trend) line despite the high correlation. Exploitation of elemental mass and COD continuity by the developed procedure keeps the results more consistent. Also, erroneous results or records of practical measurement input to the procedure were concealed in the results. For example, the procedure overestimated proteins for the paper waste, because its TAN content was not measured and all TKN was used for the protein estimation. Because the procedure applies ordered maximization, giving protein estimation precedence over carbohydrates, estimated carbohydrate COD was reduced to compensate for the extra COD estimated in protein, keeping the overall COD balance. However, such COD reduction of paper waste carbohydrates was less significant compared with the amount of fibers that could not be extracted (see Figure 1).

Lipids Estimation. Figure 3 shows the lipids results. Except in meat, either the considered waste fractions did not have lipids content, or the lipids content was too low when compared with carbohydrates and protein fractions. Except in paper and meat, there was an agreement between estimated and measured lipids, although only the phospho-lipids form was considered, and phosphorous data was collected from online solid waste and biomass databases. For meat, it is possible that the lipids extraction was overestimated, as a result of the extraction of lipoproteins. It was not possible to

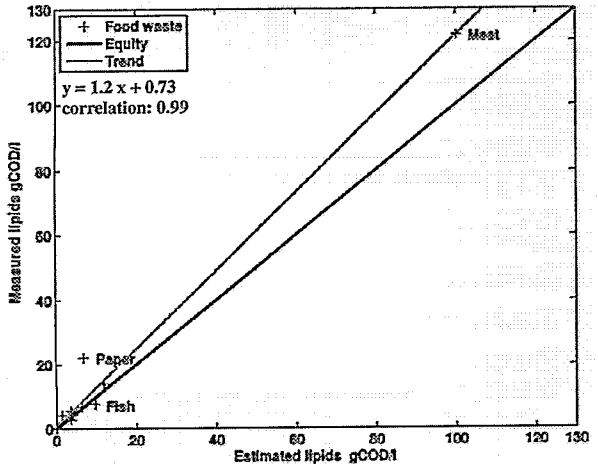

Figure 3—Comparison of the estimated and proximate analysis of lipids for the different waste types.

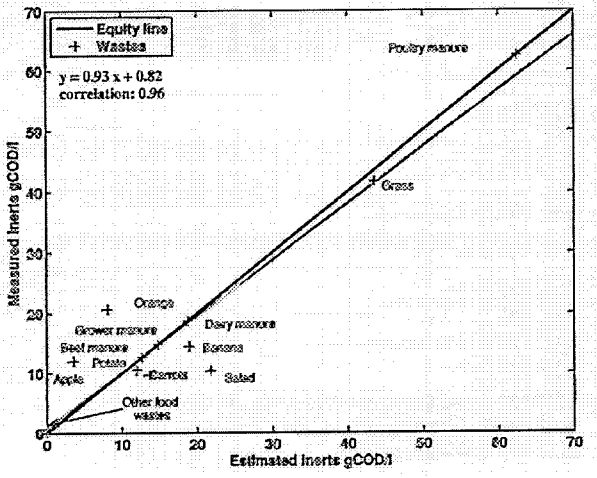

Figure 4—Comparison of the estimated and proximate analysis of inerts for the different waste types.

extract lipids from manure, as they exist in a very small fraction. However, the developed procedure could estimate such small fractions in manure. It was necessary to consider only organic phosphorous (TP – orthoP) to obtain consistent lipids estimation in manures. Kitchen food wastes' phosphorous was mainly in the organic form.

Inerts Estimation. Figure 4 shows the results of estimated inerts compared with that measured. High correlations were observed between the estimated inerts and the measured inert residues. Although the specific inerts composition of each waste was unknown, a reasonable inerts composition was estimated during the procedure development and resulted in high correlation with the measurements. Estimated and measured inerts even matched for wastes that have more inert fractions, such as grass and poultry manure. Thus, the developed procedure can accurately estimate inert fractions to assess waste treatment and handling of treated wastes.

Conclusions

The results of the developed procedure were more consistent when compared with the proximate analysis. The procedure accurately estimated the carbohydrates fraction for all waste types with high linearity over an extended measurement range. Estimated concentrations of high-protein wastes were more consistent compared with the proximate analysis, as no extraction techniques were needed. Considering phospho-lipids and total phosphorous measurement is appropriate for accurate estimation of lipids in most organic waste types. This procedure can be used to generate the complete input vector to the IWA-ADM1; thus, it is applicable to optimization and design of solid waste anaerobic digestion systems.

Credits

This work was partly funded by the Washington State Department of Ecology (Olympia, Washington), the California Energy Commission (Energy Innovation Small Grant, San Diego, California), and the Paul Allen Family Foundation (Seattle, Washington). We appreciate the editing efforts of Andrea Guss, Biological Systems Engineering, Washington State University (Pullman, Washington).

Submitted for publication July 14, 2007; revised manuscript submitted June 25, 2008; accepted for publication September 30, 2008.

The deadline to submit Discussions of this paper is July 15, 2009.

References

American Public Health Association; American Water Works Association; Water Environment Federation (2005) *Standard Methods for the Examination of Water and Wastewater,* 21st ed.; American Public Health Association: Washington, D.C.

American Society of Agricultural Engineers (1998) Manure Production and Characteristics, In *ASAE Standards,* 45th ed., section D384.1; American Society of Agricultural Engineers: St. Joseph, Michigan, 646–648.

AOAC International (2007) *AOAC Official Methods of Analysis,* 18th ed.; AOAC International: Gaithersburg, Maryland.

Association of Official Analytical Chemists (1990) *Official Methods of Analysis,* Vol. 1, 15th ed.; Association of Official Analytical Chemists: Arlington, Virginia.

Batstone, D. J.; Keller, J.; Angelidaki, R. I.; Kalyuzhnyi, S. V.; Pavlostathis, S. G.; Rozzi, A.; Sanders, W. T. M.; Siegrist, H.; Vavilin, V. A. (2002) Anaerobic Digestion Model No. 1, Scientific and Technical Report No. 13; IWA Publishing: London, United Kingdom.

Bernard, O.; Hadj-Sadok, Z.; Dochain, D.; Genovesi, A.; Steyer, J. P. (2001) Dynamical Model Development and Parameter Identification for an Anaerobic Wastewater Treatment Process. *Biotechnol. Bioeng.,* **75,** 424–438.

Buffiere, P.; Loisel, D.; Bernet, N.; Delgenes, J.-P. (2006) Towards New Indicators for the Prediction of Solid Waste Anaerobic Digestion Properties. *Water Sci. Technol.,* **53** (8), 233–241.

Copp, J.; Jeppsson, U.; Rosen, C. (2003) Towards an ASM1-ADM1 State Variable Interface for Plant-Wide Wastewater Treatment Modeling. *Proceedings of the 76th Annual Water Environment Federation Technical Exposition and Conference,* Los Angeles, California, Oct. 11–15; Water Environment Federation: Alexandria, Virginia.

Energy Research Centre of the Netherlands (2007) Phyllis Database for Biomass and Waste. Energy Research Centre of the Netherlands: Petten, Netherlands, http://www.ecn.nl/phyllis.

Garcia de Cortazar, A. L.; Monzon, I. T. (2007) MODUELO 2: A New Version of an Integrated Simulation Model for Municipal Solid Waste Landfills. *Environ. Modell. Softw.,* **22** (1), 59–72.

Goering, H. K.; Soest, P. J. (1970) Forage Fiber Analyses (Apparatus, Reagents, Procedures, and Some Applications). In *Agriculture Handbook No. 379,* Jacket No. 387-598; ARS-USDA: Washington, D.C.

Gujer, W.; Henze, M.; Mino, T.; van Loosdrecht, M. C. M. (1999) Activated Sludge Model No. 3. *Water Sci. Technol.,* **39** (1), 183–193.

Hartmann, H.; Ahring, B. K. (2006) Strategies for the Anaerobic Digestion of the Organic Fraction of Municipal Solid Waste: An Overview. *Water Sci. Technol.,* **53** (8) 7–22.

Henze, M.; Gujer, W.; Mino, T.; van Loosdrecht, M. C. M. (2000) Activated Sludge Models: ASM1, ASM2, ASM2d and ASM3, Scientific and Technical Report No 9; IWA Publishing: London, United Kingdom.

Holm-Nielsen, J. B.; Dahl, C. K.; Esbensen, K. H. (2006) Representative Sampling for Process Analytical Characterization of Heterogeneous Bioslurry Systems: A Reference Study of Sampling Issues in PAT. *Chemom. Intell. Lab. Syst.,* **83** (2), 114–126.

Islam, J.; Singhal, N. (2002) A One-Dimensional Reactive Multi-Component Landfill Leachate Transport Model. *Environ. Modell. Softw.,* **17** (6), 531–543.

Johansen, J. E.; Bakke, R. (2006) Enhancing Hydrolysis with Microaeration. *Water Sci. Technol.,* **53** (8), 43–50.

Kayhanian, M.; Tchobanoglous, G.; Mata-Alvarez, J. (1996) Development of a Mathematical Model for the Simulation of the Biodegradation of Organic Substrates in a High-Solids Anaerobic Digestion Process. *J. Chem. Technol. Biotechnol.,* **66** (3), 312–322.

Kleerebzem, R.; Van Loosdrecht, M. C. M. (2006) Waste Characterization for Implementation in ADM1. *Water Sci. Technol.,* **54** (4), 167–174.

Lowry, O. H.; Rosebrough, N. J.; Fair, A. L.; Randall, R. J. (1951) Protein Measurement with the Folin Phenol Reagent. *J. Biol. Chem.,* **193,** 265–275.

Mata-Alvarez, J.; Mace, S.; Llabres, P. (2000) Anaerobic Digestion of Organic Solid Wastes—An Overview of Research Achievements and Perspectives. *Bioresour. Technol.,* **74,** 3–16.

Moosbrugger, R. E.; Wentzel, M. C.; Loewenthal, R. E.; Ekama, G. E.; Marais, G. v. R. (1993) Alkalinity Measurement: Part 3—A 5 pH Point Titration Method to Determine the Carbonate and SCFA Weak Acid/Bases in Aqueous Solution Containing Also Known Concentrations of Other Weak Acid/Bases. *Water SA,* **19,** 29–40.

Neitsch, S. L.; Arnold, J. G.; Kiniry, J. R.; Williams, J. R. (2001) Solids and Water Assessment Tool, SWAT-Users Manual; USDA Agricultural Research Service, Grassland, Soil and Water Research Laboratory: Temple, Texas.

Reichert, P.; Borchardt, D.; Henze, M.; Rauch, W.; Shanahan, P.; Somlyo'dy, L.; Vanrolleghem, P. A. (2001) River Water Quality Model No. 1, IWA Scientific and Technical Report No. 12; IWA Publishing: London, United Kingdom.

U.S. Department of Agriculture (2007a) Agricultural Research Service 2005. USDA National Nutrient Database for Standard Reference, Release 18; U.S. Department of Agriculture: Washington, D.C., http://www.ars.usda.gov/ba/bhnrc/ndl.

U.S. Department of Agriculture (1996) *Agricultural Waste Management Field Handbook,* 210-vi–AWMFH, Rev. 1; U.S. Department of Agriculture: Washington, D.C., http://www.info.usda.gov/CED/ftp/CED/neh651-ch4.pdf.

U.S. Department of Agriculture (2007b) NRCS. Manure Characteristics, http://www.nrcs.usda.gov/technical/NRI/pubs/manntr.html.

U.S. Department of Energy (2007) Biomass Feedstock Composition and Property Database. U.S. Department of Energy: Washington, D.C., http://www.eere.energy.gov/biomass/progs/search1.cgi.

Van Soest, P. J. (1963) Use of Detergent in the Analysis of Fibrous Feeds. A Rapid Method for the Determination of Fibre and Lignin. *J. Assoc. Offic. Anal. Chem.,* **46** (5), 829–835.

Vanrolleghem, P. A.; Rosen, C.; Zaher, U.; Copp, J.; Benedetti, L.; Ayesa, E.; Jeppsson, U. (2005) Continuity-Based Interfacing of Models for Wastewater Systems Described by Petersen Matrices. *Water Sci. Technol.,* **52** (1–2), 493–500.

Yemm, E. W.; Willis, A. J. (1954) The Estimation of Carbohydrates in Plant Extracts by Anthrone. *Biochemical. J.,* **57** (3), 508–513.

Zaher, U.; Grau, P.; Benedetti, L.; Ayesa, E.; Vanrolleghem, P. A. (2007) Transformers for Interfacing Anaerobic Digestion Models to Pre- and Post-Treatment Processes in a Plant-Wide Modelling Context. *Environ. Modell. Softw.,* **22** (1), 40–58.

Zaher, U.; Vanrolleghem, P. A. (2005) Automatic Initialisation of Buffer Composition Estimation for On-Line Analysis of Unknown Buffer Solutions. *Anal. Bioanal. Chem.,* **383** (4), 605–618.

Appendix 4: GISCOD model and Experimental Analysis of Food Waste Co-digestion

Zaher U., Li R., Jeppson U., Steyer J-P., and Chen S. (2008) GISCOD: general integrated solid waste co-digestion model, Water Research (submitted)

Available at www.sciencedirect.com

ScienceDirect

journal homepage: www.elsevier.com/locate/watres

GISCOD: General Integrated Solid Waste Co-Digestion model

Usama Zaher[a,*], *Rongping Li*[a,b], *Ulf Jeppsson*[c], *Jean-Philippe Steyer*[d], *Shulin Chen*[a]

[a]*Department of Biological Systems Engineering, Washington State University, P.O. Box 646120, Pullman, WA 99164-6120, USA*
[b]*Department of Environmental Engineering, Beijing University of Chemical Technology, 100029 Beijing, PR China*
[c]*Department of Industrial Electrical Engineering and Automation, Lund University, Box 118, SE-22100, Lund, Sweden*
[d]*INRA, UR 50, Laboratoire de Biotechnologie de l'Environnement, Avenue des Etangs, F-11100 Narbonne, France*

ARTICLE INFO

Article history:
Received 22 December 2008
Received in revised form
11 March 2009
Accepted 14 March 2009
Published online 21 March 2009

Keywords:
ADM1
Co-digestion
Hydrolysis
Integrated modeling
Solid waste
Transformer model

ABSTRACT

This paper views waste as a resource and anaerobic digestion (AD) as an established biological process for waste treatment, methane production and energy generation. A powerful simulation tool was developed for the optimization and the assessment of co-digestion of any combination of solid waste streams. Optimization was aimed to determine the optimal ratio between different waste streams and hydraulic retention time by changing the digester feed rates to maximize the biogas production rate. Different model nodes based on the ADM1 were integrated and implemented on the Matlab-Simulink® simulation platform. Transformer model nodes were developed to generate detailed input for ADM1, estimating the particulate waste fractions of carbohydrates, proteins, lipids and inerts. Hydrolysis nodes were modeled separately for each waste stream. The fluxes from the hydrolysis nodes were combined and generated a detailed input vector to the ADM1. The integrated model was applied to a co-digestion case study of diluted dairy manure and kitchen wastes. The integrated model demonstrated reliable results in terms of calibration and optimization of this case study. The hydrolysis kinetics were calibrated for each waste fraction, and led to accurate simulation results of the process and prediction of the biogas production. The optimization simulated 200,000 days of virtual experimental time in 8 h and determined the feedstock ratio and retention time to set the digester operation for maximum biogas production rate.

Published by Elsevier Ltd.

1. Introduction

This paper presents GISCOD, a general integrated solid waste co-digestion model. The main goal of this study was to develop and test a simulation tool of the anaerobic digestion (AD) process that is applicable to any combinations of waste streams using the simulation platform Matlab-Simulink®. The Matlab® simulation platform was used for implementation of the risk assessment of gas emissions from solid waste incinerators (Kumar et al., 2009) and modeling solid waste landfills (García de Cortázar and Monzón, 2007), and suggested as a common interface model for solid waste management (bou Najm and El-Fadel, 2004).

A general co-digestion model is needed to support operation decisions at full-scale plants and to assist co-digestion research. The AD process is a widely applicable technology to treat and convert an organic waste stream to methane for green energy production. At wastewater treatment plants, trucked-in wastes are digested with wastewater sludge for renewable energy production (Wallis et al., 2008; Zupancic

* *Corresponding author*. Fax: +1 509 335 2722.
E-mail addresses: zaheru@wsu.edu (U. Zaher), ulf.jeppsson@iea.lth.se (U. Jeppsson), steyer@supagro.inra.fr (J.-P. Steyer), chens@wsu.edu (S. Chen).
0043-1354/$ – see front matter Published by Elsevier Ltd.
doi:10.1016/j.watres.2009.03.018

et al., 2008) as part of municipal policies for climate change mitigation and reduction of green house gas emissions. Biogas plants co-digest different solid waste feedstock to increase biogas production. However, random or heuristic decision on the ratio between waste streams or feedstock to full-scale plants often lead to process upset and significant reduction of methane production (Steyer et al., 2006). The general model would support such full-scale operation decisions. Significant research effort was devoted during the last 5 years to study the co-digestion of different combinations of municipal, industrial, agricultural and farming waste streams. A general model is needed to define optimal co-digestion experiments sparing research efforts of experimental trials, and to simulate AD improvement mechanisms that are achieved by co-digestion such as buffered pH, reduced inhibition, improved hydrolysis and/or adjusted C/N ratio. Improvement mechanisms of co-digestion can be simulated by the ADM1, International Water Association Anaerobic Digestion Model number 1, which was developed by the task group on anaerobic digestion (Batstone et al., 2002). However, the ADM1 application has practical problems related to the characterization of the digester feedstock and the associated model definition of the enzymatic disintegration and hydrolysis steps.

A generalized and separate approach is required to solve the solid waste characterization problems compared to Activated Sludge (AS) for two reasons. Firstly, ADM1 is considering constant composition of particulates with fixed fraction parameters to carbohydrates, proteins, lipids and inerts. On the contrary, solid wastes are heterogenic and dynamically changing in composition. Secondly, the lumped composite particulate model component is used as the first model input and, simultaneously, as a product from the model decay processes. This implies that the fraction parameters and hydrolysis rates of the feed substrate should match the composition and hydrolysis rates of the decaying biomass. In fact, the ADM1 was originally developed with focus on the application of AS digestion assuming similar composition of the aerobic and anaerobic bacteria. Under this assumption, there is no conflict between the feed substrate and the produced substrate from decaying bacteria. In this particular case, cell lysis (disintegration) is the limiting hydrolysis step. Such an assumption was proven to be consistent for plant-wide modeling since the AS inert fraction remains inert under anaerobic conditions (Ekama et al., 2007).

In previous applications of the ADM1, fraction parameters were estimated from experimental data (Fezzani and Cheikh, 2008a,b) or evaluated as function of VS influx (Lübken et al., 2007). Using *a priori* expert knowledge about expected wastewater characteristics and experimental measurements to estimate fraction parameters is generally applied for modeling wastewater treatment systems (Grau et al., 2007). Applying such a procedure to co-digestion is not feasible since it is difficult to find unique parameter values that are applicable to all possible combinations and ratios of solid wastes together with decaying anaerobic biomass.

Parameter estimation problems and use of fraction parameters could be avoided using a dynamic interface to ADM1 to simulate AD of animal manure and solid waste (Zaher and Chen, 2006). The interface procedure was validated by comparing the estimated carbohydrates, proteins, lipids and inerts concentrations with the proximate analysis of 17 solid wastes (Zaher et al., 2009). In the research work presented in this paper, the interface procedure is generalized and implemented with GISCOD in Matlab-Simulink as a general transformer model that interface ADM1 to any combination of co-digested wastes. The influxes of the model components from each waste are evaluated dynamically. The hydrolysis parameters are considered separately for each waste and uncoupled from the hydrolysis of the decaying biomass. Therefore, the GISCOD modeling tool is generalized to study the co-digestion of any combination of different wastes and to evaluate their independent hydrolysis rates and operation settings, i.e. their optimal feed ratio and hydraulic retention time (HRT).

2. Methods

2.1. *Process model*

The AD process was modeled using the ADM1 (Batstone et al., 2002) as a basis with phased implementation to separate the enzymatic hydrolysis of solid wastes from the metabolic reactions utilizing soluble substrates. The ADM1 model starts with a disintegration step of composite particulate material, i.e. decomposition of feed or decaying biosolids according to their predefined fractions and composition of carbohydrates, proteins, fat (lipids) and inerts. The second step is enzymatic hydrolysis of disintegrated carbohydrates, proteins and fat (lipids), which is the start of the corresponding three pathways of anaerobic degradation. The anaerobic degradation is done in three main steps—acidogenesis, acetogenesis and methanogenesis. The degradation steps are modeled by uptake kinetics of different substrates by seven bacterial groups. The decay processes of the seven bacterial groups are also considered and the decaying particulates are sent back to the disintegration step.

The implemented GISCOD model shown in Fig. 1 is generalized to consider the degradation of any other wastes that are different in composition compared to the assumed biosolids (i.e. decaying bacteria). Each waste would have different fractions of carbohydrates, proteins, lipids and inerts that may be changing dynamically (Lübken et al., 2007). Each waste would also have different hydrolysis rates of carbohydrates, proteins and lipids (Fezzani and Cheikh, 2008a,b). Carbohydrates, proteins and lipids hydrolysis of each waste is considered in separate model nodes. The disintegration step was not considered for solid wastes assuming that enzymes can diffuse in the woven structure of wastes and hydrolysis would take place before disintegration. No cell lysis is required for solid wastes compared to AS or decaying bacteria. The hydrolysis products are combined and used as input to a single digestion node where all biological reactions of ADM1 are activated. The non-hydrolyzed fractions are fed through the digestion node as a dummy vector and hydrolysis kinetics in the digestion node are only applied to the decaying biosolids. The complete structure of ADM1 is considered in the hydrolysis nodes to allow future expansion of the co-digestion model considering more complex hydrolysis kinetics. The other biological reactions are deactivated for the hydrolysis

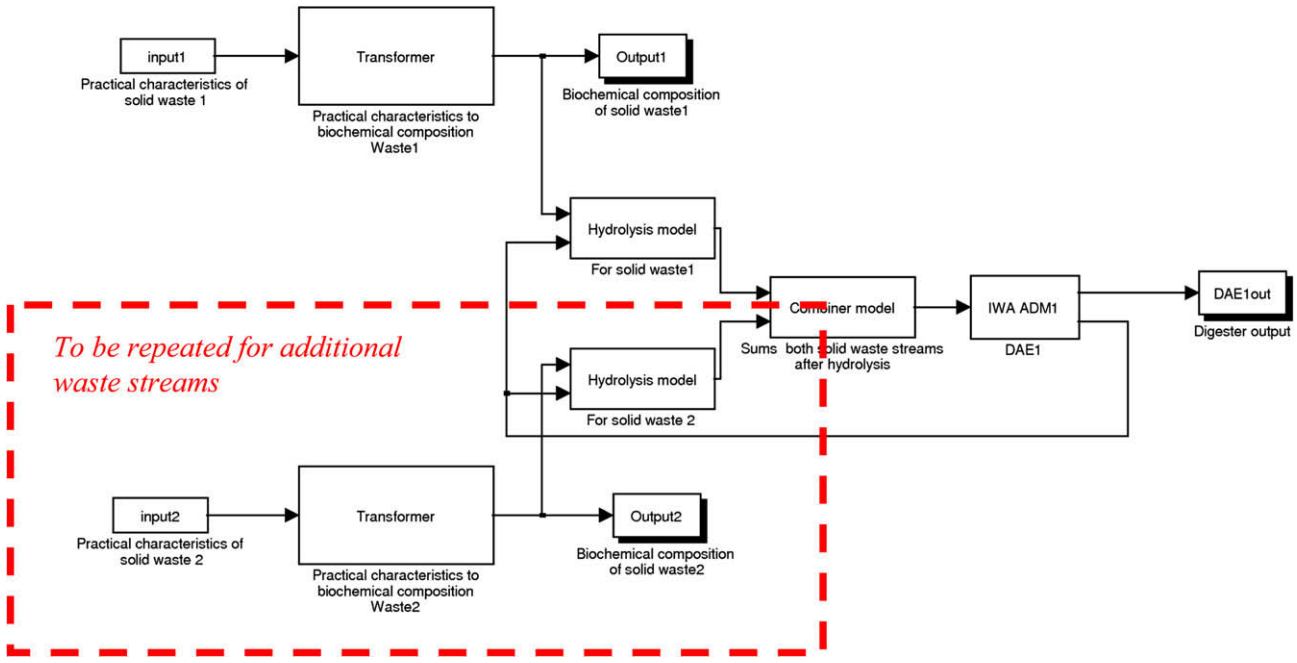

Fig. 1 – The GISCOD model in Matlab-Simulink.

nodes simply by assuming zero uptake, disintegration, decay and gas transfer rates.

In addition to the biological reactions, the ADM1 implementation considers the chemical equilibrium of all ions to evaluate the pH change. The chemical equilibrium of volatile fatty acids (VFA), the carbon and nitrogen systems is solved externally once for all hydrolysis and digestion nodes. The solution of chemical equilibrium is performed algebraically according the ADM1–DAE implementation (Rosen et al., 2006). The ADM1–DAE implementation removes stiffness from the original ADM1 Ordinary Differential Equations (ODE) system to simulate rapid dynamic changes in the anaerobic digestion process, e.g. due to changing composition of the digester feedstock.

2.2. *Transformer model*

A general transformer model to interface ADM1 to different solid waste streams was programmed in C and incorporated in the GISCOD Matlab-Simulink model as a C-MEX S-Function. The general transformer model is based on the ADM1 interface to solid wastes (Zaher and Chen, 2006; Zaher et al., 2009). The transformer model combines the advantages of previous interfacing methodologies applied to ADM1.

2.2.1. *Implemented interfacing advantages*

The general transformer model represents an enhancement of the Continuity Based Interfacing Methodology (CBIM) (Vanrolleghem et al., 2005). The CBIM applies Chemical Oxygen Demand (COD) balance, charge balance and elemental continuity to all macronutrient elements CHNOP to connect different models (Volcke et al., 2006; Zaher et al., 2007). The CBIM in the general transformer is applied to interface the ADM1 to practical characteristics of solid wastes. Kleerebezem and van Loosdrecht (2006) used practical characteristics such as COD, Total Kjeldahl Nitrogen (TKN), etc. to characterize the ADM1 influent. They assumed the digester's feedstock as a single composite particulate (Xc) with constant composition and used the practical characteristics to estimate ADM1 fraction parameters that distribute Xc after disintegration to particulate components of carbohydrates, proteins and lipids. The use of the fraction parameters does not allow dynamic simulation due to changes in the feedstock composition. The transformer model applies CBIM to estimate the influxes to ADM1 and avoids the overuse of fraction parameters to allow dynamic simulation. The transformer model robustness is increased by updating the CBIM procedure to maximize the conversions to ADM1 components in a predefined order. COD and charge balances, and the continuity of all CHNOP elements are checked after the conversion of each component. Such an ordered maximization procedure was suggested by Copp et al. (2003) to interface Activated Sludge Model no.1 (Henze et al., 1987) ASM1 with ADM1, maintaining the COD and N balances. Most recently, Nopens et al. (in press) modified the Copp et al. (2003) ASM1–ADM1 interface. They increased the robustness of the ASM1–ADM1 conversions by changing the maximization order of ADM1 components for the co-digestion of secondary sludge (from ASM1) with primary sludge (from primary settler). The conversions from ASM1 to ADM1 were extended to include carbohydrates, proteins and lipids instead of Xc. Proteins were maximized using Total Kjeldahl Nitrogen (TKN) and the remaining particulate COD was distributed between carbohydrate and lipids using fraction parameters. Extending the balance relations in the transformer model eliminates the use of fraction parameters. The transformer model is upgraded in the implementation with GISCOD to allow the user to change the maximization order of ADM1 components without changing

the transformer model algorithm. The maximization order is implemented as a one-dimensional array parameter to the transformer S-function to increase the generality of the transformer model for the application to any solid waste.

2.2.2. *Transformer algorithm*

The transformer model transforms a set of practical measurements to the input vector of ADM1 according to the stoichiometry presented in Table 1. Table 1 consists of four panes. The lower two panes shows the assumed composition of the practical measurements on the left, components 1 to 11, and the composition of the estimated ADM1 input components on the right. The upper two panes represent the stoichiometry $\nu_{j,k}$ for the conversions j and the elements k. The stoichiometry is evaluated by mass and charge balances according to Eq. (1). The stoichiometry matrix is uploaded to the Matlab work space as a two-dimensional array parameter to transformer model S-function.

$$\sum_{k} \nu_{j,k} i_{j,\mathrm{Comp}} = 0 \text{ with Comp} = \mathrm{Thod, C, N, H, O, e} \tag{1}$$

The transformation step in CBIM was changed to include the ordered maximization procedure. The original transformation of CBIM is generated by Eqs. (2) and (3). A set of algebraic equations is generated by Eq. (2) to map the influxes to vector ρ_j, $j = 1{:}n$ where n is the number of conversions, using the stoichiometry in the left pane of the transformation matrix, i.e., for $k = 1{:}P$ where P is the number of practical measurements. Then Eq. (3) calculates the outfluxes from ρ_j using the stoichiometry in the right pane of the transformation matrix, i.e., $k = P + 1{:}P + Q$ where Q is the number of the estimated composition components.

$$\sum_{j=1}^{n} \nu_{j,k}\rho_j = \mathrm{Influx}_k \quad \text{for } k = 1 : P \tag{2}$$

$$\mathrm{Outflux}_k = \sum_{j=1}^{n} \nu_{j,k}\rho_j \quad \text{for } k = P + 1 : P + Q \tag{3}$$

In the implementation for the co-digestion model Eq. (2) is replaced by a maximization procedure according to Zaher et al. (2009) to increase the transformer robustness, to conceal (correct) possible errors in the practical measurements and to maintain the elemental mass balance during the conversions. The elements of the vector ρ_j are maximized in a predefined order to make sure that the elemental influxes sourced by the input of practical measurements are sufficient before calculating the next element of ρ_j. A predefined order of ρ_z, $z = 1{:}10$, which corresponds to $j = (10, 5{:}9, 4, 3, 1, 2)$, maximizes the conversion to inert particulates, volatile fatty acids, sugars, lipids, proteins, carbohydrates, and then inorganic components. This maximization order is uploaded before simulation to the Matlab work space as a parameter to the transformer model S-function. Thus, the maximization order can be easily changed by the user. The maximization is done according to the following steps:

1. ρ_z is calculated using Eq. (4) as a function of the influx of the most correlated measurement k, i.e., corresponding to the unique value of $\nu_{z,k} = -1$ at each conversion;
2. ρ_z is verified using the conditions imposed by Eq. (5). If shown true, the next ρ_{z+1} was calculated starting from step 1 above;
3. If shown false, ρ_z is changed and calculated according to Eq. (6), the ρ_z calculation is then terminated and other rates (ρ_i, $i = z + 1{:}n$) are assigned a value of 0;
4. Any remaining fluxes are added to the relevant inorganic components; and accordingly,
5. All practical measurements are mapped to the new vector ρ. The output flux of substrate composition is then calculated using Eq. (3).

$$\rho_z = \left(\frac{\mathrm{Influx}_k - \sum_{i=1}^{z-1} \nu_{i,k}\rho_i}{\nu_{z,k}} \right) \tag{4}$$

$$\sum_{1}^{z} \nu_{z,k}\rho_z < \mathrm{Influx}_k \quad \text{for } k = 1 : P \tag{5}$$

$$\rho_z = \min \left| \frac{\mathrm{Influx}_k - \sum_{i=1}^{z-1} \nu_{i,k}\rho_i}{\nu_{z,k}} \right| \quad \text{for } k = 1 : P \tag{6}$$

2.3. *Integrated co-digestion model*

The different models integrated in GISCOD are written in C and compiled in Matlab as MEX S-functions to run simulations and optimizations using the Matlab-Simulink platform and its toolboxes. The compiled version of the model works with most Matlab-Simulink (release 14) installations on Windows XP and VISTA operating systems.

The practical characteristics and flows of all different solid wastes as well as all model parameters are arranged in Microsoft Excel file. All inputs, initial states and parameters to the co-digestion models are read from the Excel file into the Matlab work space using an automated Matlab script. The simulation starts from Simulink after configuring the numerical solution using any variable step solver that is available in Simulink. Fig. 1 shows the scheme of GISCOD in Matlab-Simulink. Practical characteristics and flows of each solid waste are inputs from the workspace to the transformer model nodes. The practical characteristics are converted to the complex composition of the ADM1 input state vector and assigned to the input of separate hydrolysis nodes. The hydrolysis output signals are rearranged by the combiner model, which generates the input to the ADM1 node. The combiner model divides the solid wastes AD process into an enzymatic hydrolysis phase in the hydrolysis nodes only and an uptake phase of the hydrolysis products in the ADM1 node. Thus, Solids Residence Time (SRT) of each waste is considered separately for each hydrolysis node according to the time its particulate components are allowed to stay in the digester (i.e. according mixing patterns) in addition to the time of any pre-hydrolysis steps. The combiner node passes the non-hydrolyzed particulates as dummy variables to the ADM1 and sums other variables on the basis of fluxes from

Table 1 – Calculated transformation and composition matrices of the transformer model.

	k	1	2	3	4	5	6	7	8	9	10	11	12	18	21	23	24	25	33	34	35	36	37	38	39
	components	CODp	DODs-VFA	VFA	TOC	Norg	TAN	TP-orthoP	orthoP	TIC	Scat	FS	S_{su}	S_{ac}	X_{I}	X_{ch}	X_{pr}	X_{li}	S_{cat}	S_{an}	S_{ic}	S_{ip}	S_{O-h}	S_{H+}	S_{an}
		(gCOD m^{-3})	(gCOD m^{-3})	(gCOD m^{-3})	(gC m^{-3})	(gN m^{-3})	(gN m^{-3})	(gP m^{-3})	(gP m^{-3})	(mol HCO_3^- m^{-3})	(eq m^{-3})	(g m^{-3})	(kgCOD m^{-3})	(kgCOD m^{-3})	(kgCOD m^{-3})	(kgCOD m^{-3})	(kgCOD m^{-3})	(kgCOD m^{-3})	(kmole m^{-3})	(kmoleN m^{-3})	(kmoleC m^{-3})	(kmolP m^{-3})	(kmole m^{-3})	kmole	(kmole m^{-3})
j	Conversion to																								
1	ammonia						-1													7.14E-05				-5.55E-20	-4.16E-20
2	bicarbonate									-1											1.00E-03				
3	ortho phosphate								-1													3.17E-05	5.43E-07	-3.23E-05	5.43E-07
4	cations										-1								0.001						
5	VFA			-1	-0.375001									0.001							1.00E-10		-7.50E-11	-2.50E-11	-5.00E-11
6	Sugars		-1		-0.375								0.001								-1.07E-18		8.07E-19	2.80E-19	5.47E-19
7	lipids	-6.457862			-2.712302			-1										0.006458					9.75E-06	-2.86E-05	-3.83E-05
8	proteins	-6.857143			-2.57143	-1											0.006857				1.00E-10		1.79E-05	5.36E-05	3.57E-05
9	carbohydrates	-1			-0.375											0.001					1.07E-18		-8.05E-19	-2.68E-19	-5.37E-19
10	organic inerts	-0.990616			-0.40463	-0.055921		-0.006388				-1			0.000991					-1.09E-07	2.85E-07	3.71E-12	-1.01E-06	-2.09E-12	8.18E-07
composition matrix	i_ThOD (gThOD/stoich.unit)	1.000	1.000	1.0000									1000	1000.0000	1000	1000	1000	1000							
	i_C (gC/stoich.unit)				1.000					12.00			375	375.0000	403.973398	375	375	420			12000				
	i_N (gN/stoich.unit)					1.00	1.00								56.3753997		145.833333			14000					
	i_O (gO/stoich.unit)	0.417	0.500	0.5000				2.07	2.07	48.00			500	500.0000	481.150513	416.666667	250	640			48000	64000	64000		
	i_H (gH/stoich.unit)	0.052	0.063	0.0469		0.14	0.29	0.03		1.00			62.5	46.8750	61.5254609	52.0833333	62.5	60		4000	1000	1000	1000	1000	
	i_P (gP/stoich.unit)							1.00	1.00						6.44793374			154.35				31500			
	i_Ch (Ch/stoich.unit)			-0.0156			0.07	-0.03	-0.10	-1.00	1.00			-15.6250				-5	1000	1000	-1000	-2000	-1000	1000	-1000
	i_Covalent Bond (Bond/stoich.unit)	-0.125	-0.125	-0.1250	0.333	-0.07		-0.03																	
	Total mass/stoich.unit											1			1009.47271										
																			Source sink components of consequently:		N	C	P	O	H	Ch

both waste streams. In the ADM1 node, non-hydrolyzed portions are not subject again to the hydrolysis kinetics and the hydrolysis in the ADM1 node is only considered for particulate fractions of the decaying biosolids (bacteria). Thus, the digester out-flux contains non-hydrolyzed carbohydrates, proteins and lipids originating from the solid wastes in addition to the corresponding components resulting from decaying biosolids. Thus the mass balance is maintained. The ADM1 is solved at each time step and the output is stored in the Matlab workspace. The chemical equilibrium is solved in the ADM1 model node and the evaluated ions and pH are shared with the hydrolysis nodes. The pH calculation is linked to the hydrolysis nodes to allow future extension of the hydrolysis kinetics to reflect the pH dependency of the hydrolysis. Although the optimal pH of methanogenesis is around pH 7.0, the optimum pH of hydrolysis and acidogenesis is between pH 5.5 and 6.5 (Ward et al., 2008).

2.4. *Calibration and optimization case study*

GISCOD robustness and simulation speed were tested by running the model in parameter estimation and optimization algorithms. Parameter estimation was done using Simulink® Parameter Estimation™ software and the simplex optimization algorithm (Nelder and Mead, 1965). Two experiments of digesting manure alone and manure with kitchen waste were performed to calibrate the hydrolysis parameters for each waste. Both waste average characteristics are listed in Table 2. Only the indicated 11 characteristics are needed as model inputs. It was not possible to digest food waste alone due to acidification and pH drop. Both wastes were homogenized and kept frozen in batches that were only thawed before feeding. The only degree of freedom used during the experiment was the daily feed rates, which were varied for each experiment according to the profiles shown in Fig. 2. The reactors for both experiments were completely mixed and arranged to have a hydrolysis step of 0.6 L volume followed by a digestion step of 2 L. All reactors were kept at 35 °C. The gas production from both steps was used for calibration. First, the manure hydrolysis parameters were estimated from the manure only digestion experiment. Secondly, the kitchen waste hydrolysis parameters were estimated from the co-digestion experiment. Carbohydrates, proteins and lipids were analyzed for each waste to validate the transformer predictions. Carbohydrates were quantified by sequential extraction using neutral and acid detergent, followed by strong acid extraction. Proteins were analyzed by the Lowry colorimetric method calibrated on bovine serum albumin. The lipids content was determined by a Soxhlet method using petroleum ether for extraction.

Optimization of the solid waste ratio and HRT was done by simulating several virtual experiments using the calibrated model. The optimal ratio and HRT were determined by comparing the steady state biogas flow rate from such virtual experiments. Virtual experiments of 200 cases were simulated varying the ratio of kitchen waste, flow and methanogenic reactor volume. Ten retention times were considered 5, 7.5, 10, 15, 20, 50, 75, 100, 150 and 200 days. The kitchen waste ratio was varied from 5% to 100% in 5% increments. The hydrolysis volume was 2 L for all the simulated cases. Two methanogenic volumes were considered: 2 L with HRT $\leq$20 days and 20 L for longer HRT. Each case was simulated until the gas flow rate reached a steady state after 1000 days of simulation time, i.e. a total virtual experimental time of 200,000 days.

Table 2 – Characteristics of diluted manure and kitchen waste.

Characteristics	Co-digestion model input no.	Unit	Diluted manure waste	Kitchen waste
Total Chemical Oxygen Demand (CODt)		(gCOD m^{-3})	27217	380647
Particulate COD (CODp)	1	(gCOD m^{-3})	23550	368400
Soluble COD (CODs)		(gCOD m^{-3})	3667	12247
Soluble COD without VFA COD(CODs-VFA)	2	(gCOD m^{-3})	2521	3500
Volatile Fatty Acids (VFA)	3	(gCOD m^{-3})	1146	8747
Total Carbon (TC)		(gC m^{-3})	10064	139760
Total Organic Carbon (TOC)	4	(gC m^{-3})	9340	139280
Total Inorganic Carbon (TIC)	9	(mol HCO_3^- m^{-3})	60	40
Total Kheldal Nitrogen (TKN)		(gN m^{-3})	882	15300
Total Organic Nitrogen (Norg)	5	(gN m^{-3})	598	14000
Total Ammonia Nitrogen (TAN)	6	(gN m^{-3})	284	1300
Total Phosphorous (TP)		(gP m^{-3})	219	1606
Organic Phosphorus (TP-orthoP)	7	(gP m^{-3})	187	720
Ortho-Phosphate (orthoP)	8	(gP m^{-3})	32	886
Total alkalinity (S cations)	10	(equ m^{-3})	60	25
Total Solids (TS)		(g m^{-3})	20697	291000
Fixed Solids (FS)	11	(g m^{-3})	5397	31000
Total Volatile Solids (TVS)		(g m^{-3})	15300	260000
Carbohydrate		(g m^{-3})	10924 $\pm$ 428	153400 $\pm$ 11180
Protein		(g m^{-3})	4069 $\pm$ 367	85800 $\pm$ 8320
Lipids		(g m^{-3})	306 $\pm$ 61.2	20800 $\pm$ 2860

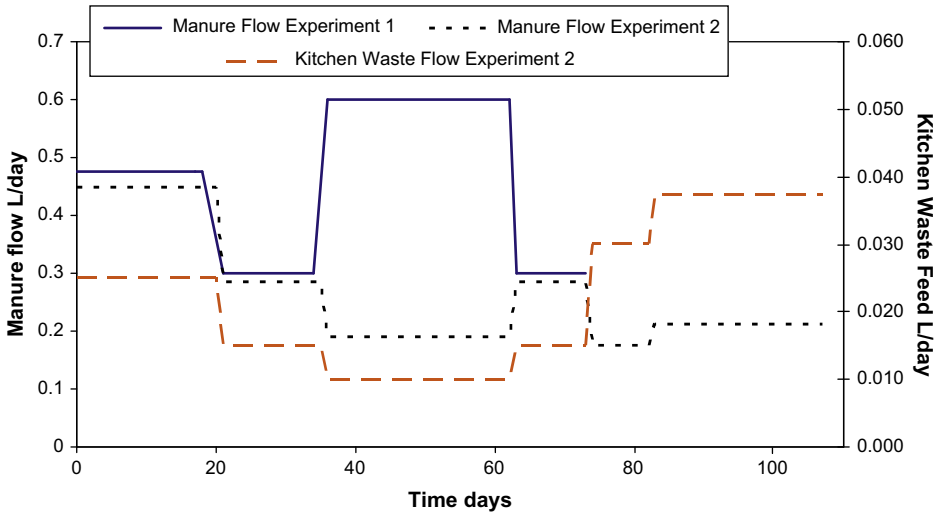

Fig. 2 – Daily feed rates implemented in the calibration experiments.

3. Results and discussion

3.1. *Transformer output*

Among other ADM1 input state variables, carbohydrates, proteins and lipids were estimated in COD units by the transformer model. The ADM1 model uses COD units for organic components and bacterial species to maintain the COD balance. The corresponding g/L concentration was evaluated according to the defined composition of ADM1 components in Table 1 and compared to the measured concentrations in Fig. 3. Generally, the estimated and measured concentrations were consistent in terms of distribution among the three main particulate components. However, some differences could be observed for each individual component when comparing the results for the manure and kitchen waste.

Carbohydrates: Estimated carbohydrates content was consistent with measured data in the case of manure but it was higher in the case of kitchen waste. The detergent extraction method is an accurate standard method to break the crystal structure of fiber, which is the main form of carbohydrates in manure. The starch content is high in kitchen waste but would not be quantified as accurately as fiber with the same extraction method. Using the carbohydrate measurements as a direct input to the ADM1 model would have introduced an error to the carbon balance kept within the model. Therefore, using the transformer model was necessary to keep the carbon balance.

Proteins: Measured and estimated protein contents were more consistent in the case of kitchen waste as compared to the case of manure. The measuring method was calibrated using bovine serum albumin, which is more relevant to the kind of proteins that normally exist in kitchen wastes, such as beef or whey. Using the protein measurements for manure as a direct input to ADM1 model would have introduced errors to the nitrogen balance. Nitrogen in solids wastes is mainly sourced by the particulate proteins. The use of the transformer model maintained the nitrogen balance.

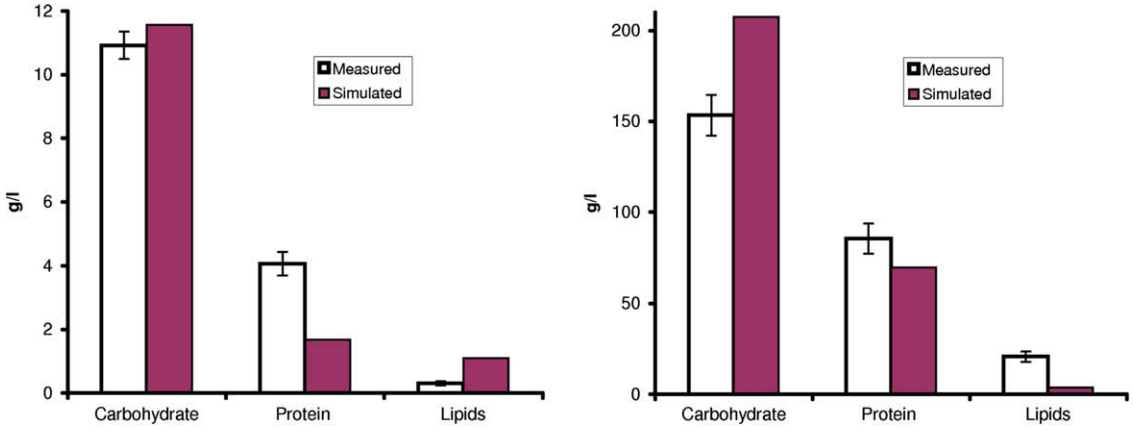

Fig. 3 – Comparison of the measured and the estimated compositions by the transformer model for diluted manure (left) and kitchen waste (right).

Lipids: Lipids were the smallest fraction of particulates in both wastes. The estimated and measured lipids contents were relatively inconsistent. On one hand, the estimated lipids composition was assumed to be in the form of phospholipids but other forms may exist in both wastes. On the other hand, Soxhlet extraction is highly biased if the sample matrix is mainly non-lipids (Manirakiza et al., 2001).

Generally, the use of the transformer model within GISCOD maintains the continuity of COD and elemental mass that are essential to guarantee accurate and reliable simulation. Direct measurements of the waste particulate fractions would not achieve the same reliability. The analytical methods are dependent on the types of the particulate fractions, which are unknown for wastes and are often different from the types defined in the model stoichiometry.

Maintaining accurate carbon and nitrogen balances during the simulation is necessary since the C:N ratio is a key factor affecting the co-digestion of different waste streams (Hartmann and Ahring, 2005; Yen and Brune, 2007; Zhang et al., 2008; Shanmugam and Horan, 2009). Also, the C and N elemental continuity preserved in the GISCOD model is important when linking the AD model to other existing models of subsequent unit processes or for integrated assessment. For instance elemental continuity is the key mechanism to evaluate pH and chemical equilibrium variables, such as CO_2/HCO_3^- and NH_4^+/NH_3 in the AD process out-flux. The evaluation of CO_2 and NH_3 emissions allows further assessment of subsequent unit processes, such as emission studies from composting (Paillat et al., 2005; Komilis and Ham, 2006), drying (Deng et al., 2009) and landfill facilities (He et al., 2006). Furthermore, estimation of the pH and NH_4^+ as well as phosphorus—evaluated from the mass balance in the transformer model—allows more integrated assessment, such as studies evaluating added fertility to soils from waste application (Alvarenga et al., 2007; Kang et al., 2008) or evaluating leachate pollution to water bodies (Singh et al., 2005).

3.2. Simulation speed

The simulation speed was kept low despite the added model complexity of separate hydrolysis and transformation model nodes. The 73 days simulation of manure digestion required less than 1 min CPU-time using the ode15s solver in Simulink with 1E-7 and 1E-6 relative and absolute tolerance, respectively. The longer and more dynamic experiment no. 2 of co-digestion required 1 min 30 s CPU-time using the same simulation settings using a standard 3 GHz PC. The efficient simulation time was achieved because of the separate algebraic solution of the chemical equilibrium. The maintenance of COD and elemental mass balances using the transformer contributes to the simulation accuracy, which also contributes to improved simulation speed.

3.3. Calibration of hydrolysis kinetics

With the reliable simulation speed, it was possible to run the model using the simplex optimization algorithm for calibration purposes. Fig. 4 shows the predictions of biogas flow rate after model calibration, which are comparable to the measurements. The hydrolysis rates of carbohydrates, proteins and lipids were estimated by fitting the biogas measurements from experiment 1, digesting diluted manure only. The estimated rates were 0.019, 0.025, 0.022 d^{-1}, respectively, for diluted manure waste. These rates are considerably lower compared to the default values of ADM1 (10 d^{-1} for each particulate component) that were originally designated for the hydrolysis of activated aerobic sludge and are still used in GISCOD for the hydrolysis of the decaying anaerobic bacteria after a disintegration step (rate $k_{dis} = 0.5$). It is noteworthy that the default hydrolysis rates presented in the ADM1 in 2002 is now considered to be at least a factor of ten too large also by the ADM1 Task Group (Batstone, 2008: personal communication). The low rates indicate that the digestion of the manure waste was limited by hydrolysis and that the amount of methane produced was mainly from soluble COD digestion. When the diluted manure was co-digested with kitchen waste the biogas production was significantly increased even at periods of similar HRT in both experiments, i.e. day 0 to 38 and day 63 to 73. The higher biogas production was not only due to the higher COD load of added kitchen waste but also because the particulate fractions of the kitchen waste were easily hydrolysable. The estimated hydrolysis rates of the kitchen waste from the second experiment were 5.22, 1.86 and 1.24 d^{-1} for carbohydrates, proteins and lipids, respectively. This indicates the necessity of separating the hydrolysis of both wastes. In a similar co-digestion study of a fixed ratio 80:20 manure liquids to cow fodder (Lübken et al., 2007), the best ADM1 simulation of biogas

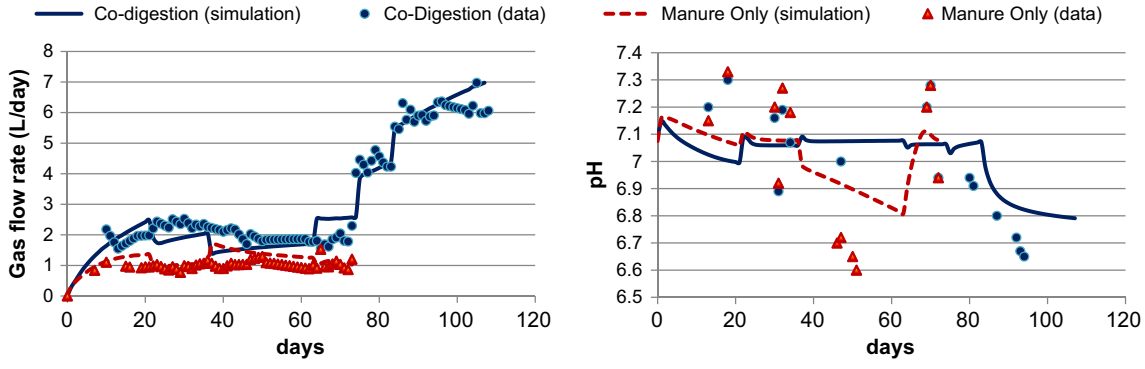

Fig. 4 – Comparison of simulated and measured biogas production (left) and pH (right) after calibration of the hydrolysis parameters.

prediction matched the experimental data at 0.3 d^{-1} hydrolysis rate for the three particulate fractions. The slightly higher hydrolysis rate compared to digesting manure is due to the addition of the cow fodder. Cow fodder hydrolysis rate is higher compared to manure that has already been passed through hydrolysis and digestion in the rumen. For reliable simulation and prediction of the biogas production at variable ratios of co-digested wastes, accurate hydrolysis rates should be estimated for each waste and each particulate fraction. Expanding the applicability of GISCOD to any waste combinations allows the integrated assessment of AD using different treatment scenarios. For instance, accurate evaluation of the biogas production co-digesting energy crops, agricultural residues and wastes would benefit LCA studies of alternative processes for bio-fuel production (Tan et al., 2004) adding the AD process to the complete process train.

3.4. *Simulation of chemical equilibrium*

The pH, presented in Fig. 4, was slightly higher during manure only digestion in Experiment 1 indicating that manure has higher alkalinity than kitchen waste. During overload periods, hydraulically during manure only digestion from day 34 to day 63 and organically by increasing the food waste ratio from day 84 till the end of the co-digestion experiment, the pH dropped rapidly but the biogas production increased. During process overloads, VFA's accumulate causing the pH to drop (Zaher et al., 2004). The drop of the pH is caused by stripping of alkalinity and higher CO_2 production in the biogas.

3.5. *Optimization of reactor design and operation*

The 200,000 days of virtual experimental time were simulated using GISCOD in 8 h of CPU-time to find the optimal operation for the co-digestion case study. Fig. 5 shows the predicted gas flow rates of the model for the 200 virtual experiments of the optimization procedure after filtering for a few anomalies due to numerical errors and the high non-linearity of the model. The optimal biogas and methane production was found at a HRT of 50 days using a pre-hydrolysis step of 2 L and a digester volume of 20 L. Increasing the HRT more than 50 days did not produce any increase in the daily gas production since the process was rate limited by the COD loading rate. At HRT <20 days the process was limited by the methanogenesis step since 2 L volume was assigned to both hydrolysis and methanogenesis steps. There was another local optimum of biogas production at HRT of 10 days that was mainly related to soluble substrates and not the particulate substrate. Inhibition due to VFA accumulation and pH started at HRT less than 20 days. However, the addition of diluted manure buffered the pH near the optimum range except for HRT <10 days. Simulations showed VFA accumulation and pH drop at HRT <10 days. Also, at 10 days HRT and an addition of kitchen waste >80%, pH dropped and VFA accumulated. During VFA accumulation and pH drop, methanogenesis was completely inhibited and biogas was mainly CO_2. Methane and total biogas production increased with the additional kitchen waste except at low HRT where the manure alkalinity could not maintain the pH in the optimal range.

The GISCOD simulated different feedstock and influent flow rates using two digester volumes to determine the optimum design and operation of an AD application to the co-digestion of two different waste streams. The simulation saved excessive experimental time, which would be needed to determine the optimum for such co-digestion applications. The determined optimal result can then be validated experimentally before full-scale implementation in a relatively short time. More generally, the model determines virtually the optimal design and operation as well as digester outputs that would benefit environmental and economic studies of AD applications. Such model-based optimization of design and operation settings is of a great practical advantage compared to "random" or "heuristic" approaches that sometimes lead to severe problems. Steyer et al. (2006) illustrated the severe consequences of using such "heuristic" approaches to make operation decisions on full-scale biogas plants. They gave a real example of a biogas plant co-digesting pig manure and industrial wastewater in Blaabjerg, Denmark that experienced a serious accident due to an overdose of the industrial waste. The consequence of such single event was the significant reduction of bio-gas production and methane content. The process did not recover for 3 months and the biogas had to be

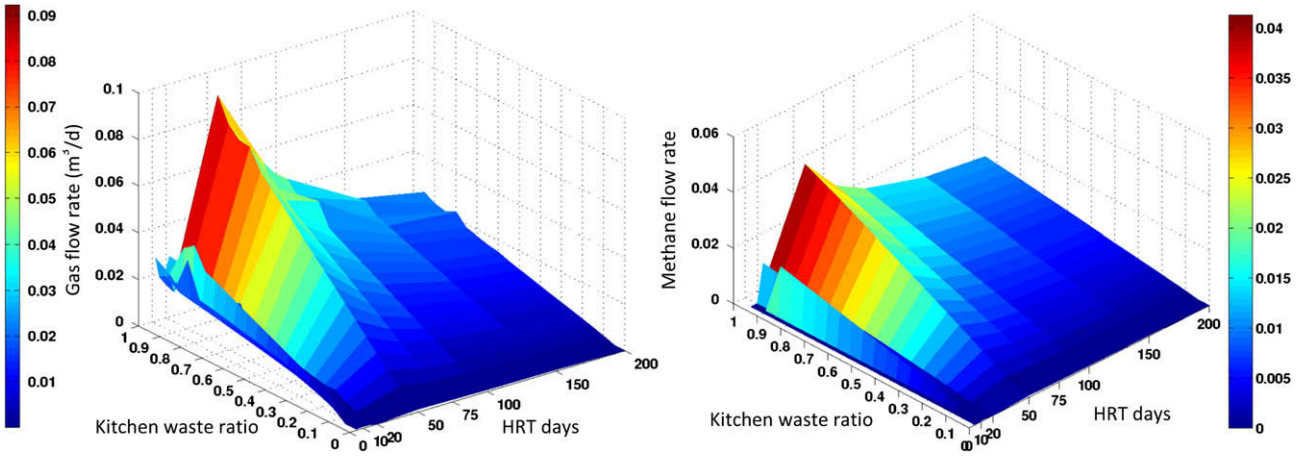

Fig. 5 – Biogas optimization results of manure and kitchen wastes co-digestion varying feedstock, flow and methanogenic volume.

flared instead of being used for power generation. The total operational loss was subsequently calculated as one million DKK (approximately US$150,000). Such example illustrates the benefit of the developed model as an optimization and decision support tool in addition to its potential application for the integrated assessment and LCA of AD applications for waste stabilization and power generation.

4. Conclusions

Feeding the digester with a combination of waste streams introduces complexities in waste characterization that requires the General Integrated Solid Waste Co-digestion (GISCOD) model to simulate improvement mechanisms of co-digestion. Maintaining the continuity of macronutrients, COD and charge during waste characterization was necessary to accurately estimate the input to the International Water Association Anaerobic Digestion Model No.1 (ADM1). In the detailed input required for ADM1, particulate components of carbohydrates, proteins and lipids vary dynamically in combined solid waste streams. Such waste heterogeneity could be resolved by applying a general transformer model to interface the ADM1 to practical characteristics of each waste stream. In co-digestion applications, it is important to consider separate hydrolysis rates for each particulate component from each waste stream. The presented case study of food waste and manure co-digestion showed that hydrolysis rates vary significantly. Also, hydrolysis rates of solid wastes differ from that of decaying biomass which is mainly limited by a disintegration step for cell lysis.

The separate characterization and phasing of the co-digested wastes hydrolysis allowed the optimization of biogas production and defined the corresponding operation settings of the digester. Therefore, the GISCOD or a similar modeling approach would support the operation decision of digesting trucked-in wastes with wastewater sludge or, generally, optimize the feedstock and operation of biogas plants.

Acknowledgments

This work was partly funded by the California Energy Commission and the Washington State Department of Ecology.

REFERENCES

Alvarenga, P., Palma, P., Gonçalves, A.P., Fernandes, R.M., Cunha-Queda, A.C., Duarte, E., Vallini, G., 2007. Evaluation of chemical and ecotoxicological characteristics of biodegradable organic residues for application to agricultural land. Environment International 33 (4), 505–513.

Batstone, D.J., 2008. Personal communication. AWMC, Advanced Water Management Centre. QLD 4072 Australia, fax +61(0)7 3365 4726. University of Queensland, Brisbane. damienb@awmc.uq.edu.au.

Batstone, D.J., Keller, J., Angelidaki, R.I., Kalyuzhnyi, S.V., Pavlostathis, S.G., Rozzi, A., Sanders, W.T.M., Siegrist, H., Vavilin, V.A., 2002. Anaerobic Digestion Model No.1. Scientific and Technical Report No. 13. IWA Publishing, London, UK.

bou Najm, M., El-Fadel, M., 2004. Computer-based interface for an integrated solid waste management optimization model. Environmental Modelling & Software 19 (12), 1151–1164.

Copp, J.B., Jeppsson U., Rosen, C., 2003. Towards an ASM1—ADM1 state variable interface for plant-wide wastewater treatment modeling. Proc. 76th Annual WEF Conference and Exposition (WEFTEC), Oct. 11–15, Los Angeles, USA.

Deng, W.Y., Yan, J.H., Li, X.D., Wang, F., Zhu, X.W., Lu, S.Y., Cen, K.F., 2009. Emission characteristics of volatile compounds during sludges drying process. Journal of Hazardous Materials 162 (1), 186–192.

Ekama, G.A., Sotemann, S.W., Wentzel, M.C., 2007. Biodegradability of activated sludge organics under anaerobic conditions. Water Research 41 (1), 244–252.

Fezzani, B., Cheikh, R.B., 2008a. Modelling of the mesophilic anaerobic co-digestion of olive mill wastewater with olive mill solid waste using anaerobic digestion model No. 1 (ADM1). Bioresource Technology 99 (14), 6565–6577.

Fezzani, B., Cheikh, R.B., 2008b. Implementation of IWA anaerobic digestion model No. 1 (ADM1) for simulating the thermophilic anaerobic co-digestion of olive mill wastewater with olive mill solid waste in a semi-continuous tubular digester. Chemical Engineering Journal 141 (1-3), 75–88.

García de Cortázar, A.L., Monzón, I.T., 2007. MODUELO 2: A new version of an integrated simulation model for municipal solid waste landfills. Environmental Modelling & Software 22 (1), 59–72.

Grau, P., Beltrán, S., de Gracia, M., Ayesa, E., 2007. New mathematical procedure for the automatic estimation of influent characteristics in WWTPs. Water Science and Technology 56 (8), 95–106.

Hartmann, H., Ahring, B.K., 2005. Anaerobic digestion of the organic fraction of municipal solid waste: Influence of co-digestion with manure. Water Research 39 (8), 1543–1552.

He, P.J., Shao, L.M., Guo, H.D., Li, G.J., Lee, D.J., 2006. Nitrogen removal from recycled landfill leachate by ex situ nitrification and in situ denitrification. Waste Management 26 (8), 838–845.

Henze, M., Grady, J.C.P.L., Gujer, W., Marais, G.v.R., Matsuo, T., 1987. Activated Sludge Model No.1. IAWQ Scientific and Technical Report #1. IWA Publishing, London, UK.

Kang, M.S., Srivastava, P., Tyson, T., Fulton, J.P., Owsley, W.F., Yoo, K.H., 2008. A comprehensive GIS-based poultry litter management system for nutrient management planning and litter transportation. Computers and Electronics in Agriculture 64 (2), 212–224.

Kleerebezem, R., van Loosdrecht, M.C.M., 2006. Waste characterization for implementation in ADM1. Water Science and Technology 54 (4), 167–174.

Komilis, D.P., Ham, R.K., 2006. Carbon dioxide and ammonia emissions during composting of mixed paper, yard waste and food waste. Waste Management 26 (1), 62–70.

Kumar, V., Mari, M., Schuhmacher, M., Domingo, J.L., 2009. Partitioning total variance in risk assessment: Application to a municipal solid waste incinerator. Environmental Modelling & Software 24 (2), 247–261.

Lübken, M., Wichern, M., Schlattmann, M., Gronauer, A., Horn, H., 2007. Modelling the energy balance of an anaerobic digester fed with cattle manure and renewable energy crops. Water Research 41 (18), 4085–4096.

Manirakiza, P., Covaci, A., Schepens, P., 2001. comparative study on total lipid determination using Soxhlet, Roese-Gottlieb, Bligh & Dyer, and modified Bligh & Dyer extraction methods. Journal of Food Composition and Analysis 14, 93–100.

Nelder, J., Mead, R., 1965. A simplex method for function minimization. Computer Journal 7, 308–313.

Nopens, I., Batstone, D.J., Copp, J.B., Jeppsson, U., Volcke, E., Alex, J., Vanrolleghem, P.A., in press. An ASM/ADM model interface for dynamic plant-wide simulation. Water Research, doi:10.1016/j.watres.2009.01.012.

Paillat, J.M., Robin, P., Hassouna, M., Leterme, P., 2005. Predicting ammonia and carbon dioxide emissions from carbon and nitrogen biodegradability during animal waste composting. Atmospheric Environment 39 (36), 6833–6842.

Rosen, C., Vrecko, D., Gernaey, K.V., Pons, M.N., Jeppsson, U., 2006. Implementing ADM1 for plant-wide benchmark simulations in Matlab/Simulink. Water Science and Technology 54 (4), 11–19.

Shanmugam, P., Horan, N.J., 2009. Simple and rapid methods to evaluate methane potential and biomass yield for a range of mixed solid wastes. Bioresource Technology 100 (1), 471–474.

Singh, K.P., Malik, A., Sinha, S., 2005. Water quality assessment and apportionment of pollution sources of Gomti river (India) using multivariate statistical techniques: a case study. Analytica Chimica Acta 538 (1–2), 355–374.

Steyer, J-P., Latrille, E., Aceves, C., Ramirez, I., Elias, A., Hess, J., Bernard, O., Nielsen, H.B., Boe, K., Angelidaki, I., 2006. Optimizing biogas production from anaerobic digestion. Water Environment Federation Technical Exhibition and Conference (WEFTEC 79th), Dallas, Texas, USA, October 21–25, 2006.

Tan, R.R., Culaba, A.B., Purvis, M.R.I., 2004. POLCAGE 1.0: a possibilistic life-cycle assessment model for evaluating alternative transportation fuels. Environmental Modelling & Software 19 (10), 907–918.

Vanrolleghem, P.A., Rosen, C., Zaher, U., Copp, J., Benedetti, L., Ayesa, E., Jeppsson, U., 2005. Continuity-based interfacing of models for wastewater systems described by Petersen matrices. Water Science and Technology 52 (1–2), 493–500.

Volcke, E.I.P., van Loosdrecht, M.C.M., Vanrolleghem, P.A., 2006. Continuity-based model interfacing for plant-wide simulation: A general approach. Water Research 40 (15), 2817–2828.

Wallis, M.J., Ambrose, M.R., Chan, C.C., 2008. Climate change: Charting a water course in an uncertain future. E-Journal AWWA 100 (6), 70–79.

Ward, A.J., Hobbs, P.J., Holliman, P.J., Jones, D.L., 2008. Optimisation of the anaerobic digestion of agricultural resources. Bioresource Technology 99 (17), 7928–7940.

Yen, H.W., Brune, D.E., 2007. Anaerobic co-digestion of algal sludge and waste paper to produce methane. Bioresource Technology 98 (1), 130–134.

Zaher, U., Chen, S., 2006. Interfacing the IWA anaerobic digestion model no1 (ADM1) with manure and solid waste characteristics. Proc. 79th Annual WEF Conference and Exposition (WEFTEC), October 21–25, Dallas, USA.

Zaher, U., Bouvier, J.C., Steyer, J.-P., Vanrolleghem, P.A., 2004. Titrimetric monitoring of anaerobic digestion: VFA, alkalinities and more. Proc. 10th World Congress on Anaerobic Digestion (AD10), August 29–September 2, Montreal, Canada, Vol. 1, pp. 330-336.

Zaher, U., Grau, P., Benedetti, L., Ayesa, E., Vanrolleghem, P.A., 2007. Transformers for interfacing anaerobic digestion models to pre- and post-treatment processes in a plant-wide modelling context. Environmental Modelling & Software 22 (1), 40–58.

Zaher, U., Buffiere, P., Steyer, J.-P., Chen, S., 2009. A procedure to estimate proximate analysis of mixed organic wastes. Water Environment Research 81 (4), 407–415.

Zhang, P., Zeng, G., Zhang, G., Li, Y., Zhang, B., Fan, M., 2008. Anaerobic co-digestion of biosolids and organic fraction of municipal solid waste by sequencing batch process. Fuel Processing Technology 89 (4), 485–489.

Zupancic, G.D., Uranjek-Zevart, N., Ros, M., 2008. Full-scale anaerobic co-digestion of organic waste and municipal sludge. Biomass and Bioenergy 32 (2), 162–167.

Appendix 5: ADM1 Process model parameters

Parameter	Unit	Value	Definition
Stoichiometric parameters			
$f_{sI,xc}$	–	0.1	Yield of soluble inerts from disintegration of complex particulates
$f_{xI,xc}$	–	0.2	Yield of particulate inerts from disintegration of complex particulates
$f_{ch,xc}$	–	0.2	Yield of carbohydrates from disintegration of complex particulates
$f_{pr,xc}$	–	0.2	Yield of proteins from disintegration of complex particulates
$f_{li,xc}$	–	0.3	Yield of lipids from disintegration of complex particulates
N_{xc}	kmole N (kg COD)$^{-1}$	0.00221	Nitrogen content of particulate degradable COD
N_I	kmole N (kg COD)$^{-1}$	0.00414	Nitrogen content of soluble inert COD
		0.00414	Nitrogen content of particulate inert COD
N_{aa}	kmole N (kg COD)$^{-1}$	0.0071	Nitrogen content of amino acids
C_{xc}	kmole C (kg COD)$^{-1}$	0.0258	Carbon content of complex particulates
C_{sI}	kmole C (kg COD)$^{-1}$	0.03	Carbon content of soluble inert COD
C_{ch}	kmole C (kg COD)$^{-1}$	0.0313	Carbon content of carbohydrates
C_{pr}	kmole C (kg COD)$^{-1}$	0.03	Carbon content of proteins
C_{li}	kmole C (kg COD)$^{-1}$	0.022	Carbon content of lipids
C_{xI}	kmole C (kg COD)$^{-1}$	0.03	Carbon content of particulate inert COD
C_{su}	kmole C (kg COD)$^{-1}$	0.0313	Carbon content of sugars
C_{aa}	kmole C (kg COD)$^{-1}$	0.03	Carbon content of amino acids
$f_{fa,li}$	–	0.95	Yield of long chain fatty acids (as opposed to glycerol) from lipids
C_{fa}	kmole C (kg COD)$^{-1}$	0.0217	Carbon content of long chain fatty acids
$f_{h2,su}$	–	0.19	Yield of hydrogen from monosaccharide degradation
$f_{bu,su}$	–	0.13	Yield of butyrate from monosaccharide degradation
$f_{pro,su}$	–	0.27	Yield of propionate from monosaccharide degradation
$f_{ac,su}$	–	0.41	Yield of acetate from sugar degradation
N_{bac}	kmole N (kg COD)$^{-1}$	0.0062	Nitrogen content of biomass

Parameter	Unit	Value	Definition
C_{bu}	kmole C (kg COD) $^{-1}$	0.025	Carbon content of butyrate
C_{pro}	kmole C (kg COD) $^{-1}$	0.0268	Carbon content of propionate
C_{ac}	kmole C (kg COD) $^{-1}$	0.0313	Carbon content of acetate
C_{bac}	kmole C (kg COD) $^{-1}$	0.0313	Carbon content of biomass
Y_{su}	–	0.1	Yield of biomass on uptake of monosaccharides
$f_{h2,aa}$	–	0.06	Yield of hydrogen from amino acid degradation
$f_{va,aa}$	–	0.23	Yield of valerate from amino acid degradation
$f_{bu,aa}$	–	0.26	Yield of butyrate from amino acid degradation
$f_{pro,aa}$	–	0.05	Yield of propionate from amino acid degradation
$f_{ac,aa}$	–	0.4	Yield of acetate from amino acid degradation
C_{va}	kmole C (kg COD) $^{-1}$	0.024	Carbon content of valerate
Y_{aa}	–	0.08	Yield of biomass on uptake of amino acids
Y_{fa}	–	0.06	Yield of biomass on uptake of long chain fatty acids
Y_{c4}	–	0.06	Yield of biomass on uptake of valerate or butyrate
Y_{pro}	–	0.04	Yield of biomass on uptake of propionate
C_{ch4}	kmole C (kg COD) $^{-1}$	0.0156	Carbon content of methane
Y_{ac}	–	0.05	Yield of biomass on uptake of acetate
Y_{h2}	–	0.06	Yield of biomass on uptake of elemental hydrogen
Kinetic parameters			
k_{dis}	d^{-1}	0.5	Complex particulate disintegration first order rate constant
$k_{hyd,ch}$	d^{-1}	10	Carbohydrate hydrolysis first order rate constant
$k_{hyd,pr}$	d^{-1}	10	Protein hydrolysis first order rate constant
$k_{hyd,li}$	d^{-1}	10	Lipid hydrolysis first order rate constant
$K_{S,IN}$	M	0.0001	Inorganic nitrogen concentration at which growth ceases
$k_{m,su}$	d^{-1}	30	Maximum uptake rate for monosaccharide degrading organisms
$K_{S,su}$	kg COD m^{-3}	0.5	Half saturation constant for monosaccharide degradation
$pH_{UL,aa}$		5.5	pH level at which there is no inhibition…(for bacteria in general e.g. aa and fa degraders)
$pH_{LL,aa}$		4	pH level at which there is full inhibition …(for bacteria in general e.g. aa and fa degraders)
$k_{m,aa}$	d^{-1}	50	Maximum uptake rate amino acid degrading organisms
$K_{S,aa}$	kg COD m^{-3}	0.3	Half saturation constant for amino acid degradation
$k_{m,fa}$	d^{-1}	6	Maximum uptake rate for long chain fatty acid degrading organisms
$K_{S,fa}$	kg COD m^{-3}	0.4	Half saturation constant for long chain fatty acids degradation
$K_{Ih2,fa}$	kg COD m^{-3}	5E-6	Hydrogen inhibitory concentration for FA degrading organisms
$k_{m,c4}$	d^{-1}	20	Maximum uptake rate for C4 degrading

Parameter	Unit	Value	Definition
			organisms
$K_{S,c4}$	kg COD m^{-3}	0.2	Half saturation constant for butyrate and valerate degradation
$K_{Ih2,c4}$	kg COD m^{-3}	1E-5	Hydrogen inhibitory concentration for C4 degrading organisms
$k_{m,pro}$	d^{-1}	13	Maximum uptake rate for propionate degrading organisms
$K_{S,pro}$	kg COD m^{-3}	0.1	Half saturation constant for propionate degradation
$K_{Ih2,pro}$	kg COD m^{-3}	3.5E-6	Inhibitory hydrogen concentration for propionate degrading organisms
$k_{m,ac}$	d^{-1}	8	Maximum uptake rate for acetate degrading organisms
$K_{S,ac}$	kg COD m^{-3}	0.15	Half saturation constant for acetate degradation
$K_{I,nh3}$	M	0.0018	Inhibitory free ammonia concentration for acetate degrading organisms
$pH_{UL,ac}$		7	pH level at which there is no inhibition of acetate degrading organisms
$pH_{LL,ac}$		6	pH level at which there is full inhibition of acetate degradation
$k_{m,h2}$	d^{-1}	35	Maximum uptake rate for hydrogen degrading organisms
$K_{S,h2}$	kg COD m^{-3}	7E-6	Half saturation constant for uptake of hydrogen
$pH_{UL,h2}$		6	pH level at which there is no inhibition of hydrogen degrading organisms
$pH_{LL,h2}$		5	pH level at which there is full inhibition of hydrogen degrading organisms
$k_{dec,Xsu}$	d^{-1}	0.02	Decay rate for monosaccharide degrading organisms
$k_{dec,Xaa}$	d^{-1}	0.02	Decay rate for amino acid degrading organisms
$k_{dec,Xfa}$	d^{-1}	0.02	Decay rate for long chain fatty acid degrading organisms
$k_{dec,Xc4}$	d^{-1}	0.02	Decay rate for butyrate and valerate degrading organisms
$k_{dec,Xpro}$	d^{-1}	0.02	Decay rate for propionate degrading organisms
$k_{dec,Xac}$	d^{-1}	0.02	Decay rate for acetate degrading organisms
$k_{dec,Xh2}$	d^{-1}	0.02	Decay rate for hydrogen degrading organisms
Physiochemical parameters			
R	bar M^{-1} K^{-1}	0.08314	Gas law constant
T_{base}	K	--	" Not used " … i.e. operating temperature (T_{op}) is considered constant and parameter values should correspond to this operational temperature
T_{op}	K	308.15	Temperature
K_w	M	2.08E-14	Water acidity constant (temperature correction needed)
$K_{a,va}$	M	1.38E-5	Valerate acidity constant (temperature correction can be ignored)
$K_{a,bu}$	M	1.5E-5	Butyrate acidity constant (temperature correction can be ignored)
$K_{a,pro}$	M	1.32E-5	Propionate acidity constant (temperature correction can be ignored)
$K_{a,ac}$	M	1.74E-5	Acetate acidity constant (temperature correction can be ignored)
$K_{a,co2}$	M	4.94E-7	CO_2 acidity constant (temperature correction needed)

Parameter	Unit	Value	Definition
$K_{a,IN}$	M	1.11E-9	NH_4^+ acidity constant (temperature correction needed)
P_{atm}	Bar	1.013	Pressure of atmosphere
$p_{gas,h2o}$	Bar	0.0557	Partial pressure of water (Note: can be defined empirically)
k_La	d^{-1}	200	Gas liquid transfer coefficient (Note: dependent on the reactor type)
$K_{H,co2}$	$M_{liq}\,bar^{-1}$	0.0271	Henry's law constants for carbon dioxide
$K_{H,ch4}$	$M_{liq}\,bar^{-1}$	0.00116	Henry's law constants for methane
$K_{H,h2}$	$M_{liq}\,bar^{-1}$	0.000738	Henry's law constants for hydrogen
Physical parameters			
V_{liq}	m^3	varies	Volume of liquid in the reactor
V_{gas}	m^3	varies	Volume of the gas vessel
f_{xout}	–	1 (CSTR) 0 (FBR)	Fraction of the anaerobic particulate matter that leaves the reactor